UNIVERSIDAD DE LA REPÚBLICA

Facultad de Ingeniería

Tesis para optar al Título de
Doctor en Ingeniería Eléctrica

ON SOME DYNAMIC PROPERTIES OF ELECTRICAL POWER SYSTEMS

(Sobre algunas propiedades dinámicas de los sistemas eléctricos de potencia)

Autor:
Alvaro Giusto
Director de Tesis:
Alex Stankovic

Montevideo, Uruguay
2010

.

UNIVERSIDAD DE LA REPÚBLICA ORIENTAL DEL URUGUAY
INSTITUTO DE INGENIERíA ELÉCTRICA

Los abajo firmantes certificamos que hemos leído el presente trabajo titulado "**On some dynamic properties of electrical power systems (Sobre algunas propiedades dinámicas de los sistemas eléctricos de potencia)**" hecho por **Alvaro Giusto** y encontramos que el mismo satisface los requerimientos curriculares que la Facultad de Ingeniería exige para la tesis del título de **Doctor en Ingeniería Eléctrica**.

Fecha: 23 de junio 2010

Director Académico: _____
Prof. César Briozzo

Director de Tesis: _____
Dr. Alex Stankovic

Tribunal examinador: _____
Dr. Fernando Paganini

_____
Prof. Glauco N. Taranto

_____
Dr. Ing. Pablo Monzón

ISSN: 1688-2784 (printed version)
ISSN: 1688-2776 (electronic version)
Alvaro Giusto (alvaro@fing.edu.uy)
Tesis de Doctorado en Ingeniería Eléctrica
Facultad de Ingeniería
Universidad de la República
Montevideo, Uruguay, 2010.

UNIVERSIDAD DE LA REPÚBLICA ORIENTAL DEL URUGUAY

Fecha: **23 de junio 2010**

Autor:	**Alvaro Giusto**
Titulo:	**On some dynamic properties of electrical power systems (Sobre algunas propiedades dinámicas de los sistemas eléctricos de potencia)**
Instituto:	**Ingeniería Eléctrica**
Grado:	**Doctor en Ingeniería Eléctrica** (**Dr. Ing.**)

.

Para Gladys, Camilo, Joaquín y Lucía.

Para mis padres.

Table of Contents

Gracias

Esta tesis se valió de aportes valiosos de muchas personas que quiero agradecer en estas líneas.

Mi esposa Gladys y mis hijos así como mis padres le dieron, cada uno a su modo y en su tiempo, razón de ser a este esfuerzo y a todo lo demás.

Maruja, Oscar y Cristina aportaron, entre otras cosas, su apoyo y su solidaridad.

Pablo Monzón y César Briozzo me han brindado su apoyo y la posibilidad de discutir diversos aspectos de esta tesis en un momento por demás oportuno.

A los compañeros del Grupo de Estabilidad y Control de Sistemas Eléctricos de Potencia les agradezco su apoyo y el haber convertido el grupo en un ámbito muy estimulante de trabajo y estudio.

Muchos compañeros del Instituto–¿ porqué nombrar solo a unos pocos?–me han apoyado cotidianamente.

Quiero agradecer al Prof. Romeo Ortega su talento, su generosidad y su tiempo al colaborar activamente en una parte de los trabajos reportados en esta tesis.

Quiero agradecer a los Prof. Glauco N. Taranto y Fernando Paganini su participación en el tribunal y la revisión de esta tesis. Sus comentarios y sugerencias han sido útiles para mejorar la misma.

I want to thank Prof. Alex Stankovic for advising my thesis and for his gentile support in this period.

Abstract

This thesis treats some dynamic properties of power system models. An extension of the classical concept of dissipativity is formulated to deal with these systems described by differential-algebraic equations on phasor variables. A class of models of these systems–the same that is known to admit an energy function–is shown to be dissipative in the sense mentioned above, to later be extended to include realistic models of synchronous machines and other devices.

The small signal models are shown to satisfy a convex constraint in the frequency domain that is later articulated with Integral Quadratic Constraints, a well-known stability analysis tool.

Specific features of realistic power system models, as the effect of voltage regulation and damping injection, are precisely captured and incorporated into the analysis. It is shown that a trade-off between the mentioned control actions and the voltage sensitivity is a sufficient condition to establish the robustness of the electromechanical modes. This result and others mentioned above are validated through several examples.

Resumen

Esta tesis trata algunas propiedades dinámicas de los sistemas eléctricos de potencia. Se formula una extensión del concepto clásico de disipatividad compatible con estos sistemas, descritos por ecuaciones algebraico-diferenciales sobre variables fasoriales. Se muestra que una clase de modelos de estos sistemas satisface este concepto de disipatividad y se muestra que también lo hacen modelos detallados de máquinas síncronas y otros dispositivos de potencia.

Se demuestra que los modelos en pequeña señal satisfacen una restricción convexa en el dominio de la frecuencia, capaz de ser articulada con herramientas bien conocidas de análisis de estabilidad.

Características específicas de los sistemas eléctricos reales, tales como la acción de la regulación de tensión y las señales estabilizadoras, son precisamente definidas e incorporadas al análisis. Se demuestra que un adecuado balance entre las acciones de control mencionadas y la sensibilidad a variaciones de tensión es una condición suficiente para la robustez de los modos electromecánicos del sistema. Este resultado y otros mencionados anteriormente son validados mediante el análisis de varios ejemplos.

Notation

$\mathbb{R}, \mathbb{C}, \mathbb{N}$	real, complex and natural numbers
I_n	$n \times n$ identity matrix
$0_{m\times n}$	$m \times n$ zero matrix
$A^\top, A^{-\top}$	transpose and its inverse
A^*, A^{-*}	complex conjugate transpose and its inverse
$\bar{\sigma}(A)$	maximum singular value of matrix A
Re, Im	real and imaginary part
$j\Omega$	the set $s = j\omega, \omega \in \Omega \subset \mathbb{R}$
$\mathcal{L}_2[0,\infty)$	space of functions of energy $\int_0^\infty \lvert f(t)\rvert^2 dt$ finite
$\mathcal{L}_2^e[0,\infty)$	square integrable functions on finite intervals.
$\mathcal{L}_\infty^{m\times n}(\Omega)$	$m \times n$ bounded functions on the set $j\Omega$.
$\mathbf{R}\mathcal{L}_\infty^{m\times n}(\Omega)$	$m \times n$ rational proper transfer matrices with no poles on $j\Omega$
$\mathbf{R}\mathcal{H}_\infty^{m\times n}$	$m \times n$ stable rational transfer matrices bounded on the imaginary axis
$\tilde{V}_j \in \mathbb{C}$	voltage phasor at the bus j
$\mathrm{V}_j = [\mathrm{V}_{Rj}\ \mathrm{V}_{Ij}]^\top$	Cartesian description of voltage phasor at the bus j.
$\mathcal{V}_j, \theta_j$	module and angle of the voltage phasor
I_j^d	Cartesian description of current phasor, entering device d at the bus j.
P_j^d, Q_j^d	active and reactive power entering device d at bus j
$\mathrm{V}_j^\star, I_j^{d\star}, P_j^{d\star}, Q_j^{d\star}$	electrical magnitudes at the equilibrium
$\mathrm{v}_j, \mathrm{i}_j^d, p_j^d, q_j^d$	small signal electrical magnitudes around the equilibrium.
$\mathrm{v}_j = [\mathrm{v}_{Rj}\ \mathrm{v}_{Ij}]^\top$	Cartesian description of small signal voltage phasor at the bus j.

v_j, ϑ_j	small signal voltage module and angle
$\lambda_j = \dot{\vartheta}_j$	small signal frequency deviation at bus j
$\hat{x}$	Laplace transform of temporal function $x(t)$
$\mathbb{B} \subset \mathbb{N}$	index set of buses in a network
$\mathbb{M}, \mathbb{L}, \mathbb{E} \subset \mathbb{B}$	index sets associated to machines, static loads and external injections
$\mathbb{M}_3 \subset \mathbb{M}$	index set associated to third order models of synch. machines
$\mathbb{M}_6 \subset \mathbb{M}$	index set associated to sixth order models of synch. machines
$\mathcal{M} \subset \mathbb{N}$	index set of a given set of close loop modes
g_r, g_d, g_g	auxiliary functions on complex matrices
$\gamma_r(\cdot, \cdot; \omega)$	voltage regulation function
$\gamma_d(\cdot; \omega)$	damping performance function
$\gamma_g(\cdot; \omega)$	voltage sensitivity function
J	auxiliary matrix, 90 degrees counter-clockwise rotation in $\mathbb{R}^2$
$\mathbf{J} := diag_{j \in \mathbb{B}}(J)$	auxiliary matrix $\mathbf{J} \in \mathbb{R}^{2m \times 2m}$
$\mathbf{J}^E := diag_{j \in \mathbb{E}}(J)$	auxiliary matrix $\mathbf{J}^E \in \mathbb{R}^{2m_E \times 2m_E}$
U_θ	auxiliary matrix, θ clockwise rotation in $\mathbb{R}^2$
k_v, k_θ	versors co-linear and orthogonal to equilibrium voltage
$\mathbf{Z}$	matrix transfer function $\hat{\mathrm{i}} \to \hat{\mathrm{v}}$
$\mathbf{Y}$	matrix transfer function $\hat{\mathrm{v}} \to \hat{\mathrm{i}}$
$col_{j \in \mathbb{B}}\ x_j$	vector column, ordered stacking of the vectors $x_j, j \in \mathbb{B}$.
$diag_{j \in \mathbb{B}}\ M_j$	block diagonal matrix, with $M_j, j \in \mathbb{B}$ at its diagonal
$\nabla_x f(x);\ \nabla f(x)$	(column) gradient vector of the function $f : \mathbb{R}^n \to \mathbb{R}$
$\nabla_x f(x, y);\ \nabla_y f(x, y)$	(column) partial derivative vector of the function $f : \mathbb{R}^n \times \mathbb{R}^m \to \mathbb{R}$

$\Sigma_i^{M_3}, \Sigma_i^{M_6}$	PCH third (sixth) order model of synchronous machine
Σ_i^M	PCH generic model of synch. machine, $i \in \mathbb{M}$
Σ_l^L	PCH description for the ZIP model of the power system loads
Σ^N	PCH description for the network model
$S^N, S_l^L, S_i^{M_3}, S_i^{M_6}, S_i^M$	storage functions associated to the respective devices
W, W_{fd}, W^N, W^E	power supply rate functions
Ψ^N, Ψ_l^L	terms associated to the network and loads that impede dissipativity
$\mathcal{F}_u$	upper LFT
$\mathcal{F}_l$	lower LFT
$\left[\begin{array}{c\|c} A & B \\ \hline C & D \end{array}\right]$	$:= C(sI - A)^{-1}B + D$: transfer matrix of state space model.

Glossary

AC	Alternating Current
AC	Alternating Current
AVR	Automatic Voltage Regulator
DAE	Differential-Algebraic Equations
FACTS	Flexible AC Transmission System
FDLMI	Frequency Dependent Linear Matrix Inequality
GKYP	Generalized Kalman-Yakubovic-Popov lemma
IQC	Integral Quadratic Constraint
KYP	Kalman-Yakubovic-Popov lemma
LFT	Linear Fractional Transformation
LHP	Left-half plane: $Re(s) < 0$
LMI	Linear Matrix Inequality
ODE	Ordinary Differential Equations
PCH	Port-Controlled Hamiltonian
PD	Proportional + derivative control law
PSS	Power System Stabilizer
RHP	Right-half plane: $Re(s) \geq 0$
SVC	Static Var Compensator
TCR	Thyristor-Controlled Reactor
ZIP	Constant Impedance, Current and Power load model

Introduction

The dynamic behavior of power systems is very complex due to nonlinearity, high order dynamics, topological changes and parametric variations. The scenario is complex also because of the influence of manifold control actions, necessary to ensure proper performance and operation. A rich set of theoretical and technological tools are nowadays available to engineers to cope with this complexity in modeling, planning, design and operation of power systems. Powerful software packages along with a well established theoretical framework assist the engineer in simulating and analyzing the dynamic behavior of power systems. However, the need to *conceptually* deal with this complexity is always present.

Power systems constitute a special case of electrical network. However, some peculiarities of power systems models impede that certain basic dynamic properties of the classical Circuit Theory can be applied. The AC modulation and the presence of multiple control actions are shown to hamper the direct application of the idea of passivity, so essential in circuit theory.

A long line of research rooted with the classical Equal Area Criterion (Kimbark, 1948) and the application of Lyapunov theory (Athay et al., 1979) has contributed with a characterization of power systems from an energy perspective which has been used as a direct method to study the transient stability of a class of power systems models. The examination of the terms composing this energy function illuminates the peculiarities of the power system dynamics. Kinetic and potential energies depending on the phasorial description of electrical variables highlight the electromechanical nature of the basic power system dynamics. However, the application of these analysis techniques requires the absence of resistive losses or loads and the absence of control, conditions that are in general very restrictive. These facts open some general questions:

Does the concept of energy–from the dynamic perspective–lose its sense for realistic models of power systems?

Are the power system models *passive* in a sense different from the classical one?

In this thesis the general dissipativity framework proposed in (Willems, 1972) is adopted and extended to study the power systems dynamics. Roughly speaking, a system is dissipative if it satisfies a dynamical balance between the storage of a generalized energy and a suitably defined power supply from the environment. In terms also general, the *cyclo-dissipative* systems satisfy the same energy balance, but the conditions to be met by the generalized energy are less restrictive.

A first original contribution of this thesis is the formulation of a specific concept of dissipativity suitable for the algebraic–differential description of power systems. The particularities of these systems require, for instance, storage functions also depending on the link variables and the definition of a specific supply rate function having derivative terms on the input.

This approach allows one to establish connections with previous results and to provide other contributions. It is shown that, in absence of control and resistive load or losses, the different network components–and their interconnection–admit a Port-Controlled Hamiltonian (PCH) description (Van der Schaft, 2000) and are, therefore, *cyclo–dissipative* in the sense above mentioned.

This is also true for a full order, conventional model of the synchronous machine, including field and damping rotor windings. As a consequence, a complete energy characterization of these machines is provided—avoiding oversimplified models that have been used in the past—which constitutes an original contribution of this work.

The analysis is based on structure–preserving models, see (Bergen and Hill, 1981). A PCH model for the power system including the power exchanges with outer subsystems is provided, and its links with the classical energy function are discussed. Small signal models around the equilibrium are then obtained with the help of the PCH formalism. These linear models are shown to satisfy a convex constraint in frequency domain that presents similarities–and significant differences–with the familiar concept of passivity. The *phase* of the transfer matrix is constrained, but in a different way.

The frequency characterization of small signal models of power systems constitutes another original contribution of this work, and it can be articulated with well known stability analysis tools: the Integral Quadratic Constraints (IQC), see (Megretski and Rantzer, 1997). This fact facilitates the inclusion of

power systems models into a very general framework of robustness analysis.

The mentioned dynamic properties, both the cyclo–dissipativity and the frequency domain constraint, withstand significant parametric variations. On the other hand, several important features of realistic models of power systems cannot be incorporated to this framework. The inclusion of resistive components and realistic models of voltage regulation compromises the cyclo–dissipativity. The reflection of this property on the frequency domain is shown to be very useful to quantify these adverse effects: a simple example allows one to appreciate how the frequency domain constraint is violated at low and high frequencies, but it is significantly preserved at the frequency band associated to the electromechanical modes. This observation and the will to study power system models closer to the real ones open new questions:

To what extent is the cyclo–dissipativity preserved in realistic models?

How can this concept of dissipativity be modified to cope with voltage regulation and damping injection?

The final part of the thesis, Chapter 4, abandons the simplifying modeling assumptions mentioned above, and treats generic small signal models of power systems. The analysis is done with independence of modeling details of the different devices, by focusing on the effects of the classical control actions on the input-output maps of small signal models of power systems. A first contribution of this chapter is a precise definition of the performance of voltage regulation and damping injection, which are discussed with the help of examples. These measures of control performance constitute quadratic constraints–on a finite band of frequencies–that recognize links with the phase constraint mentioned above and also with some familiar concepts in power system community.

The implications of these control actions on the system stability are then investigated through a procedure that, although based on IQCs, has some peculiarities. First, the constraints are satisfied only on a finite range of frequencies. Second, the use of numerical optimization is purposely avoided. This approach has the virtue of keeping direct links with the well known power system concepts mentioned above. In this way, it is shown that a certain balance between damping, voltage regulation and voltage sensitivity constitutes a sufficient condition for the robust stability of the electromechanical modes. This result, another original contribution of this thesis, is validated through the analysis of a classical example.

The structure of the thesis is as follows. Chapter 1 begins by introducing the mathematical model of the various elements comprising the power system, gives their PCH representation and obtains a model for interconnected subsystems.

Chapter 2 introduces the specific dissipativity framework used in this work. The nonlinear models of the different devices are shown to be cyclo–dissipative in the mentioned sense. When small signal models are considered, this property is shown to imply a convex constraint in the frequency domain given by a multiplier $\Pi_d(\omega)$. The dissipativity of detailed models of synchronous machines and of a standard model of Static Var Compensator (SVC), controller included, are studied in detail.

Chapter 3 is focused on applications of the above-mentioned properties. In Section 3.1 the PCH description of a class of power systems is used for the design of excitation controllers to ensure stability and performance in the presence of non-dissipative terms. Section 3.2 studies the application of quadratic frequency domain constraints to the stability analysis of linear interconnected systems. An example involving the design of an SVC voltage regulator is considered. The robust stability is later assessed through the computation of IQC multipliers. The significance of the *a priori* knowledge of multiplier Π_d in the frequency band associated to the electromechanical modes is highlighted and, in some sense, quantified.

Chapter 4 treats general small signal models of controlled power systems, with no restrictive assumptions on losses or control. We investigate how the classical control actions–voltage regulation and damping injection–influence the power system dynamics. A frequency domain characterization of voltage regulation and damping performance is proposed that, in addition, provides a sufficient condition to ensure the robust stability of the electromechanical modes in a sense that is precisely stated.

Chapter 5 completes the main body of the thesis with some concluding remarks and comments on future research.

Appendix A presents the classical definition of dissipativity and briefly discuss its links with passivity and Lyapunov stability. Appendix B gathers the demonstrations of some auxiliary or intermediate results whose details do not contribute to a better understanding of the main topics. A brief introduction to Linear Fractional Transformations (LFT) is included in Appendix C along with the demonstration of an auxiliary lemma used in Chapter 4. Appendix D analyzes the small signal models of static ZIP loads.

The main original contributions of the research described in this thesis are briefly commented:

1. Section 2.1 introduces an extension of the classical concept of dissipativity, intended to cope with differential–algebraic descriptions of power systems. The dissipative properties of a class of non linear models of power systems are demonstrated.

2. The small signal models of the mentioned class of power systems are shown to meet a convex constraint in the frequency domain. Section 2.2.

3. Detailed non linear models of synchronous machines are shown to be cyclo-dissipative. Its linear model is shown to satisfy the frequency domain constraint. Section 1.3.2 and Chapter 2.

4. The dissipativity of standard non linear model of *controlled* SVC is studied in detail. A complete characterization of the linear controllers preserving this property for the small signal is provided. Section 2.3 of this thesis.

5. The content of Chapter 4, including the frequency characterization of classical control actions (Definitions 2-4) and the sufficient condition for the robustness of electromechanical modes, Theorem 1.

Most of the content of this thesis was reported in publications or international events, has been accepted for publication, or it is currently being prepared to be submitted for review.

References (Giusto et al., 2006a; Giusto et al., 2006b) include most of the Chapters 1 and 2 along with the control application of Section 3.1. Some aspects involving notation have been improved for this thesis.

References (Giusto, 2007a; Giusto, 2007b) includes mainly contribution 2, Section 2.2, although the demonstration included in this thesis is preferred by the author.

The studies involving detailed models of synchronous machines, contribution 3, were published in (Giusto et al., 2008).

The application of the frequency properties of power systems to the stability analysis of these systems, Section 3.2, was accepted for publication in (Giusto, 2010).

Contribution 5 is being prepared to be submitted to a journal.

Chapter 1

Power System Modeling

In this thesis we consider the power system models usually employed for transient stability analysis. It is assumed that the electrical magnitudes can be represented through their phasors by neglecting the fast dynamics associated to electromagnetic phenomena on the network. Only the first harmonic of the positive sequence is included in the analysis which has been shown to be sufficient to study the transient phenomena of interest, see e.g. (Kundur, 1994).

The literature on power system dynamics usually describes the phasors by the respective angle and modulus. We, instead, have chosen the Cartesian description via the real and imaginary parts. This fact and the use of currents (instead of powers) to model external injections allows the work with a more linear model and the direct use of the models built with the software package DSAT (Powertech Labs Inc., n.d.). Since several classical models are written in polar coordinates, we sometimes will consider temporarily both notations.

We will work with a *structure–preserving* power system model in a similar way to (Bergen and Hill, 1981). It is a disaggregated model that preserves the original topology of the network, comprised basically by synchronous machines and loads interconnected by a constant impedance network. To facilitate in later sections the derivation of the dissipativity properties of each element, we first show that they can be described by a PCH model.

The reference to PCH models is done with certain abuse of notation, since the systems considered in this thesis are algebraic–differential and the port variables do not respect *stricto sensu* the framework described, e.g. in (Van der Schaft, 2000). The analysis takes advantage, certainly, of the usefulness of this type of models and the implications on the dissipativity of the systems.

The system comprises a set of buses that interconnect load, machines and other devices through the transmission network. Each bus has an associated

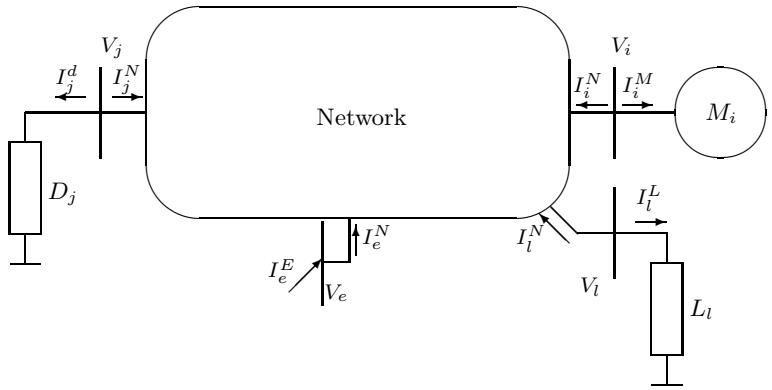

Figure 1.1: Notational conventions

identifier $j \in \mathbb{B} := \{1, .., m\}$. The generators and loads are respectively labeled with indices $i \in \mathbb{M} \subset \mathbb{B}$ and $l \in \mathbb{L} \subset \mathbb{B}$. Generic buses are denoted by identifiers j or k with $j, k \in \mathbb{B}$. The interconnection with external systems is modeled by current injections at a set of buses[1] $\mathbb{E} \subset \mathbb{B}$. $\mathbb{M}, \mathbb{L}, \mathbb{E}, \mathbb{B}$–whose respective cardinalities are m_M, m_L, m_E, m–are *ordered* sets which is taken into account when composite vectors or matrices be built with functions as *col* or *diag*.

The voltage phasor is expressed in Cartesian notation V_{R_j}, V_{I_j} that we collect in vectors

$$\mathrm{V}_j := \begin{bmatrix} \mathrm{V}_{R_j} \\ \mathrm{V}_{I_j} \end{bmatrix} \in \mathbb{R}^2. \tag{1.1}$$

Associated to each bus are the current phasors entering the machine, the load, or a generic device that will be denoted

$$\mathrm{I}_i^M = \begin{bmatrix} \mathrm{I}_{R_i}^M \\ \mathrm{I}_{I_i}^M \end{bmatrix}, \ \mathrm{I}_l^L = \begin{bmatrix} \mathrm{I}_{R_l}^L \\ \mathrm{I}_{I_l}^L \end{bmatrix}, \mathrm{I}_j^d = \begin{bmatrix} \mathrm{I}_{R_j}^d \\ \mathrm{I}_{I_j}^d \end{bmatrix}, \tag{1.2}$$

respectively. We denote respectively

$$\mathrm{I}_j^N := \begin{bmatrix} \mathrm{I}_{R_j}^N & \mathrm{I}_{I_j}^N \end{bmatrix}^\top, \ \mathrm{I}_e^E := \begin{bmatrix} \mathrm{I}_{R_e}^E & \mathrm{I}_{I_e}^E \end{bmatrix}^\top$$

the current entering the network interconnecting the system and the external current injection at bus $e \in \mathbb{E}$. Fig. 1 schematically depicts the notational conventions. We take a current as positive when it *enters* to its component.

[1] To avoid cluttering we reserve the subindex i to variables ranging in the index set $\mathbb{M}$ without explicit reference to it. The same for indices $l \in \mathbb{L}$, $e \in \mathbb{E}$ and $j, k \in \mathbb{B}$. For the same reason, we also omit the subindices when the context avoids any confusion.

The voltage phasor can also be represented by the complex number $\tilde{V}_j$, whose magnitude and angle are respectively denoted $\mathcal{V}_j$ and θ_j. Thus

$$\tilde{V}_j = \mathcal{V}_j \angle \theta_j,\ \theta_j = \arctan \frac{\mathrm{V}_{I_j}}{\mathrm{V}_{R_j}},\ \mathcal{V}_j = \sqrt{\mathrm{V}_{R_j}^2 + \mathrm{V}_{I_j}^2}. \tag{1.3}$$

The following differential expressions will be useful in our development:

$$\left\{ \begin{array}{rclcrcl} \frac{\partial \theta_l}{\partial \mathrm{V}_{R_l}} & = & -\frac{\mathrm{V}_{I_l}}{\mathrm{V}_{R_l}^2} \frac{1}{1+\frac{\mathrm{V}_{I_l}^2}{\mathrm{V}_{R_l}^2}} = -\frac{\mathrm{V}_{I_l}}{\mathcal{V}_l^2}; & & \frac{\partial \mathcal{V}_l}{\partial \mathrm{V}_{R_l}} & = & \frac{\mathrm{V}_{R_l}}{\mathcal{V}_l}; \\ \frac{\partial \theta_l}{\partial \mathrm{V}_{I_l}} & = & \frac{1}{\mathrm{V}_{R_l}} \frac{1}{1+\frac{\mathrm{V}_{I_l}^2}{\mathrm{V}_{R_l}^2}} = \frac{\mathrm{V}_{R_l}}{\mathcal{V}_l^2}; & & \frac{\partial \mathcal{V}_l}{\partial \mathrm{V}_{I_l}} & = & \frac{\mathrm{V}_{I_l}}{\mathcal{V}_l}. \end{array} \right. \tag{1.4}$$

Some devices are typically described in function of active and reactive powers. The respective definitions and basic relationships are given next.

$$\left\{ \begin{array}{rclcrcl} P_j^d & := & Re(\tilde{V}_j \tilde{I}_j^{d*}) & = & \mathrm{V}_{R_j}\mathrm{I}_{R_j}^d + \mathrm{V}_{I_j}\mathrm{I}_{I_j}^d & = & \mathrm{V}_j^\top \mathrm{I}_j^d, \\ Q_j^d & := & Im(\tilde{V}_j \tilde{I}_j^{d*}) & = & -\mathrm{V}_{R_j}\mathrm{I}_{I_j}^d + \mathrm{V}_{I_j}\mathrm{I}_{R_j}^d & = & \mathrm{V}_j^\top J \mathrm{I}_j^d, \end{array} \right. \tag{1.5}$$

where we introduced the auxiliary matrix $J \in \mathbb{R}^{2\times 2}$

$$J := \begin{bmatrix} 0 & -1 \\ 1 & 0 \end{bmatrix},\ J^{-1} = J^\top = -J. \tag{1.6}$$

Algebraic manipulations of equations (1.5) yields

$$\mathrm{V}_j = \frac{1}{(\mathcal{I}_j^d)^2} \begin{bmatrix} P_j^d & -Q_j^d \\ Q_j^d & P_j^d \end{bmatrix} \mathrm{I}_j^d;\quad \mathrm{I}_j^d = \frac{1}{\mathcal{V}_j^2} \begin{bmatrix} P_j^d & Q_j^d \\ -Q_j^d & P_j^d \end{bmatrix} \mathrm{V}_j. \tag{1.7}$$

We will use

$$\Sigma_i^M : (\mathrm{I}_i^M, \mathrm{V}_i; E_{fd_i}, I_{fd_i}),\quad \Sigma_l^L : (\mathrm{I}_l^L, \mathrm{V}_l),$$

to denote the subsystems associated to the synchronous machines and loads, with their respective port variables. These subsystems will, in their turn, be coupled by the power network that interconnects all buses through transmission lines. The port (E_{fd_i}, I_{fd_i}) in the synchronous machine model is the one associated to the excitation circuit.

1.1 Bus Equations

From Kirchhoff's current law we have that the sum of all currents entering a bus must be zero. Consequently,

$$0 = -\mathrm{I}_j^N - \mathrm{I}_j^M - \mathrm{I}_j^L + \mathrm{I}_j^E\ \forall j \in \mathbb{B}. \tag{1.8}$$

Notice that, at a given bus j, some terms can vanish: i.e. $\mathrm{I}_j^M = 0\ \forall j \notin \mathbb{M}$. Analogously $\mathrm{I}_j^E = 0$ for all buses where the interconnection with other systems does not occur. Equation (1.8) establishes the electrical interconnection of loads, machines, network and external injections at each bus. Trivially, we can write equation (1.8) as

$$\Sigma_j^B : \ 0 = -J\mathrm{I}_j^N - J\mathrm{I}_j^M - J\mathrm{I}_j^L + J\mathrm{I}_j^E \ \forall j \in \mathbb{B}. \tag{1.9}$$

1.2 Static Loads

Loads are described by the standard ZIP model (Kundur, 1994) that represents the contribution of each type of load (constant impedance, current or power) to the active and reactive powers through the coefficients $p_r \geq 0, q_r \geq 0, r = 1..3$:

$$\left\{ \begin{array}{rcl} P_l^L & = & P^\star[p_1(\frac{\mathcal{V}_l}{\mathcal{V}_l^\star})^2 + p_2\frac{\mathcal{V}_l}{\mathcal{V}_l^\star} + p_3], \\ Q_l^L & = & Q^\star[q_1(\frac{\mathcal{V}_l}{\mathcal{V}_l^\star})^2 + q_2\frac{\mathcal{V}_l}{\mathcal{V}_l^\star} + q_3], \end{array} \right. \tag{1.10}$$

The equilibrium values, denoted with the super-index $\star$, imply

$$\sum_r p_r = 1; \sum_r q_r = 1.$$

See Appendix D for a more general model and further discussion.

Fact 1. *The load model (*1.10*) defines an operator $\Sigma_l^L : (\mathrm{I}_l^L, \mathrm{V}_l)$ described by the (memory–less) PCH system*

$$0 = -\nabla_{\mathrm{V}_l} S_l^L(\mathrm{V}_l) + J\mathrm{I}_l^L - \Psi_l^L(\mathrm{V}_l) \tag{1.11}$$

with storage function[2] *$S_l^L : \mathbb{R}^2 \to \mathbb{R}$,*

$$S_l^L(\mathrm{V}_l) \triangleq P^\star p_3\theta_l + Q^\star[\frac{q_1}{2}(\frac{\mathcal{V}_l}{\mathcal{V}_l^\star})^2 + q_2\frac{\mathcal{V}_l}{\mathcal{V}_l^\star} + q_3\ln(\mathcal{V}_l)], \tag{1.12}$$

where

$$\Psi_l^L(\mathrm{V}_l) \triangleq \frac{P^\star}{\mathcal{V}_l^{\star 2}}[p_1 + p_2\frac{\mathcal{V}_l^\star}{\mathcal{V}_l}]J\mathrm{V}_l.$$

Proof: The proof is immediate from the computation of the gradient of the function S_l^L. By invoking expressions (1.12), (1.5), (1.4) and model (1.10) we have:

$$\nabla_{\mathrm{V}_l} S_l^L(\mathrm{V}_l) = \left[\begin{array}{c} \frac{\partial S_l^L(\mathrm{V}_l)}{\partial \mathrm{V}_{R_l}} \\ \frac{\partial S_l^L(\mathrm{V}_l)}{\partial \mathrm{V}_{I_l}} \end{array} \right] = \left[\begin{array}{c} P^\star p_3\frac{\partial \theta_l}{\partial \mathrm{V}_{R_l}} + Q^\star[q_1(\frac{\mathcal{V}_l}{\mathcal{V}_l^{\star 2}}) + \frac{q_2}{\mathcal{V}_l^\star} + \frac{q_3}{\mathcal{V}_l}]\frac{\partial \mathcal{V}_l}{\partial \mathrm{V}_{R_l}} \\ P^\star p_3\frac{\partial \theta_l}{\partial \mathrm{V}_{I_l}} + Q^\star[q_1(\frac{\mathcal{V}_l}{\mathcal{V}_l^{\star 2}}) + \frac{q_2}{\mathcal{V}_l^\star} + \frac{q_3}{\mathcal{V}_l}]\frac{\partial \mathcal{V}_l}{\partial \mathrm{V}_{I_l}} \end{array} \right] =$$

[2] *The use of the name "storage function" will be justified in the Chapter* 2 *where $S^L(\cdot)$ will be used to establish the cyclo–dissipativity of Σ^L. See also Remark* 1.

$$= \frac{1}{\mathcal{V}_l^2} \begin{bmatrix} -P^\star p_3 \mathrm{V}_{I_l} + Q_l^L \mathrm{V}_{R_l} \\ P^\star p_3 \mathrm{V}_{R_l} + Q_l^L \mathrm{V}_{I_l} \end{bmatrix} = \frac{1}{\mathcal{V}_l^2} \begin{bmatrix} Q_l^L & -P^\star p_3 \\ P^\star p_3 & Q_l^L \end{bmatrix} \mathrm{V}_l =$$

$$= \frac{1}{\mathcal{V}_l^2} \begin{bmatrix} Q_l^L & -P_l^L + P^\star [p_1 (\frac{\mathcal{V}_l}{\mathcal{V}_l^\star})^2 + p_2 \frac{\mathcal{V}_l}{\mathcal{V}_l^\star}] \\ P_l^L - P^\star [p_1 (\frac{\mathcal{V}_l}{\mathcal{V}_l^\star})^2 + p_2 \frac{\mathcal{V}_l}{\mathcal{V}_l^\star}] & Q_l^L \end{bmatrix} \mathrm{V}_l =$$

$$= \frac{1}{\mathcal{V}_l^2} \begin{bmatrix} Q_l^L & -P_l^L \\ P_l^L & Q_l^L \end{bmatrix} \mathrm{V}_l + \frac{P^\star}{\mathcal{V}_l^2} [p_1 (\frac{\mathcal{V}_l}{\mathcal{V}_l^\star})^2 + p_2 \frac{\mathcal{V}_l}{\mathcal{V}_l^\star}] \begin{bmatrix} \mathrm{V}_{I_l} \\ -V_{R_l} \end{bmatrix}.$$

By recalling expressions (1.6) and (1.7), we get

$$\nabla_{\mathrm{V}_l} S_l^L(\mathrm{V}_l) = J\mathrm{I}_l^L - \frac{P^\star}{\mathcal{V}_l^2} [p_1 (\frac{\mathcal{V}_l}{\mathcal{V}_l^\star})^2 + p_2 \frac{\mathcal{V}_l}{\mathcal{V}_l^\star}] J\mathrm{V}_l,$$

which completes the proof along the definition of function Ψ_l^L. □□□

Remark 1. Denoting the algebraic model (1.11), or the DAE models to be introduced below, as " PCH systems" is done with some abuse of notation. Indeed, the formal definition of PCH systems given, e.g. in Subsection 4.2 of (Van der Schaft, 2000) implies other considerations that are not met in our case. We instead refer to the more abstract notion of "generalized energy" introduced by (Willems, 1972) that is captured by the storage function S^L.

Remark 2. As will become clear below, the term $\Psi_l^L(\mathrm{V}_l)$ introduces sign–indefinite terms in the derivative of the storage function, hampering the establishment of the cyclo–dissipativity of the subsystem Σ_l^L. Notice that Ψ_l^L vanishes if the active power is supposed constant, i.e. $p_1 = p_2 = 0$—an assumption that is *necessary* for the derivation of energy functions, (Tsolas et al., 1985).

1.3 Synchronous machine models

The synchronous machines are usually modeled in stability studies with different degrees of complexity. Second and third order models are the common choice in the energy function literature. Fifth and sixth order models are the common practice in time simulations for transient stability studies, (Kundur, 1994). We first consider a third order model that represents the rotor dynamics and a simple model of the flux decay, (Varaiya et al., 1985). These models will be associated to the index set $\mathbb{M}_3 \subset \mathbb{M}$. Later we will consider detailed sixth order models, labeled with indices in $\mathbb{M}_6 \subset \mathbb{M}, \mathbb{M}_3 \cup \mathbb{M}_6 = \mathbb{M}$.

1.3.1 Third order model

Consider the following model, equations (3.6) in (Varaiya et al., 1985):

$$\left\{\begin{array}{rcl} \dot{\delta}_i & = & \omega_i, \\ M_i\dot{\omega}_i & = & P_{m_i} - D_i\omega_i - P_i^M, \\ \tau_i\dot{E}_i & = & -\frac{x_{d_i}}{x'_{d_i}}E_i + \frac{x_{d_i}-x'_{d_i}}{x'_{d_i}}\mathcal{V}_i\cos(\delta_i-\theta_i) + E_{fd_i}, \\ P_i^M & = & -\frac{1}{x'_{d_i}}E_i\mathcal{V}_i\sin(\delta_i-\theta_i) - \frac{x'_{d_i}-x_{q_i}}{2x_{q_i}x'_{d_i}}\mathcal{V}_i^2\sin(2(\delta_i-\theta_i)), \\ Q_i^M & = & \frac{x'_{d_i}+x_{q_i}}{2x_{q_i}x'_{d_i}}\mathcal{V}_i^2 - \frac{1}{x'_{d_i}}E_i\mathcal{V}_i\cos(\delta_i-\theta_i) - \frac{x'_{d_i}-x_{q_i}}{2x_{q_i}x'_{d_i}}\mathcal{V}_i^2\cos(2(\delta_i-\theta_i)), \end{array}\right. \tag{1.13}$$

where the *state variables*

$$X_i := \left[\begin{array}{c} \delta_i \\ \omega_i \\ E_i \end{array}\right] \tag{1.14}$$

denote the rotor angle, the rotor speed and the quadrature axis internal e.m.f., respectively, and E_{fd_i} is the field voltage. The interaction of this model with its environment is given through the active and reactive powers P_i^M, Q_i^M and the phasor of terminal voltage in polar coordinates $\theta_i, \mathcal{V}_i$. The parameters M_i, P_{m_i},D_i, x_{d_i}, x'_{d_i}, x_{q_i} are denoted as in (Varaiya et al., 1985), and their detailed description may be found in any basic power systems textbook (Kundur, 1994; Anderson and Fouad, 1993). Following standard convention, we will make the physically reasonable assumptions $D_i > 0,\ x_{d_i} - x'_{d_i} > 0$.

For convenience, we will separate the field voltage in two terms,

$$E_{fd_i} = E^\star_{fd_i} + e_{fd_i}, \tag{1.15}$$

the first one is constant and fixes the equilibrium value, while the second one is the field voltage deviation. Also, to simplify notation, we define the constants

$$Y_{2i} \triangleq \frac{x'_{d_i}-x_{q_i}}{2x_{q_i}x'_{d_i}},\ Y_{E_i} \triangleq \frac{x_{d_i}}{x'_{d_i}(x_{d_i}-x'_{d_i})},\ Y_{F_i} \triangleq \frac{1}{x_{d_i}-x'_{d_i}},\ Y_{Vi} \triangleq \frac{x'_{d_i}+x_{q_i}}{2x_{q_i}x'_{d_i}},$$

and the matrices

$$K_i \triangleq \left[\begin{array}{ccc} 0 & \frac{1}{M_i} & 0 \\ -\frac{1}{M_i} & 0 & 0 \\ 0 & 0 & 0 \end{array}\right],\ R_i \triangleq \left[\begin{array}{ccc} 0 & 0 & 0 \\ 0 & \frac{D_i}{M_i^2} & 0 \\ 0 & 0 & \frac{1}{\tau_i Y_{F_i}} \end{array}\right],\ B_{fd_i} \triangleq \left[\begin{array}{c} 0 \\ 0 \\ \frac{1}{\tau_i} \end{array}\right]. \tag{1.16}$$

Notice that the definition of K_i, R_i implies the properties

$$K_i = -K_i^\top,\ R_i = R_i^\top \geq 0,\ det(K_i - R_i) \neq 0. \tag{1.17}$$

Recalling the definitions (1.1), (1.2) we have the following simple fact, whose proof is established by direct substitution. The computations are similar to the introduced in the preceding section and are omitted.

Fact 2. *The synchronous machine model (*1.13*) defines an operator* $\Sigma_i^{M_3} : (\mathrm{I}_i^M, \mathrm{V}_i)$ *described by the PCH system*

$$\left\{ \begin{array}{rcl} \dot{X}_i & = & (K_i - R_i)\nabla_{X_i} S_i^{M_3}(X_i, \mathrm{V}_i) + B_{fd_i} e_{fd_i} \\ 0 & = & -\nabla_{\mathrm{V}_i} S_i^{M_3}(X_i, \mathrm{V}_i) + J\mathrm{I}_i^M \end{array} \right. \tag{1.18}$$

with storage function $S_i^{M_3} : \mathbb{R}^3 \times \mathbb{R}^2 \to \mathbb{R}$,

$$\begin{array}{l} S_i^{M_3}(X_i, \mathrm{V}_i) \triangleq \frac{1}{2} M_i \omega_i^2 - P_{mi}\delta_i - \frac{E_i \mathcal{V}_i}{x'_{d_i}} \cos(\theta_i - \delta_i) - \\ -\frac{Y_{2i}}{2}\mathcal{V}_i^2 \cos 2(\theta_i - \delta_i) + \frac{Y_{E_i}}{2} E_i^2 - Y_{F_i} E_{F_i}^\star E_i + \frac{Y_{Vi}}{2}\mathcal{V}_i^2, \end{array} \tag{1.19}$$

with $\theta_i, \mathcal{V}_i$ *given by equation (*1.3*).*

We will consider now a complete, detailed model for the synchronous machine. It includes three damping circuits at the rotor, salient poles, and the complete dynamics at the stator.

1.3.2 Sixth order model

In this subsection we will introduce two detailed models for the synchronous machine. The first one, equation (1.20) below, has order eight and it is closely related with the machine's physics. On the other hand, it involves some fast stator dynamics that is usually neglected in stability studies. This is the reason of the interest on the sixth order model, to be introduced later in this subsection, that will be the one employed in later chapters.

The standard eighth order model, equations 3.120 to 3.134 in (Kundur, 1994), is given by:

$$\left\{ \begin{array}{rcl} E_d & = & \frac{d}{dt}\Phi_d - \Phi_q \omega_r - R_a I_d, \\ E_q & = & \frac{d}{dt}\Phi_q + \Phi_d \omega_r - R_a I_q, \\ E_{fd} & = & \frac{d}{dt}\Phi_{fd} + R_{fd} I_{fd}, \\ 0 & = & \frac{d}{dt}\Phi_{1d} + R_{1d} I_{1d}, \\ 0 & = & \frac{d}{dt}\Phi_{1q} + R_{1q} I_{1q}, \\ 0 & = & \frac{d}{dt}\Phi_{2q} + R_{2q} I_{2q}, \\ \frac{d}{dt}\delta & = & \Omega_0(\omega_r - 1), \\ h\frac{d}{dt}\omega_r & = & T_m - d(\omega_r - 1) - T_e, \\ T_e & = & \Phi_d I_q - \Phi_q I_d. \end{array} \right. \tag{1.20}$$

The subindices d, q denote, as usual, the components of the different variables along the direct and quadrature axes. Φ_d, Φ_q represent the components of the stator flux linkage. $\Phi_{1d}, \Phi_{1q}, \Phi_{2q}, \Phi_{fd}$ are the respective rotor flux linkages associated to the damping and field circuits. The currents $I_d, I_q, I_{fd}, I_{1d}, I_{1q}, I_{2q}$ obey to the same notation. We will assume, by physical reasons, that the damping coefficient $d \geq 0$, the resistances $R_k > 0$, and the inertia $h > 0$.

The electrical variables at the stator in the $d-q$ frame (see equation 13.31 in (Kundur, 1994)) are:

$$\begin{cases} \tilde{E}_s & := & E_d + jE_q & = & je^{-j\delta}\tilde{V}, \\ \tilde{I}_s & := & I_d + jI_q & = & -je^{-j\delta}\tilde{I}^M, \end{cases} \tag{1.21}$$

where $\tilde{V}$ is the terminal voltage phasor, and δ is the rotor position both referred to the synchronous reference. The negative signal at $\tilde{I}_s$ comes from the convention used to define this stator current as positive when salient, opposite to our convention.[3]. Equations (1.21) can be written

$$\mathrm{E}_s := \begin{bmatrix} E_d \\ E_q \end{bmatrix} = JU_\delta \mathrm{V}, \;\; \mathrm{I}_s = \begin{bmatrix} I_d \\ I_q \end{bmatrix} = -JU_\delta \mathrm{I}^M \tag{1.22}$$

with $U_\delta \in \mathbb{R}^{2\times 2}$ the matrix associated to the clockwise rotation[4] in the plane:

$$U_\delta = \begin{bmatrix} \cos\delta & \sin\delta \\ -\sin\delta & \cos\delta \end{bmatrix},$$

that satisfies

$$\begin{cases} U_\delta^{-1} = U_\delta^\top = U_{-\delta}, \\ \frac{dU_\delta}{d\delta} = -JU_\delta = -U_\delta J. \end{cases} \tag{1.23}$$

The properties of U_δ and J, equations (1.23) and (1.6), will be used so often in this section that no explicit reference to them will be done.

The entering complex power C^M results:

$$C^M := \tilde{E}_s(-\tilde{I}_s)^* = -(E_d + jE_q)(I_d - jI_q) = -\mathrm{E}_s^\top \mathrm{I}_s + j\mathrm{I}_s^\top J\mathrm{E}_s. \tag{1.24}$$

The model is completed with the relationship between the flux linkages and the respective currents, but some notation will be introduced before to get

[3]The subindex identifying the machine bus is omitted to improve readability

[4]This matrix also appears in Chapter 4 where is defined in a slightly different way.

a compact description. We introduce the sub-indices s and r to respectively denote the stator and rotor variables:

$$\Phi_s := \begin{bmatrix} \Phi_d \\ \Phi_q \end{bmatrix}; \quad \Phi_r := \begin{bmatrix} \Phi_{1d} \\ \Phi_{1q} \\ \Phi_{2q} \end{bmatrix}, \; I_r := \begin{bmatrix} I_{1d} \\ I_{1q} \\ I_{2q} \end{bmatrix}. \tag{1.25}$$

The relationship between fluxes and currents is

$$\Phi := \begin{bmatrix} \Phi_s \\ \Phi_{fd} \\ \Phi_r \end{bmatrix} = L \begin{bmatrix} -I_s \\ I_{fd} \\ I_r \end{bmatrix} = LI, \tag{1.26}$$

with

$$L = \begin{bmatrix} L_{ad} + L_l & 0 & L_{ad} & L_{ad} & 0 & 0 \\ 0 & L_{aq} + L_l & 0 & 0 & L_{aq} & L_{aq} \\ L_{ad} & 0 & L_{ffd} & L_{f1d} & 0 & 0 \\ L_{ad} & 0 & L_{f1d} & L_{11d} & 0 & 0 \\ 0 & L_{aq} & 0 & 0 & L_{11q} & L_{aq} \\ 0 & L_{aq} & 0 & 0 & L_{aq} & L_{22q} \end{bmatrix}.$$

The stator equations in (1.20) can be now written as:

$$\mathrm{E}_s = \frac{d}{dt}\Phi_s + J\Phi_s\omega_r - R_a\mathrm{I}_s \tag{1.27}$$

We shall state the assumptions we need to proceed with our development.

Assumption 1. *The terms $\frac{d}{dt}\Phi$ and R_aI_s in equation (*1.27*) are neglected. The term $J\Phi_s\omega_r$ is approximated by $J\Phi_s$. So, equation (*1.27*) will be substituted by*

$$E_s = J\Phi_s. \tag{1.28}$$

Notice that the terms $\frac{d}{dt}\Phi$ are typically neglected all along the power system since the electrical network is studied with the help of phasors and a quasi-stationary hypotheses. By neglecting the terms $\frac{d}{dt}\Phi$ in the stator equations, we are treating the machine's stator as the remainder of the network. Assumption 1 is fairly standard in stability studies, see (Kundur, 1994). The neglect of the term R_aI_s is justified as a simplifying assumption given its little significance in the transient behavior. Its effect on the dissipativity of the machine model is quantified numerically in Section 2.2.1.

The electrical torque T_e, from the respective equation in (1.20) and equations (1.28) and (1.24), results

$$T_e = \Phi_d I_q - \Phi_q I_d = \begin{bmatrix} I_d \\ I_q \end{bmatrix}^\top J \begin{bmatrix} \Phi_d \\ \Phi_q \end{bmatrix} = \mathrm{I}_s^\top J \Phi_s = I_s^\top \mathrm{E}_s = -P^M. \tag{1.29}$$

With these simplification, we get the sixth order model

$$\begin{cases} \frac{d}{dt}\delta &= \Omega_0(\omega_r - 1), \\ h\frac{d}{dt}\omega_r &= T_m - d(\omega_r - 1) + P^M, \\ \frac{d}{dt}\Phi_{fd} &= E_{fd} - R_{fd} I_{fd}, \\ \frac{d}{dt}\Phi_r &= -R_r I_r, \\ E_s &= J\Phi_s, \\ \Phi &= LI, \end{cases} \tag{1.30}$$

which is completed with equation (1.22), and definitions (1.25), (1.26). We denote $X := [\delta\ \omega_r\ \Phi_{fd}\ \Phi_r^\top]^\top \in R^6$ the state vector.

We assume that the mechanical torque T_m is constant. Let us express again the excitation voltage E_{fd} as the sum of a constant term $E_{fd}^\star$ which sets the operating point, and the control action e_{fd}: $E_{fd} = E_{fd}^\star + e_{fd}$. Analogously, denote $I_{fd}^\star$ the field current at the equilibrium ($I_{fd}^\star = \frac{E_{fd}^\star}{R_{fd}}$) and the incremental field current $i_{fd} := I_{fd} - I_{fd}^\star$.

Consider the function $S^{M_6} : R^6 \times R^2 \to R$:

$$S^{M_6}(X, \mathrm{V}) := \frac{1}{2}\Omega_0 h(\omega_r - 1)^2 + \frac{1}{2}\Phi^\top L^{-1}\Phi - T_m\delta - I_{fd}^\star \Phi_{fd}. \tag{1.31}$$

We state the PCH model for (1.30), that is demonstrated in Appendix B:

Fact 3. *The synchronous machine model (*1.30*) defines an operator* $\Sigma_i^{M_6} : (\mathrm{I}_i^M, \mathrm{V}_i; e_{fd_i}, i_{fd_i})$ *described by the PCH system*

$$\Sigma_i^{M_6} : (\mathrm{I}_i^M, \mathrm{V}_i; e_{fd_i}, i_{fd_i}) \begin{cases} \dot{X}_i &= (K_i - R_i)\nabla_X S_i^{M_6}(X_i, \mathrm{V}_i) + B_{fd} e_{fd_i} \\ 0 &= -\nabla_{\mathrm{V}_i} S_i^{M_6}(X_i, \mathrm{V}_i) + J\mathrm{I}_i^M \end{cases} \tag{1.32}$$

with storage function $S_i^{M_6}$ *given by (*1.31*) with*

$$K_i = -K_i^\top = \frac{1}{h_i}\left[\begin{array}{cc|c} 0 & 1 & \\ -1 & 0 & 0_{2\times 4} \\ \hline \multicolumn{2}{c|}{0_{4\times 2}} & 0_{4\times 4} \end{array}\right] \tag{1.33}$$

$$R_i = \begin{bmatrix} 0 & 0 & 0 & 0 & 0 & 0 \\ 0 & \frac{d_i}{h_i^2\Omega_0} & 0 & 0 & 0 & 0 \\ 0 & 0 & R_{fdi} & 0 & 0 & 0 \\ 0 & 0 & 0 & R_{1di} & 0 & 0 \\ 0 & 0 & 0 & 0 & R_{1qi} & 0 \\ 0 & 0 & 0 & 0 & 0 & R_{2qi} \end{bmatrix} \geq 0, \tag{1.34}$$

$$B_{fd} = \left[\begin{array}{cccccc} 0 & 0 & 1 & 0 & 0 & 0 \end{array} \right]^\top .$$

Other models can also be considered, e.g. the classical second order model. This has no theoretical difficulty since it can be seen as an special case of one of the models above mentioned. In the sequel we will use the symbols Σ_i^M, S_i^M to refer generically to any of the models studied.

1.4 Network

The network is composed by m generic nodes labeled $j \in \mathbb{B}$ interconnected by series devices as transformers, reactors or transmission lines modeled as classical circuits of lumped parameters. Each node feeds a shunt impedance associated to it. Constant impedance loads can also be incorporated to the network.

The classical power system literature usually models the electrical magnitudes all along the network with the help of phasors collected in complex vectors of dimension m. The phasorial description is of course valid for steady state and its use can be extended to quasi-statical trajectories. The use of conventional phasors to study the transient behavior in power systems, our choice, is nevertheless justified by the engineering practice and the difficulties to simulate the full response of complex and very high order dynamic systems, (Kundur, 1994; Anderson and Fouad, 1993). Of course, more detailed models exist: models for electromagnetic simulation (see e.g. (Dommel, 1969)), and simulation based on dynamic phasors (Sanders et al., 1991; Mattavelli et al., 1997; Stankovic and Aydin, 2000).

Denote $\tilde{\mathbf{I}}^{\mathbf{N}}, \tilde{\mathbf{V}} \in \mathbb{C}^m$ the vectors of current and voltage phasors

$$\tilde{\mathbf{I}}^{\mathbf{N}} := col_{j\in\mathbb{B}}(\tilde{I}_j^N);\ \tilde{\mathbf{V}} := col_{j\in\mathbb{B}}(\tilde{V}_j).$$

With these definitions, the network is modeled with the help of the *node admittance matrix* $\tilde{Y} \in \mathbb{C}^{m\times m}$ (Anderson and Fouad, 1993; Kundur, 1994):

$$\tilde{\mathbf{I}}^{\mathbf{N}} = \tilde{Y}\tilde{\mathbf{V}}. \tag{1.35}$$

We have been treating the phasorial variables through their Cartesian description. So, we will write $\tilde{Y} = Y_R + jY_I$ and describe the network through the

vectors $\mathbf{I^N}, \mathbf{V} \in \mathbb{R}^{2m}$:

$$\begin{array}{rcl} \mathbf{I}^N := col_{j\in\mathbb{B}}(I_j^N) & = & col_{j\in\mathbb{B}}(\left[\begin{array}{c} I_{R_j}^N \\ I_{I_j}^N \end{array}\right]); \\ \mathbf{V} := col_{j\in\mathbb{B}}(V_j) & = & col_{j\in\mathbb{B}}(\left[\begin{array}{c} V_{R_j} \\ V_{I_j} \end{array}\right]). \end{array} \tag{1.36}$$

Let us denote $\mathbf{I}_R^N, \mathbf{I}_I^N \in \mathbb{R}^m$ the respective vectors of real and imaginary parts

$$\mathbf{I}_R^N := col_{j\in\mathbb{B}}(I_{R_j}^N);\ \mathbf{I}_I^N := col_{j\in\mathbb{B}}(I_{I_j^N}),$$

and take the analogous definitions for voltages $\mathbf{V}_R, \mathbf{V}_I \in \mathbb{R}^m$. Define the matrix $\mathcal{U} \in \mathbb{R}^{2m\times 2m}$ such that

$$\mathbf{V} = \mathcal{U}\left[\begin{array}{c} \mathbf{V}_R \\ \mathbf{V}_I \end{array}\right]; \mathbf{I}^N = \mathcal{U}\left[\begin{array}{c} \mathbf{I}_R^N \\ \mathbf{I}_I^N \end{array}\right]. \tag{1.37}$$

$\mathcal{U}$ is simply a permutation of rows of the identity matrix. Thus, it is a unitary matrix and satisfies $\mathcal{U}^{-1} = \mathcal{U}^\top$. So, the inverse relations of equation (1.37) are

$$\left[\begin{array}{c} \mathbf{V}_R \\ \mathbf{V}_I \end{array}\right] = \mathcal{U}^\top\mathbf{V}; \left[\begin{array}{c} \mathbf{I}_R^N \\ \mathbf{I}_I^N \end{array}\right] = \mathcal{U}^\top\mathbf{I}^N. \tag{1.38}$$

Also define $\mathbf{J} \in \mathbb{R}^{2m\times 2m}$ as

$$\mathbf{J} := diag_{j\in\mathbb{B}}(J). \tag{1.39}$$

Fact 4. *The power network model (*1.35*) defines an operator* $\Sigma^N : (\mathbf{I}^N, \mathbf{V})$ *described by a PCH system*

$$\Sigma^N : (\mathbf{I}^N, \mathbf{V}) \ \left\{ \begin{array}{rcl} 0 & = & -\nabla_{\mathbf{V}} S^N(\mathbf{V}) + \mathbf{J}\mathbf{I}^N - \Psi_N(\mathbf{V}), \end{array} \right. \tag{1.40}$$

with storage function $S^N : \mathbb{R}^{2m} \to \mathbb{R}$,

$$S^N(\mathbf{V}) \triangleq -\frac{1}{2}\mathbf{V}^\top\mathcal{Y}_I\mathbf{V}, \tag{1.41}$$

function $\Psi^N : \mathbb{R}^{2m} \to \mathbb{R}^{2m}$

$$\Psi^N(\mathbf{V}) \triangleq \mathcal{Y}_R\mathbf{V},$$

and the matrices $\mathcal{Y}_I, \mathcal{Y}_R \in \mathbb{R}^{2m\times 2m}$*:*

$$\mathcal{Y}_I := \mathcal{U}\left[\begin{array}{cc} Y_I & 0 \\ 0 & Y_I \end{array}\right]\mathcal{U}^\top;\ \mathcal{Y}_R := \mathcal{U}\left[\begin{array}{cc} 0 & -Y_R \\ Y_R & 0 \end{array}\right]\mathcal{U}^\top. \tag{1.42}$$

Proof: With the introduction of the respective real and imaginary parts $Y_R, Y_I \in \mathbb{R}^{m\times m}$ of the admittance matrix, equation (1.35) can be written

$$(\mathbf{I}_R^N + j\mathbf{I}_I^N) = (Y_R + jY_I)(\mathbf{V}_R + j\mathbf{V}_I).$$

Thus

$$j(\mathbf{I}_R^N + j\mathbf{I}_I^N) = j(Y_R + jY_I)(\mathbf{V}_R + j\mathbf{V}_I)) = -Y_I\mathbf{V}_R - Y_R\mathbf{V}_I + j(Y_R\mathbf{V}_R - Y_I\mathbf{V}_I),$$

or equivalently

$$\begin{bmatrix} -\mathbf{I}_I^N \\ \mathbf{I}_R^N \end{bmatrix} = \begin{bmatrix} -Y_R\mathbf{V}_I \\ Y_R\mathbf{V}_R \end{bmatrix} + \begin{bmatrix} -Y_I\mathbf{V}_R \\ -Y_I\mathbf{V}_I \end{bmatrix} =$$

$$= \begin{bmatrix} 0 & -Y_R \\ Y_R & 0 \end{bmatrix} \begin{bmatrix} \mathbf{V}_R \\ \mathbf{V}_I \end{bmatrix} - \begin{bmatrix} Y_I & 0 \\ 0 & Y_I \end{bmatrix} \begin{bmatrix} \mathbf{V}_R \\ \mathbf{V}_I \end{bmatrix}. \tag{1.43}$$

Hence, by recalling the definitions of $\mathbf{J}$ and $\mathbf{I}^N$:

$$\mathbf{JI}^N = diag_{j\in\mathbb{B}}(J)col_{j\in\mathbb{B}}(I_j^N) = col_{j\in\mathbb{B}}(JI_j^N) = col_{j\in\mathbb{B}}(\begin{bmatrix} -\mathrm{I}_{I_j}^N \\ \mathrm{I}_{R_j}^N \end{bmatrix}) = \mathcal{U}\begin{bmatrix} -\mathbf{I}_I^N \\ \mathbf{I}_R^N \end{bmatrix}.$$

By invoking equations (1.43) and (1.38), we have

$$\mathbf{JI}^N = \mathcal{U}\begin{bmatrix} 0 & -Y_R \\ Y_R & 0 \end{bmatrix}\mathcal{U}^\top\mathbf{V} - \mathcal{U}\begin{bmatrix} Y_I & 0 \\ 0 & Y_I \end{bmatrix}\mathcal{U}^\top\mathbf{V}.$$

Notice that the symmetry of matrix $\tilde{Y}$, see (Kundur, 1994), implies the symmetry of the matrices Y_R, Y_I. So, the definitions (1.42) imply

$$\mathcal{Y}_I^\top = \mathcal{Y}_I,\ \mathcal{Y}_R^\top = -\mathcal{Y}_R.$$

Hence

$$\mathbf{JI}^N = -\mathcal{Y}_I\mathbf{V} + \mathcal{Y}_R\mathbf{V} = \nabla_{\mathbf{V}}S^N(\mathbf{V}) + \Psi^N(\mathbf{V}),$$

which concludes the proof. □□□

Remark 3. The role of term Ψ^N in (1.40) is similar to Ψ^L in (1.11), commented in Remark 2 for the loads models. Notice that $\Psi^N(\mathbf{V}) = 0$ if and only if $Y_R = 0$, i.e., the network has no electrical losses nor resistive loads.

1.5 Power system model

We are now in position to use the external power injections to *model the interactions between adjacent subsystems*. The system interacts with its environment trough the pairs (I_e^E, V_e), i.e. the phasors at the frontier buses $e \in \mathbb{E}$. The *power system model* results from the models already introduced, equations (1.9), (1.11), (1.18), (1.32), (1.40), and some notational convention. The equations are repeated and reordered here to facilitate later references:

$$\begin{array}{rcll} \dot{X}_i & = & (K_i - R_i)\nabla_{X_i} S_i^M(X_i, \mathrm{V}_i) + B_{v_i} e_i, & \forall i \in \mathbb{M} \\ J\mathrm{I}_i^M & = & \nabla_{\mathrm{V}_i} S_i^M(X_i, \mathrm{V}_i), & \forall i \in \mathbb{M} \\ J\mathrm{I}_l^L & = & \nabla_{\mathrm{V}_l} S_l^L(\mathrm{V}_l) + \Psi_l^L(\mathrm{V}_l), & \forall l \in \mathbb{L} \\ \mathbf{J}\mathbf{I}^N & = & \nabla_{\mathbf{V}} S^N(\mathbf{V}) + \Psi_N(\mathbf{V}) & \\ 0 & = & -J\mathrm{I}_j^N - J\mathrm{I}_j^M - J\mathrm{I}_j^L + J\mathrm{I}_j^E, & \forall j \in \mathbb{B} \end{array} \tag{1.44}$$

Clearly, the currents $\mathrm{I}^M, \mathrm{I}^L, \mathbf{I}^N$ can be eliminated by direct substitution to get a more compact description. With that objective, denote n the dimension of the state space, define $X, \mathbf{e}_{fd}$ the state and control vector of the system, and name $\mathbf{I}^E, \mathbf{V}^E$ the electrical variables at the frontier buses:

$$\begin{array}{rcl} X: & = & \mathrm{col}_{i \in \mathbb{M}}(X_i), \\ \mathbf{e}_{fd} & = & col_{i \in \mathbb{M}}(e_{fd_i}) \\ \mathbf{V}^E & := & col_{e \in \mathbb{E}}(\mathrm{V}_e), \\ \mathbf{I}^E & := & col_{e \in \mathbb{E}}(\mathrm{I}_e^E). \end{array} \tag{1.45}$$

With these conventions and after the elimination of the internal currents, one can describe the equations (1.44) with the differential-algebraic (DAE) system

$$\left\{ \begin{array}{rcl} \dot{X} & = & f(X, \mathbf{V}, \mathbf{e}_{fd}) \\ 0 & = & g(X, \mathbf{V}, \mathbf{I}^E) \end{array} \right. \tag{1.46}$$

The functions $f : \mathbb{R}^n \times \mathbb{R}^{2m} \times \mathbb{R}^{m_M} \to \mathbb{R}^n$ and $g : \mathbb{R}^n \times \mathbb{R}^{2m} \times \mathbb{R}^{2m_E} \to \mathbb{R}^{2m}$ gather, respectively, the differential and algebraic equations. f and g will be supposed smooth enough to ensure, along with the assumptions stated below, the existence and uniqueness of the trajectories. We will suppose that:

Assumption 2. *There exists a set* $\mathcal{D} \in \mathbb{R}^n \times \mathbb{R}^{2m} \times \mathbb{R}^{2m_E}$ *satisfying*

$$\mathcal{D} \triangleq \{(X, \mathbf{V}, \mathbf{I}^E) | g(X, \mathbf{V}, \mathbf{I}^E) = 0 \text{ and } \nabla_{\mathbf{V}} g(X, \mathbf{V}, \mathbf{I}^E) \text{ is non singular}\},$$

*where the solutions of (*1.46*) are unique and well defined.*

Notice that, since the Jacobian of function g with respect to $\mathbf{V}$ is supposed to be non singular, it will be possible, at least locally, to solve $g(\cdot) = 0$ to get

$$\mathbf{V} = \mathbf{V}(X, \mathbf{I}^E),$$

see (Hill and Mareels, 1990). This fact makes possible the substitution of the so-called *link variables* in $f(\cdot)$ to get an ordinary differential system.

The second assumption we will need is the existence of an equilibrium point:

Assumption 3. *There exists an* open loop equilibrium *of the system, that is, a point* $(X^\star, \mathbf{V}^\star, \mathbf{I}^{E\star}) \in \mathcal{D}$ *where*

$$\begin{cases} 0 &= f(X^\star, \mathbf{V}^\star, 0) \\ 0 &= g(X^\star, \mathbf{V}^\star, \mathbf{I}^{E\star}). \end{cases} \tag{1.47}$$

We will work on the PCH models obtained in this chapter, to get a compact description of the overall system. We will begin by applying the operation $col_{j\in\mathbb{B}}(\cdot)$ to each term in the last equation in (1.44). Thus

$$col_{j\in\mathbb{B}}(-J\mathrm{I}_j^N) = -\mathbf{J}\mathbf{I}^N = -\nabla_{\mathbf{V}} S^N(\mathbf{V}) - \Psi_N(\mathbf{V}), \tag{1.48}$$

where the definitions (1.39), (1.36) and equation (1.44) were employed. Compute now

$$col_{j\in\mathbb{B}}(-J\mathrm{I}_j^M) = -\nabla_{\mathbf{V}}(\sum_{i\in\mathbb{M}} S_i^M(X_i, \mathrm{V}_i)), \tag{1.49}$$

and

$$col_{j\in\mathbb{B}}(-J\mathrm{I}_j^L) = -\nabla_{\mathbf{V}}(\sum_{l\in\mathbb{L}} S_l^L(\mathrm{V}_l)) - col_{j\in\mathbb{B}}\Psi_j^L(\mathrm{V}_j), \tag{1.50}$$

Compare the definitions of vectors $\mathbf{V}$ and $\mathbf{V}^E$ in equations (1.36) and (1.45). Clearly, the entries in $\mathbf{V}^E \in \mathbb{R}^{2m_E}$ are a subset of the entries in $\mathbf{V} \in \mathbb{R}^{2m}$. So, define the auxiliary matrix $\mathcal{T} \in \mathbb{R}^{2m_E \times 2m}$ such that

$$\mathbf{V}^E = \mathcal{T}\mathbf{V}. \tag{1.51}$$

Let us define the matrix $\mathbf{J}^E \in \mathbb{R}^{2m_E \times 2m_E}$ as

$$\mathbf{J}^E = diag_{\mathbb{E}}(J), \tag{1.52}$$

i.e., the block diagonal matrix whose diagonal blocks are all equal to J. Thus,

$$col_{e\in\mathbb{E}}(J\mathrm{I}_e^E) = \mathbf{J}^E\mathbf{I}^E, \;\; col_{j\in\mathbb{B}}(J\mathrm{I}_j^E) = \mathcal{T}^\top\mathbf{J}^E\mathbf{I}^E. \tag{1.53}$$

Consider now the last equation in (1.44) and substitute the vector associated to each term with the help of equations (1.48), (1.49), (1.50) and (1.53):

$$0 = -\nabla_{\mathbf{V}}(S^N(\mathbf{V}) + \sum_{i\in\mathbb{M}} S_i^M(X_i, \mathrm{V}_i) + \sum_{l\in\mathbb{L}} S_l^L(\mathrm{V}_l)) -$$

$$-\Psi_N(\mathbf{V}) - col_{j\in\mathbb{B}}\Psi_j^L(\mathrm{V}_j) + \mathcal{T}^\top \mathbf{J}^E \mathbf{I}^E. \tag{1.54}$$

The last equation suggest us to define the functions $S_0 : \mathbb{R}^n \times \mathbb{R}^{2m} \to \mathbb{R}$:

$$S_0(X, \mathbf{V}) := \sum_i S_i^M(X_i, \mathrm{V}_i) + \sum_l S_l^L(\mathrm{V}_l) + S^N(\mathbf{V}). \tag{1.55}$$

and $\Psi : \mathbb{R}^{2m} \to \mathbb{R}^{2m}$

$$\Psi(\mathbf{V}) := \Psi^N(\mathbf{V}) + col_{j\in\mathbb{B}}\Psi_j^L(\mathrm{V}_j).$$

Remark 4. *Notice that, when the synchronous machines are described with third (or second) order models, the function S_0 coincides, beyond minor details associated to the notation, with the classical energy function, see e.g. (Varaiya et al., 1985). The links of the work described in this thesis with the energy function theory are discussed in remark* 8 *in Section* 2.1.

It is important to underscore that $\Psi(\mathbf{V})$ is not a gradient vector field, that is, it cannot be expressed as the gradient of a scalar function. This is the main stumbling block for the generation of energy functions for non–ideal power systems models, a difficulty that has been widely documented in the power systems literature, see e.g. (Chiang, 1989). Equation (1.54) can now be written

$$0 = -\nabla_{\mathbf{V}} S_0(X, \mathbf{V}) - \Psi(\mathbf{V}) + \mathcal{T}^\top \mathbf{J}^E \mathbf{I}^E. \tag{1.56}$$

It is very convenient that a function candidate to be a storage function for the overall system be singular[5], ideally having a local minimum, at the equilibrium. Notice that S_0 does not qualify because of terms involving Ψ and $\mathbf{I}^E$ in equation (1.56). Therefore we will add some linear terms to S_0 in order to get null partial derivatives at the equilibrium: define the function $S : \mathbb{R}^n \times \mathbb{R}^{2m} \to \mathbb{R}$:

$$S(X, \mathbf{V}) := S_0(X, \mathbf{V}) + \mathbf{V}^\top \Psi(\mathbf{V}^\star) - \mathbf{V}^{E\top} \mathbf{J}^E \mathbf{I}^{E\star}, \tag{1.57}$$

with $\mathbf{V}^\star \in \mathbb{R}^{2m}, \mathbf{I}^{E\star} \in \mathbb{R}^{2m_E}$ the equilibrium value of the variables $\mathbf{V}, \mathbf{I}^E$.

Define also and the block–diagonal matrices

$$K := \mathrm{diag}_{i\in\mathbb{M}}\{K_i\}, R := \mathrm{diag}_{i\in\mathbb{M}}\{R_i\}, B_u := \mathrm{diag}_{i\in\mathbb{M}}\{B_{fd}\}, \tag{1.58}$$

[5] In the sense that its gradient vanishes.

Notice that, the definition of K and R and the properties of K_i, R_i, equations (1.17), (1.33), (1.34) imply

$$K = -K^\top,\ R = R^\top \geq 0,\ det(K - R) \neq 0. \tag{1.59}$$

This allows us to rewrite the overall system given by equation (1.44) as

$$\begin{cases} \dot{X} &= (K-R)\nabla_X S(X, \mathbf{V}) + B_u \mathbf{e}_{fd} \\ 0 &= -\nabla_{\mathbf{V}} S(X, \mathbf{V}) - \Psi(\mathbf{V}) + \Psi(\mathbf{V}^\star) + \mathcal{T}^\top \mathbf{J}^E (\mathbf{I}^E - \mathbf{I}^{E\star}). \end{cases} \tag{1.60}$$

Notice the presence of the "incremental term" $-\Psi(\mathbf{V})+\Psi(\mathbf{V}^\star)$ that, as we know, captures the effects of the loads with constant current and lossy network.

Notice that the function S has a singular point at the equilibrium, since

$$\begin{cases} 0 &= \nabla_X S(X^\star, \mathbf{V}^\star) \\ 0 &= \nabla_{\mathbf{V}} S(X^\star, \mathbf{V}^\star). \end{cases} \tag{1.61}$$

Chapter 2

Dynamic Properties

As indicated in the Introduction we adopt the dissipativity framework proposed in (Willems, 1972) and extended in (Hill and Moylan, 1980). The dissipativity implies a dynamical balance between the storage of a generalized energy and a power supply from the environment. This concept, with deep roots in Physics must nevertheless be tailored to the specific dynamics under study.

The electro-mechanical nature of the basic power system dynamics and the analysis based on phasors generate some surprises to any observer familiar with Circuit Theory and with Mechanics. When slow electro-mechanical transients are under study, the inductances can be interpreted as elements storing potential energy–no novelty here–but its role reminds more a spring than a magnetic device. The confusion can even be stronger with the role of the resistances on the AC network since these elements do not contribute to dissipate the electro-mechanical energy accumulated in a transient, due e.g. to a fault. The reader is referred to the classical literature on power systems energy function for a deep discussion, see e.g. (Pai, 1989; Tsolas et al., 1985; Varaiya et al., 1985).

On the other hand, the dissipativity based on conventional definitions of electrical energy and power is almost useless in the study of transient stability. The standard constant power static loads do not fit in this framework and the conventional energy does not know minima or singular points at the equilibria, see e.g. (Ortega et al., 1998).

Of course, we always can base our analysis on ordinary differential equations, control theory and a generic "signal processing" approach. This thesis, and in particular this chapter, is intended to show that the dissipativity concept, suitably adapted, can be useful to extract valuable information on the power system dynamics.

The content of this chapter is closely related with very deep and interesting

topics both in System and Control Theory on the one hand and in Power System Analysis on the other. The chapter is intended to introduce the specific concept of dissipativity for power systems models and its links with the energy functions theory in this context. Appendix A introduces *briefly* the classical definition of dissipativity and presents some links with passivity and other concepts.

Section 2.1 introduces the dissipativity framework to be used in the sequel. It is shown that, in absence of control and resistive elements, the different network components–and their interconnection–are *cyclo–dissipative*. Small signal models around the equilibrium are considered in Section 2.2. Finally, Section 2.3 analyzes the dissipativity properties of controlled SVC systems.

2.1 Dissipativity Properties

To establish our results a slight variation of the classical formulation is needed—this requirement is related to the fact that the supply rate functions that we consider are functions, not of the port variables (I, V), but of $(I, \dot{V})$. Another difference with respect to the standard dissipativity framework is that our systems are characterized by DAEs[1], instead of ODEs and readout maps. But this difference is not essential as we suppose that the algebraic constraints can be solved for the "link variables" (Hill and Mareels, 1990) leading to the standard formulation, see Assumption 2.

Definition 1. *Consider a dynamical system $\Sigma : (u, v)$ represented by the DAEs*

$$\left\{ \begin{array}{rcl} \dot{x} & = & F(x, y, u) \\ 0 & = & G(x, y, u) \\ v & = & r(x, y, u) \end{array} \right. \tag{2.1}$$

where $x \in \mathbb{R}^n$ is the state and $(u, v) \in \mathbb{R}^p \times \mathbb{R}^p$ are the port variables. The function $r : \mathbb{R}^n \times \mathbb{R}^m \times \mathbb{R}^p \to \mathbb{R}^p$ is the so-called read-out function and $G : \mathbb{R}^n \times \mathbb{R}^m \times \mathbb{R}^p \to \mathbb{R}^m$ establishes the algebraic constraint that links the $y \in \mathbb{R}^m$ variables to the state and the input. We will assume the existence and uniqueness of the solutions of system Σ on a set $\mathcal{D} \subset \mathbb{R}^n \times \mathbb{R}^m \times \mathbb{R}^p$. Suppose $v(t)$ continuously differentiable and let $w : \mathbb{R}^p \times \mathbb{R}^p \to \mathbb{R}$ be locally integrable along trajectories of Σ, i.e.

$$\int_{t_1}^{t_2} w(u(t), \dot{v}(t))dt < \infty, \quad \forall\, t_1, t_2 \in \mathbb{R}.$$

We say that Σ is cyclo–dissipative *with respect to the supply rate $w(u, \dot{v})$ if and only if there exists a differentiable function $S : \mathbb{R}^n \times \mathbb{R}^m \to \mathbb{R}$, called storage*

[1]The reader, if confused by notation or acronyms, can consult the Glossary.

function, such that all solution $(x(t), y(t), u(t)) \in \mathcal{D}$ *satisfies*

$$S(x(t_2), y(t_2)) - S(x(t_1), y(t_1)) \leq \int_{t_1}^{t_2} w(u(t), \dot{v}(t))dt \quad \forall t_2 \geq t_1. \tag{2.2}$$

We also define the dissipation function $d : \mathbb{R}^n \times \mathbb{R}^m \times \mathbb{R}^p \to \mathbb{R}$

$$\int_{t_1}^{t_2} d(x(t), y(t), u(t))dt = S(x(t_2), y(t_2)) - S(x(t_1), y(t_1)) - \int_{t_1}^{t_2} w(u(t), \dot{v}(t))dt \quad \forall t_2 \geq t_1.$$

$\Sigma : (u, y)$ *is* cyclo–lossless *if the dissipation inequality (*2.2*) holds with identity, the same to say* $d \equiv 0$*. Finally, if the storage function is* non–negative *we say that* Σ *is dissipative with respect to the supply rate* $w(u, \dot{v})$*.*

As seen from the definition above, the distinction between cyclo–dissipative and dissipative systems is the non–negativity of the storage function[2]. It can be shown that a system is cyclo–dissipative when it cannot create (abstract) energy *over closed paths* in the space (x, y). In effect, if the trajectory describes a cycle in the period t_1, t_2, it is satisfied

$$S(x(t_1), y(t_1)) = S(x(t_2), y(t_2)),$$

and

$$\int_{t_1}^{t_2} w(u(t), \dot{v}(t))dt \geq 0.$$

In this case, the environment *delivers* (abstract) work, but the system is not able to *storage* it as an increase of the generalized energy S. This does not impede that at an initial portion of the trajectory the system delivers energy to the environment leading to a temporary decrease of the storage function. On the other hand, if the system is dissipative and the trajectory starts from a point with minimum (zero) energy, the above-mentioned behavior is not possible because S is impeded to decrease below zero.

The presence or not of a lower bound of the generalized energy S also has an important influence on the local shape of the storage function and the existence of a class of these functions that can be demonstrated with variational arguments, see (Willems, 1972).

In the power systems case, the interest resides in the dynamic behavior of the system around multiple equilibrium points that depend on parametrical and topological changes. In a certain sense[3], the absence of a point with absolute minimum energy is not important.

[2]Actually, as one can always add a constant to the storage function, the question is whether it is bounded from below or not.

[3]The existence of such a point is of course essential when the system is being shut off.

A noticeable difference between the concept of dissipativity introduced in this chapter and the classical one introduced in (Willems, 1972) and extended in (Hill and Moylan, 1980) is that the supply rate function w also depends in our case on the derivatives of the port variables. This fact nevertheless does not constitutes any obstacle, as it can be seen below. It is interesting to note that in (Ortega et al., 2003) classes of nonlinear RLC circuits have been identified that are dissipative with respect to supply rates of the form $\dot{V}^\top I$ or $\dot{I}^\top V$—which is in the spirit of the results that we derive below.

In this section it will be shown that, *in the absence* of control action and disturbance terms, each device of our power systems model is cyclo–dissipative with respect to the supply rate function[4] $W : \mathbb{R}^2 \times \mathbb{R}^2 \to \mathbb{R}$:

$$W(\mathrm{I}_j, \dot{\mathrm{V}}_j) \triangleq \dot{\mathrm{V}}_j^\top J \mathrm{I}_j = -\mathrm{I}_j^\top J \dot{\mathrm{V}}_j = -\dot{\mathrm{V}}_{R_j} \mathrm{I}_{I_j} + \dot{\mathrm{V}}_{I_j} \mathrm{I}_{R_j}. \tag{2.3}$$

A straightforward, but quite tedious, algebraic computation involving equations (1.4) and (1.5) allows us to write the power supply function in terms of the polar description of voltage phasor and the power:

$$W(\mathrm{I}_j, \dot{\mathrm{V}}_j) = P_j \dot{\theta}_j + \frac{Q_j}{\mathcal{V}_j} \dot{\mathcal{V}}_j. \tag{2.4}$$

The analysis of the dissipativity properties developed in this chapter is entirely based on the Cartesian description of bus variables, since this option allows us to work with functions closer to be quadratic. On the other hand, the polar coordinates are closer to the way as the power engineers usually reason.

Remark 5. *Before entering to the formal machinery of this chapter, let us discuss–in an informal way–the meaning of dissipativity for a power system. Think in a power system (a single device or a subsystem) operating at constant voltage. In such a case, the power supply function can be approximated by*

$$W(\mathrm{I}_j, \dot{\mathrm{V}}_j) \approx P_j \dot{\theta}_j.$$

The dissipativity with respect to W implies that a closed trajectory satisfies

$$\int_{t_1}^{t_2} W dt = \int_{t_1}^{t_2} P_j \dot{\theta}_j dt \geq 0,$$

that enforces a certain proximity between the waveforms of power and bus frequency ($\dot{\theta}_j$). Increases of bus frequency must accompany slow increases of active power, which is a behavior very natural in power system. The dissipativity goes beyond at enforcing that this proximity also must be maintained for dynamic, faster, power variations. In particular, if the power variations are sinusoidal, at

[4] We are supposing, see definition 1, that the port variables V, I are differentiable.

any frequency, the difference of phase between both waveforms will be less than 90 degrees. A similar reasoning is possible involving the waveforms of Q and $\dot{\mathcal{V}}$ at constant frequency, which also has a direct engineering meaning: reactive power injections will be accompanied by positive increases of bus voltage.

In the case of the synchronous machine an additional supply rate function $W_{fd} : \mathbb{R} \times \mathbb{R} \to \mathbb{R}$ arises, associated to the excitation system:

$$W_{fd}(e_{fd}, i_{fd}) := e_{fd} i_{fd}. \tag{2.5}$$

To establish the cyclo–dissipativity properties we make the following (temporary) assumptions.

Assumption 4. *The field voltages of the synchronous machines are constant, i.e., $E_{fd_i} = E^{\star}_{fd_i}$.*

Assumption 5. *The active component of loads are modeled as constant power, i.e. $p_1 = p_2 = 0$ in equation (1.10).*

Assumption 6. *The network has no resistive element: $Y_R = 0$.*

Proposition 1. *The operator $\Sigma_i^{M_6} : (\mathrm{I}_i^M, \mathrm{V}_i; e_{fd_i}, i_{fd_i})$ defined by the sixth order synchronous machine model (1.32) is cyclo–dissipative with respect to the supply rate $W(\mathrm{I}_i^M, \dot{\mathrm{V}}_i) + W_{fd}(e_{fd_i}, i_{fd_i})$. More precisely,*

$$\frac{dS_i^{M_6}(X_i, \mathrm{V}_i)}{dt} \leq W(\mathrm{I}_i^M, \dot{\mathrm{V}}_i) + W_{fd}(e_{fd_i}, i_{fd_i}).$$

If, in addition, Assumption 4 is satisfied, $\Sigma_i^{M_6} : (\mathrm{I}_i^M, \mathrm{V}_i; 0, i_{fd_i})$ is cyclo–dissipative with respect to the supply rate $W(\mathrm{I}_i^M, \dot{\mathrm{V}}_i)$ and

$$\frac{dS_i^{M_6}(X_i, \mathrm{V}_i)}{dt} \leq W(\mathrm{I}_i^M, \dot{\mathrm{V}}_i).$$

If Assumption 5 holds, the operator $\Sigma_l^L : (I_l^L, V_l)$ defined by the model (1.11) is cyclo–dissipative lossless with respect to the supply rate $W(I_l^L, \dot{V}_l)$:

$$\frac{dS_l^L(\mathrm{V}_l)}{dt} = W(\mathrm{I}_l^L, \dot{\mathrm{V}}_l).$$

If Assumption 6 holds, the operator $\Sigma^N : (\mathbf{I}, \mathbf{V})$ defined by (1.40) is cyclo–dissipative lossless with respect to the supply rate $W_N : \mathbb{R}^{2m} \times \mathbb{R}^{2m} \to \mathbb{R}$:

$$W_N(\mathbf{I}, \dot{\mathbf{V}}) := \dot{\mathbf{V}}^{\top} \mathbf{J} \mathbf{I} = \sum_{j \in \mathbb{B}} W(I_j, \dot{V}_j). \tag{2.6}$$

More precisely,

$$\frac{dS^N(\mathbf{V})}{dt} = W_N(\mathbf{I}, \dot{\mathbf{V}}).$$

Finally, the bus equations (1.9) may be written as

$$W(\mathrm{I}_j^E, \dot{\mathrm{V}}_j) = W(\mathrm{I}_j, \dot{\mathrm{V}}_j) + W(\mathrm{I}_j^M, \dot{\mathrm{V}}_j) + W(\mathrm{I}_j^L, \dot{\mathrm{V}}_j) \; \forall j \in \mathbb{B}. \tag{2.7}$$

Proof Some simple computations from (1.31), (1.32) yield

$$\frac{dS^{M_6}(X,\mathrm{V})}{dt} = \frac{\partial S^{M_6}}{\partial X}\dot{X} + \frac{\partial S^{M_6}}{\partial \mathrm{V}}\dot{\mathrm{V}} =$$

$$= \left[\nabla_X S^{M_6}(X,\mathrm{V})\right]^\top \left[(K-R)\nabla_X S^{M_6}(X,\mathrm{V}) + B_{fd}e_{fd}\right] + [J\mathrm{I}^M]^\top \dot{\mathrm{V}} =$$

$$- \left[\nabla_X S^{M_6}(X,\mathrm{V})\right]^\top R\nabla_X S^{M_6}(X,\mathrm{V}) + e_{fd}i_{fd} + [J\mathrm{I}^M]^\top \dot{\mathrm{V}} \leq$$

$$\leq W_{fd}(e_{fd}, i_{fd}) + W(\mathrm{I}^M, \dot{\mathrm{V}}). \tag{2.8}$$

The inequality results from equations (1.33), (1.34), and definitions (2.3), (2.5).

Notice that, if Assumption 4 is also satisfied, $e_{fd} = 0$, $W_{fd}(e_{fd}, i_{fd}) = 0$ and the cyclo–dissipativity of the generator with respect to W follows.

Similarly, from the loads equation (1.11) and (2.3), we get

$$\frac{dS_l^L(\mathrm{V}_l)}{dt} = \frac{\partial S_l^L}{\partial \mathrm{V}_l}\dot{\mathrm{V}}_l = \nabla_{\mathrm{V}_l} S_l^L(\mathrm{V}_l)^\top \dot{\mathrm{V}}_l = (J\mathrm{I}_l^L)^\top \dot{\mathrm{V}}_l - \Psi_l^L(\mathrm{V}_l)^\top \dot{\mathrm{V}}_l =$$

$$= W(\mathrm{I}_l^L, \dot{\mathrm{V}}_l) - \dot{\mathrm{V}}_l^\top \Psi_l^L(\mathrm{V}_l),$$

establishing cyclo–dissipativity for load models satisfying Assumption 5, since $\Psi_l^L(\mathrm{V}_l) = 0$. For the electrical network we get from (1.40) and (2.6)

$$\frac{dS_N(\mathbf{V})}{dt} = \dot{\mathbf{V}}^\top \mathbf{J}\mathbf{I}^N - \dot{\mathbf{V}}^\top \Psi_N(\mathbf{V}) = W_N(\mathbf{I}, \dot{\mathbf{V}}) - \dot{\mathbf{V}}^\top \Psi_N(\mathbf{V})$$

proving the system is cyclo–lossles if $\Psi_N(\mathbf{V}) = 0$—that is, in the absence of resistive components. Finally, (2.7) follows multiplying (1.9) by $\dot{\mathrm{V}}_j$ and taking the transpose. □□□

In reference (Giusto et al., 2006a) it was shown that Proposition 1 is also met by classical second and third order generator models with constant excitation. These results are not included in Proposition 1 for the sake of brevity.

Remark 6. The cyclo–dissipativity of the synchronous machines deserves some comments. Compute the dissipation function from (2.8) and definition (1.31):

$$d(X_i, V_i) = -\nabla_X S^{M_6\top} R\nabla_X S^{M_6} = -d\Omega_0(\omega_r - 1)^2 - R_{fd}i_{fd}^2 - I_r^T R_r I_r.$$

As it can be seen, the dissipation is composed by mechanical and electrical losses. The rotor circuits are not AC modulated and their resistances appear dissipating energy as usual. The supply rate function has two components: W is the one associated to the stator variables and to the energy interchange all along the network. The term $W_{fd} = e_{fd}i_{fd}$ is, naturally, the electrical power supplied to the machine by the excitation system. Finally, the storage function S^{M_6}, equation (1.31) exhibits noticeable terms that emphasize its electromechanical

nature: the rotational kinetic energy $\frac{1}{2}\Omega_0(\omega_r - 1)^2$ and the electromagnetical potential energy $\frac{1}{2}\Phi^\top L^{-1}\Phi$. The term $T_m\delta$ is a direct consequence of assuming constant torque; the linear term involving Φ_{fd} was introduced to ensure the absence of linear terms around the equilibrium, remember (1.61).

Remark 7. Of course, we always can consider the physically natural supply rate function defined as the sum of $\hat{W} = -E_s^T I_s = P^M$ for the stator and W_{fd} for the field. By doing so, we recover the familiar energy balance at the machine, see (Ortega et al., 1998) and references therein. This study is very interesting, since it establishes links with very well-known physical concepts. However, the election of $\hat{W}$ as supply rate function (and its corresponding storage function) faces serious drawbacks when analyzing the stability of a non zero equilibrium, since the dissipativity is not satisfied by the incremental model around the equilibrium. The power supply rate W defined in (2.3) does not have these drawbacks as it will be shown below.

Notice that the addition in $j \in \mathbb{B}$ of equation (2.7) yields

$$\sum_{\mathbb{E}} W(I_e^E, \dot{V}_e^E) = W_N(\mathbf{I}, \dot{\mathbf{V}}) + \sum_{j\in\mathbb{M}} W(I_j^M, \dot{V}_j) + \sum_{j\in\mathbb{L}} W(I_j^L, \dot{V}_j), \tag{2.9}$$

which motivates the definition of the external supply rate function[5] $W^E : \mathbb{R}^{2m_E} \times \mathbb{R}^{2m_E} \to \mathbb{R}$:

$$W^E(\mathbf{I}^E, \dot{\mathbf{V}}^E) \triangleq \sum_{\mathbb{E}} W(I_e^E, \dot{\mathbf{V}}_e) = \sum_{\mathbb{E}} \dot{V}_e^\top J I_e^E = \dot{\mathbf{V}}^{E\top}\mathbf{J}^E\mathbf{I}^E, \tag{2.10}$$

with the matrix $\mathbf{J}^E$ defined in (1.52). Define now the incremental variables

$$\mathbf{i}^E := \mathbf{I}^E - \mathbf{I}^{E\star},\ \mathbf{v}^E := \mathbf{V}^E - \mathbf{V}^{E\star},$$

and the function $w^E : \mathbb{R}^{2m_E} \times \mathbb{R}^{2m_E} \to \mathbb{R}$:

$$w^E(\mathbf{i}^E, \dot{\mathbf{v}}^E) \triangleq \dot{\mathbf{v}}^{E\top}\mathbf{J}^E\mathbf{i}^E. \tag{2.11}$$

The first order terms around the equilibrium were suppressed in w^E, as it was done in Section 1.5 for the storage function S, equation (1.57). The links between both functions are highlighted in the following Proposition that establishes the cyclo-dissipativity of the power system model:

Proposition 2. *If Assumptions* 4-6 *are satisfied, the system given by equation (*1.60*) is cyclo-dissipative with respect to supply rate function W^E:*

$$\frac{dS_0(X, \mathbf{V})}{dt} \leq W^E(\mathbf{I}^E, \dot{\mathbf{V}}^E),$$

[5]The reader familiar with reference (Willems, 1972) will recognize, behind the equation (2.9), the concept of *neutral interconnection* that establishes the way how the internal interactions compensate each other.

with S_0 given by (1.55). The system also is cyclo-dissipative with respect to w^E:

$$\frac{dS(X,\mathbf{V})}{dt} \leq w^E(\dot{\mathbf{i}}^E, \dot{\mathbf{v}}^E),$$

with S given by (1.57).

Proof From the previous derivations and equations (2.9) and (2.10), we have

$$\begin{aligned}\frac{dS_0(X,\mathbf{V})}{dt} &= \sum_i \frac{d}{dt}S_i^M(X_i,\mathrm{V}_i) + \sum_l \frac{d}{dt}S_l^L(\mathrm{V}_l) + \frac{d}{dt}S_N(\mathbf{V}) \leq \\ &\leq \sum_i W(\mathrm{I}_i^M, \dot{\mathrm{V}}_i) + \sum_l W(\mathrm{I}_l^L, \dot{\mathrm{V}}_l) + \sum_{j\in\mathbb{B}} W(\mathrm{I}_j^N, \dot{\mathrm{V}}_j) = \\ &= W^E(\mathbf{I}^E, \dot{\mathbf{V}}^E)\end{aligned}$$

that proves the first part of the thesis. The second affirmation can be easily proved directly from equation (1.60):

$$\begin{aligned}\frac{dS(X,\mathbf{V})}{dt} &= \nabla_X S(X,\mathbf{V})^\top \dot{X} + \nabla_{\mathbf{V}} S(X,\mathbf{V})^\top \dot{\mathbf{V}} = \\ = \nabla_X S(X,\mathbf{V})^\top [(K-R)\nabla_X S(X,\mathbf{V})] &+ [\mathcal{T}^\top \mathbf{J}^E(\mathbf{I}^E - \mathbf{I}^{E\star})]^\top \dot{\mathbf{V}} \leq \\ \leq \dot{\mathbf{V}}^\top [\mathcal{T}^\top \mathbf{J}^E(\mathbf{I}^E - \mathbf{I}^{E\star})] &= \mathbf{V}\dot{^E}^\top \mathbf{J}^E(\mathbf{I}^E - \mathbf{I}^{E\star}) = \mathbf{v}\dot{^E}^\top \mathbf{J}^E \mathbf{i}^E.\end{aligned}$$

The latter identities were obtained with equation (1.51) and definition (2.11). Thus

$$\frac{dS(X,\mathbf{V})}{dt} \leq w^E(\dot{\mathbf{i}}^E, \dot{\mathbf{v}}^E),$$

that concludes the proof. □□□

Notice that, when the system is isolated, the model (1.46) results

$$\dot{X} = f(X, \mathbf{V}(X), 0) := \bar{f}(X), \tag{2.12}$$

where the links variables $\mathbf{V}$ were substituted by a function on the states, by virtue of Assumption 2. In these conditions, Proposition 2 yields

$$\frac{dS(X,\mathbf{V})}{dt} = \frac{dS(X,\mathbf{V}(X))}{dt} := \frac{d\bar{S}(X)}{dt} \leq 0,$$

The function $S(X,\mathbf{V})$, see definition (1.57) and equations (1.12),(1.19), (1.31) and (1.41), is not bounded from below nor radially unbounded: it is only non-increasing along the trajectories. Its local properties around the equilibria depend on each case. Consequently, the function $\bar{S}$ *can not* be used as a Lyapunov function for the system (2.12) without further considerations. These functions nevertheless have been successfully used in the power system literature with different objectives. In this context, see e.g. (Chiang et al., 1987; Varaiya et al., 1985), a differentiable function $\bar{S} : \mathbb{R}^n \to \mathbb{R}$ is called an *energy function* of system (2.12) if the following three conditions are met:

1. $\bar{S}$ is non–increasing along the trajectories of (2.12): $\dot{\bar{S}}((X(t)) \leq 0$,

2. the set $\{t \in \mathbb{R} : \dot{\bar{S}}(X(t)) = 0\}$ has measure zero in $\mathbb{R}$ for all non trivial trajectory $X(t)$,

3. if a trajectory has a bounded value of $\bar{S}(X(t))$ on $t \geq 0$, then $X(t)$ is also bounded.

The energy function has been employed, among others objectives, to investigate the dynamic properties of the stability boundary of stable equilibrium points (s.e.p), to estimate attraction regions of s.e.p, to compute security margins to the voltage collapse in power systems, to obtain quantitative measures of transient stability, and to provide *on line* analysis tools to assess dynamic security. See, e.g. references (Chiang et al., 1987; Varaiya et al., 1985; Overbye and DeMarco, 1991; Chiang et al., 1994; Paganini and Lesieutre, 1999), for a deep discussion and applications.

The application of energy function theory to power systems has faced serious obstacles due to the size and complexity of these systems. It is not a simple task to rigourously verify properties 2 and 3 above. Among the legitime responses to these obstacles it is possible to find the use of simplified dynamic models and the development of computational procedures based partial *and explicitly* on the heuristics.

Remark 8. *The contributions of the work reported in this thesis to the analysis techniques based on the energy function are the following:*

- *A characterization of the dynamic properties to be met by each component, Definition* 1 *and Proposition* 1*, in order to ensure that the power system possesses a storage function satisfying Condition 1 above.*

- *The inclusion of detailed full order synchronous machine models to the classical energy function: Fact* 3 *and Proposition* 1*.*

- *The inclusion of a class of controlled SVC systems to the classical energy function, see Section* 2.3*.*

The latter two statements are valid provided that Conditions 2 and 3 of the energy function can be established for the overall system by some mean.

*The expression in polar coordinates of the function W, equation (*2.4*) have been implicitly employed in a procedure of construction of energy functions, first reported in (Van Cutsem and Ribbens-Pavella, 1985) and, more recently, applied in reference (Azbe et al., 2005) and others of the same authors.*

2.2 Input-output properties for small signal models

We have seen in the previous section that the power system model (1.60) satisfies a fundamental internal property: the balance between the storage of energy and the interaction with the environment. We will study how this property is also satisfied by small signal models. Later, we will exploit the versatility of linear models to study the dissipativity in the frequency domain.

Variables at the equilibrium will be denoted with a supra-index $\star$: $X^\star, \mathbf{V}^\star, I^\star_{fd}$, etc. Lowercase will denote the incremental variables around the equilibrium point: $i_{fd} = I_{fd} - I^\star_{fd}, \tilde{x} = X - X^\star$, etc.

Consider the Jacobian matrix of function $\Psi(\mathbf{V})$ at the equilibrium

$$J_\psi := \frac{d}{d\mathbf{V}}\Psi(\mathbf{V})|_\star,$$

and its symmetric and skew-symmetric parts:

$$J^S_\Psi := \frac{1}{2}(J_\psi + J_\psi^\top); J^A_\Psi \ :== \frac{1}{2}(J_\psi - J_\psi^\top);$$

The Hessian of function S, equation (1.57), at the equilibrium:

$$\mathbf{H} := \frac{\partial^2 S(X,\mathbf{V})}{\partial (X,\mathbf{V})^2}|_\star,$$

allows us to define $H : \mathbb{R}^n \times \mathbb{R}^{2m} \to \mathbb{R}$:

$$H(x,\mathbf{v}) := \frac{1}{2}\begin{bmatrix} x \\ \mathbf{v} \end{bmatrix}^\top \mathbf{H} \begin{bmatrix} x \\ \mathbf{v} \end{bmatrix} + \frac{1}{2}\mathbf{v}^\top J^S_\Psi \mathbf{v}, \tag{2.13}$$

and obtain, by invoking (1.60) and (1.61), the small signal model:

$$\begin{cases} \dot{x} &= (K-R)\nabla_x H(x,\mathbf{v}) + B_u \mathbf{e}_{fd} \\ 0 &= -\nabla_{\mathbf{v}} H(x,\mathbf{v}) - J^A_\Psi \mathbf{v} + \mathcal{T}^\top \mathbf{J}^E \mathbf{i}^E \\ \mathbf{v}^E &= \mathcal{T}\mathbf{v} \end{cases} \tag{2.14}$$

If the excitation is held constant (Assumption 4), and if the network is free from resistive losses or loads (Assumptions 5-6), $\mathbf{\Psi} \equiv 0$:

$$\begin{cases} \dot{x} &= (K-R)\nabla_x H(x,\mathbf{v}) \\ 0 &= -\nabla_{\mathbf{v}} H(x,\mathbf{v}) + \mathcal{T}^\top \mathbf{J}^E \mathbf{i}^E \\ \mathbf{v}^E &= \mathcal{T}\mathbf{v} \end{cases} \tag{2.15}$$

In these conditions,

$$\frac{d}{dt}H = \nabla_x^\top H \dot{x} + \nabla_{\mathbf{v}}^\top H \dot{\mathbf{v}} \leq \dot{\mathbf{v}}^{E\top} \mathbf{J}^E \mathbf{i}^E = w_E(\mathbf{i}^E, \dot{\mathbf{v}}^E),$$

and the dissipation inequality is recovered:

$$\frac{d}{dt}H \leq w_E(\mathbf{i}^E, \dot{\mathbf{v}}^E). \tag{2.16}$$

If we denote

$$\mathbf{H} = \begin{bmatrix} H_x & H_{xv} \\ H_{xv}^\top & H_v \end{bmatrix},$$

in full accordance with equation (2.13), we obtain

$$\nabla_x H(x, \mathbf{v}) = \begin{bmatrix} H_x & H_{xv} \end{bmatrix} \begin{bmatrix} x \\ \mathbf{v} \end{bmatrix},$$

$$\nabla_{\mathbf{v}} H(x, \mathbf{v}) = \begin{bmatrix} H_{xv}^\top & H_v \end{bmatrix} \begin{bmatrix} x \\ \mathbf{v} \end{bmatrix}.$$

Since H_v is invertible (because of Assumption 3), a straightforward computation allow us to get the state space model

$$\begin{cases} \dot{x} &= (K-R)[H_x - H_{xv}H_v^{-1}H_{xv}^\top]x + (K-R)H_{xv}H_v^{-1}\mathcal{T}^\top \mathbf{J}^E \mathbf{i}^E \\ \mathbf{v}^E &= \mathcal{T}H_v^{-1}[-H_{xv}^\top]x + \mathcal{T}H_v^{-1}\mathcal{T}^\top \mathbf{J}^E \mathbf{i}^E. \end{cases} \tag{2.17}$$

Notice that the election of the pair $\mathbf{v}^E, \mathbf{i}^E$ respectively as output and input is merely conventional. The inverse map $\mathbf{v}^E \to \mathbf{i}^E$ exists since the matrix

$$\tilde{D} := \mathcal{T}H_v^{-1}\mathcal{T}^\top \mathbf{J}^E$$

is invertible because, by construction, $\mathcal{T}$ has full rank and $\mathbf{J}^E$ is invertible.

Equation (2.15), or equivalently equation (2.17), is the state space representation of the small signal response of the power system. It determines the dynamic matrix

$$\tilde{A} := (K-R)[H_x - H_{xv}H_v^{-1}H_{xv}^\top], \tag{2.18}$$

and also the input-output relationship between $\mathbf{i}^E$ and $\mathbf{v}^E$. Denote $\mathbf{Z}(s)$ and $\mathbf{Y}(s)$ the corresponding transfer matrices

$$\begin{aligned} \hat{\mathbf{v}}^E(s) &= \mathbf{Z}(s)\hat{\mathbf{i}}^E(s), \forall \mathbf{i}^E \in \mathcal{L}_2^e, x(0) = 0, \\ \hat{\mathbf{i}}^E(s) &= \mathbf{Y}(s)\hat{\mathbf{v}}^E(s), \forall \mathbf{v}^E \in \mathcal{L}_2^e, x(0) = 0, \end{aligned} \tag{2.19}$$

where we have used the symbol $\hat{\cdot}$ to denote the Laplace transform and $s \in \mathcal{C}$ the Laplace variable.

The dissipation inequality (2.16) and the classical Kalman-Yakubovic-Popov lemma, see references (Rantzer, 1996), (Willems, 1971), enable us to think that

these systems satisfy some constraint in the frequency domain. Our concept of dissipativity possesses some differences from the original setting. For this reason, we will prove the mentioned property independently.

Proposition 3. *Suppose the Assumptions* 4-6 *hold and* $det(jwI - \tilde{A}) \neq 0 \forall \omega \in \mathbb{R}$. *Then the transfer matrices* $\mathbf{Z}, \mathbf{Y}$ *given by equation (*2.19*) satisfy*

$$\begin{bmatrix} I \\ \mathbf{Z}(j\omega) \end{bmatrix}^* \Pi_d(j\omega) \begin{bmatrix} I \\ \mathbf{Z}(j\omega) \end{bmatrix} \geq 0 \ \ \forall w \in \mathbb{R}, \tag{2.20}$$

$$\begin{bmatrix} I \\ \mathbf{Y}(j\omega) \end{bmatrix}^* \Pi_d(j\omega) \begin{bmatrix} I \\ \mathbf{Y}(j\omega) \end{bmatrix} \geq 0 \ \ \forall w \in \mathbb{R}, \tag{2.21}$$

$$\Pi_d(j\omega) := |h_d(j\omega)|^2 \begin{bmatrix} 0 & j\omega \mathbf{J}^{E\top} \\ -j\omega \mathbf{J}^E & 0 \end{bmatrix} \tag{2.22}$$

for all function $h_d(s)$ *real rational stable and strictly proper.*

Proof: Consider $x(0) = 0$ and take Laplace transform at equation (2.15):

$$\begin{cases} s\hat{x} &= (K-R) \begin{bmatrix} H_x & H_{xv} \end{bmatrix} \begin{bmatrix} \hat{x} \\ \hat{\mathbf{v}} \end{bmatrix} \\ \mathcal{T}^\top \mathbf{J}^E \hat{\mathbf{i}^E} &= \begin{bmatrix} H_{xv}^\top & H_v \end{bmatrix} \begin{bmatrix} \hat{x} \\ \hat{\mathbf{v}} \end{bmatrix} \\ \hat{\mathbf{v}^E} &= \mathcal{T}\hat{\mathbf{v}}. \end{cases}$$

The first two equations can be written

$$\begin{bmatrix} s\hat{x} \\ \mathcal{T}^\top \mathbf{J}^E \hat{\mathbf{i}^E} \end{bmatrix} = \begin{bmatrix} (K-R) & 0 \\ 0 & I_{2m} \end{bmatrix} \mathbf{H} \begin{bmatrix} \hat{x} \\ \hat{\mathbf{v}} \end{bmatrix}, \ \forall \mathbf{i}^E \in \mathcal{L}_2^e$$

As $(K-R)$ is invertible, see equation (1.59), we can write

$$\begin{bmatrix} (K-R)^{-1} & 0 \\ 0 & I_{2m} \end{bmatrix} \begin{bmatrix} s\hat{x} \\ \mathcal{T}^\top \mathbf{J}^E \hat{\mathbf{i}^E} \end{bmatrix} = \mathbf{H} \begin{bmatrix} \hat{x} \\ \hat{\mathbf{v}} \end{bmatrix}, \ \forall \mathbf{i}^E \in \mathcal{L}_2^e$$

If we pre multiply by the vector

$$|h_d(s)|^2 s^* \begin{bmatrix} \hat{x} \\ \hat{\mathbf{v}} \end{bmatrix}^*,$$

we obtain

$$|h_d(s)|^2 s^* \begin{bmatrix} \hat{x} \\ \hat{\mathbf{v}} \end{bmatrix}^* \begin{bmatrix} (K-R)^{-1} & 0 \\ 0 & I_{2m} \end{bmatrix} \begin{bmatrix} s\hat{x} \\ \mathcal{T}^\top \mathbf{J}^E \hat{\mathbf{i}^E} \end{bmatrix} = |h_d(s)|^2 s^* \begin{bmatrix} \hat{x} \\ \hat{\mathbf{v}} \end{bmatrix}^* \mathbf{H} \begin{bmatrix} \hat{x} \\ \hat{\mathbf{v}} \end{bmatrix},$$

or, equivalently

$$|h_d(s)|^2 s^* \hat{x}^* (K-R)^{-1} s\hat{x} + |h_d(s)|^2 s^* \hat{\mathbf{v}}^{E*} \mathbf{J}^E \hat{\mathbf{i}}^E = |h_d(s)|^2 s^* \begin{bmatrix} \hat{x} \\ \hat{\mathbf{v}} \end{bmatrix}^* \mathbf{H} \begin{bmatrix} \hat{x} \\ \hat{\mathbf{v}} \end{bmatrix}, \tag{2.23}$$

where we have used the last equation in (2.15). If we take $s = j\omega, \omega \in \mathbb{R}$, the right hand side of equation (2.23) is purely imaginary since $\mathbf{H}$ is a symmetrical real matrix. Thus, $\forall \mathbf{i}^E \in \mathcal{L}_2^e$

$$|h_d(j\omega)|^2 \omega^2 \hat{x}(j\omega)^* [(K-R)^{-1} + (K-R)^{-\top}] \hat{x}(j\omega) -$$
$$-j\omega |h_d(j\omega)|^2 \hat{\mathbf{v}}^E(j\omega)^* \mathbf{J}^E \hat{\mathbf{i}}^E(j\omega) + j\omega |h_d(j\omega)|^2 \hat{\mathbf{i}}^E(j\omega)^* \mathbf{J}^{E\top} \hat{\mathbf{v}}^E(j\omega) = 0.$$

The absence of imaginary poles of $\tilde{A}$ implies that $\hat{x}(j\omega)$ is bounded $\forall \mathbf{i}^E \in \mathcal{L}_2^e$. The assumptions on h_d imply that $|h_d(j\omega)|^2\omega^2$ is also bounded on $\mathbb{R}$. Finally, the sign definition of $(K-R)$ and the introduction of the transfer matrix $\mathbf{Z}$, equation (2.19), implies

$$|h_d(j\omega)|^2 \hat{\mathbf{i}}^E(j\omega)^* [-\mathbf{Z}(j\omega)^* j\omega \mathbf{J}^E + j\omega \mathbf{J}^{E\top} \mathbf{Z}(j\omega)] \hat{\mathbf{i}}^E(j\omega) \geq 0, \ \ \forall \mathbf{i}^E \in \mathcal{L}_2^e$$

Since $\mathbf{i}^E \in \mathcal{L}_2^e$ is arbitrary:

$$|h_d(j\omega)|^2 [-\mathbf{Z}(j\omega)^* j\omega \mathbf{J}^E + j\omega \mathbf{J}^{E\top} \mathbf{Z}(j\omega)] \geq 0 \ \forall \omega \in \mathbb{R}. \tag{2.24}$$

The equation (2.20) results of a simple reordering of this inequality. Notice that the introduction of the factor $|h_d(\cdot)|^2$ ensures that Π_d is bounded on $\mathbb{R}$. By pre and post multiplying equation (2.24) by $\mathbf{Y}^*$ and $\mathbf{Y}$ we have

$$|h_d(j\omega)|^2 [-j\omega \mathbf{J}^E \mathbf{Y}(j\omega) + \mathbf{Y}(j\omega)^* j\omega \mathbf{J}^{E\top}] \geq 0 \ \forall \omega \in \mathbb{R}.$$

Since $\mathbf{J}^{E\top} = -\mathbf{J}^E$, we can write

$$|h_d(j\omega)|^2 [j\omega \mathbf{J}^{E\top} \mathbf{Y}(j\omega) - \mathbf{Y}(j\omega)^* j\omega \mathbf{J}^E] \geq 0 \ \forall \omega \in \mathbb{R},$$

which allows us to obtain equation (2.21) that concludes the proof. □□□

The condition (2.20) is equivalent, see equation (2.24), to

$$j\omega |h_d(j\omega)|^2 \mathbf{J}^{E\top} \mathbf{Z}(j\omega) + [j\omega |h_d(j\omega)|^2 \mathbf{J}^{E\top} \mathbf{Z}(j\omega)]^* \geq 0 \ \forall \omega \in \mathbb{R}.$$

If $\mathbf{Z}(s)$ is stable and strictly proper, the condition above is equivalent to

$$s\mathbf{J}^{E\top} \mathbf{Z}(s) \textit{ is positive real},$$

in the sense established, e.g. in (Khalil, 1996). This condition does not constrain the *size* of the map $\mathbf{Z}(s)$ but, in the matrix sense, its *phase*[6].

Equations (2.20)-(2.22) constitute frequency-weighted convex conditions for the small signal systems $\mathbf{Z}$ and $\mathbf{Y}$. This statement can be easily verified with the help of Lemma 2 in Section 3.2.

2.2.1 Numerical example

We consider a classical benchmark of power system stability studies: the Example 12.6 in (Kundur, 1994). A single-line diagram of this example is depicted in Figure 4.6. The objective of the analysis is to verify the fulfillment of the frequency domain condition in Proposition 3 and the way this property is affected by the inclusion of resistive losses, magnetic saturation and excitation control. The linear models around the equilibrium system were computed with the package DSAT (Powertech Labs Inc., n.d.).

The eigenvalues of the matrix function

$$\sigma(j\omega) := \sigma_l(\mathbf{Z}(j\omega), \Pi_d(j\omega))(j\omega) \;\; \forall \omega \in \mathbb{R},$$

for each generator were computed. The generators are modeled in full accordance with (Kundur, 1994), with the exceptions mentioned below in each case. All the machines models have sixth order. The model of generator $G1$ does not include the effect of magnetic saturation nor the resistance R_a. The excitation is kept constant. Figure 2.1 shows the eigenvalues of $\sigma(j\omega)$ for generator $G1$: both positive, which provide us a numerical validation of Proposition 3.

The remaining machines were modeled with magnetic saturation. The model of generator G3 includes also the statorical resistance Ra. The eigenvalues of σ for G3 are depicted in Fig. 2.2. As it can be seen, the influence of Ra is negligible for frequencies up to 1000 rad/sec, beyond the reasonable limits of validity for the class of models used in transient stability studies.

Generator $G4$ includes the following AVR:

$$E_{fd} = 200\frac{1+s}{1+10s}(E_t - V_{ref}),$$

with a relatively high gain. The eigenvalues of $\sigma(j\omega)$ for this case are represented in Fig. 2.3. The AVR naturally affects the frequency response at low frequencies, just below the natural frequencies of the system, around 1 rad/sec.

[6]We refer to the polar decomposition of the complex matrices, see e.g. (Conway, 1985).

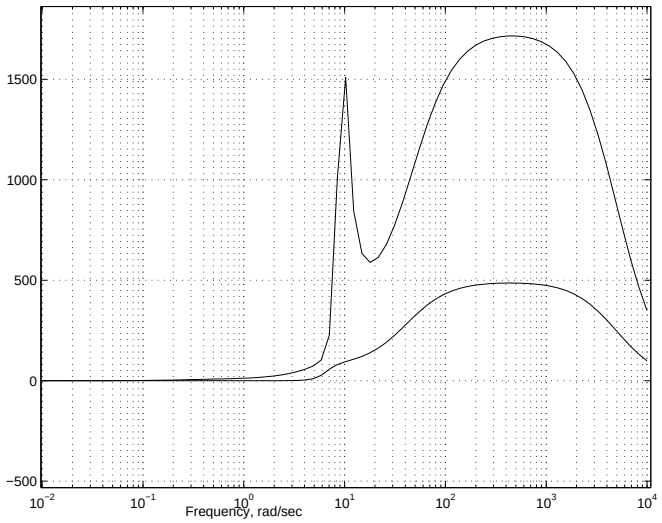

Figure 2.1: Eigenvalues of function $\sigma(j\omega)$ for $G1$: no magnetic saturation, $R_a = 0$, constant excitation.

Figures 2.1-2.3 allow us graphically appreciate the influence of R_a and the AVR on the cyclo-dissipativity of the generator model. Notice that this property remains valid in the presence of active excitation control for medium frequencies comprising the basic natural frequencies of electromechanical oscillations. This fact encourages the employment of multiplier Π_d, at least at medium frequencies, for robustness analysis of power systems.

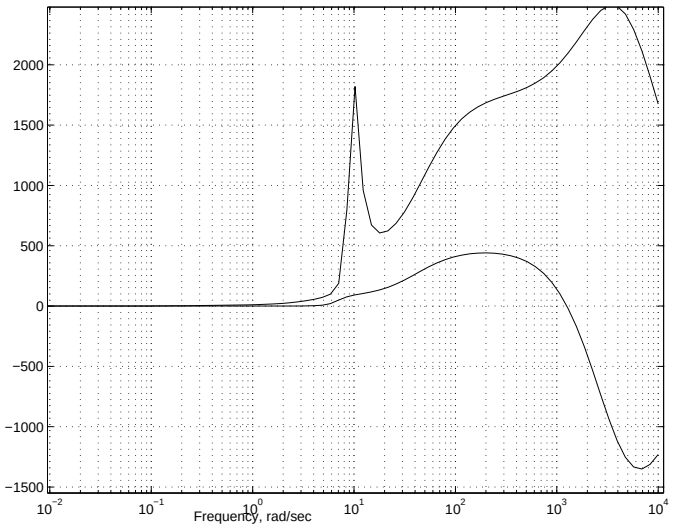

Figure 2.2: Eigenvalues of function $\sigma(j\omega)$ for $G2$. It includes the effect of R_a.

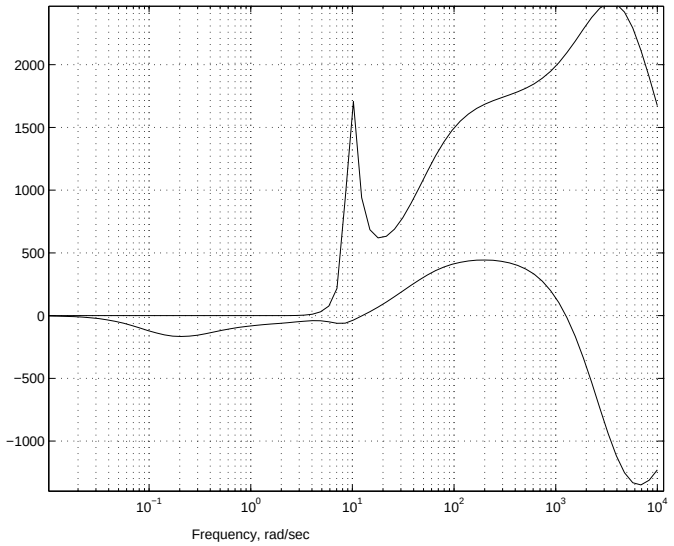

Figure 2.3: Eigenvalues of function $\sigma(j\omega)$ for $G4$. It includes the effect of R_a and excitation control.

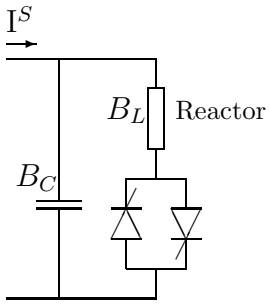

Figure 2.4: Schematic one-line diagram of a SVC

2.3 Dissipativity properties of SVC models

This section focuses on the properties of Static Var Compensators (SVC) models. A schematic diagram of a basic configuration is shown in Figure 2.4. The model considered here is the one typically used for power system stability studies (Kundur, 1994): balanced system, oriented to transient phenomena and describing the behavior of the phasor associated to the fundamental frequency[7].

We will show that for a broad class of SVC voltage regulators–namely, the PD controllers–, these models satisfy the cyclo-dissipativity property defined in Section 2.1. This fact has particular relevance since it allows to incorporate the model of the SVC with PD controller to classical energy functions used to analyze power system stability, see Remark 8 in Section 2.1. As we know, the dissipation inequality implies also that the linear model around the equilibrium meets a convex condition in the frequency domain; a complete characterization of the set of controllers that ensure this property is obtained.

Typically, the SVC have been treated in the energy function literature either as a constant impedance or as a constant voltage load (Hiskens and Hill, 1992). The first situation corresponds to a saturated control action and the second one to an instantaneous control response. However, at the best of our knowledge, no energy function is known for the SVC when its control dynamics is considered.

The Figure 2.4 represents a fixed bank capacitor with susceptance $-B_C$ and a Thyristor-Controlled Reactor (TCR) with a susceptance B_L which is controlled by the voltage regulator, see (Kundur, 1994). Figure 2.5 graphically describes the control loop: the controller $k(s)$ operates on the voltage error to contribute to the adjust of the SVC susceptance B_S, positive when inductive.

As it was mentioned, the energy function for the saturated cases ($B_S = -B_C$

[7]Harmonics and electromagnetic fast transients are not considered.

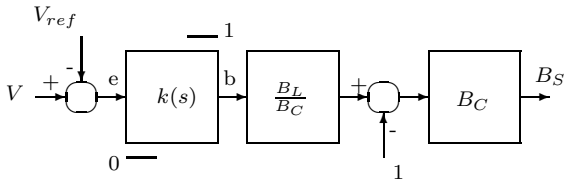

Figure 2.5: Basic model of the SVC

or $B_S = -B_C + B_L$) is well known. For this reason, no explicit mention is done in the sequel on the fixed operating limits.

The controlled SVC susceptance can be written

$$B_S = -B_C + B_L b(t). \tag{2.25}$$

So, the specific model of the SVC controlled by a PD regulator[8] is

$$\left\{ \begin{array}{rcl} P^S & = & 0 \\ Q^S & = & (-B_C + B_L b)\mathcal{V}^2 \\ b(t) & = & k_P e + k_D \dot{e} \\ e & = & \mathcal{V} - \mathcal{V}_{ref}. \end{array} \right. \tag{2.26}$$

It will be shown, in a first instance, that the SVC controller with a PD voltage regulator admits a PCH model.

Fact 5. *The model of the SVC with PD control, equation (*2.26*) can be represented as the operator* $\Sigma^S_{pd} : (\mathrm{I}^S, \mathrm{V})$ *described by the system*

$$\Sigma^S_{pd} : (\mathrm{I}^S, \mathrm{V}) \left\{ \begin{array}{rcl} 0 & = & -\nabla_{\mathrm{V}} S^S_{pd}(\mathrm{V}) + J\mathrm{I}^S - B_L k_D \dot{\mathcal{V}}\mathrm{V}, \end{array} \right. \tag{2.27}$$

with storage function $S^S_{pd} : R^2 \to R$

$$S^S_{pd}(\mathrm{V}) := -\frac{B_C \mathcal{V}^2}{2} + B_L k_P [\frac{\mathcal{V}_{ref}}{2}(\mathcal{V} - \mathcal{V}_{ref})^2 + \frac{(\mathcal{V} - \mathcal{V}_{ref})^3}{3}]. \tag{2.28}$$

Proof: The gradient can be computed from equation (2.28), the model (2.26), and the identity (1.4):

$$\nabla_{\mathrm{V}} S^{SVC}(\mathrm{V}) = \frac{S^{PD}_{SVC}}{d\mathcal{V}} \left[\begin{array}{c} \frac{\partial \mathcal{V}}{\partial \mathrm{V}_R} \\ \frac{\partial \mathcal{V}}{\partial \mathrm{V}_I} \end{array} \right] =$$

$$= \{-B_C \mathcal{V} + B_L k_P [\mathcal{V}_{ref}(\mathcal{V} - \mathcal{V}_{ref}) + (\mathcal{V}_{ref} - \mathcal{V}_{ref})^2]\} \frac{1}{\mathcal{V}} \left[\begin{array}{c} \mathrm{V}_R \\ \mathrm{V}_I \end{array} \right] =$$

[8]The index S stands for SVC, the bus identifier is omitted.

$$= [-B_C + B_L k_P(\mathcal{V} - \mathcal{V}_{ref}] \begin{bmatrix} \mathrm{V}_R \\ \mathrm{V}_I \end{bmatrix} = [-B_C + B_L k_P e]\mathrm{V}.$$

Compute $J\mathrm{I}^S$ from the model (2.26) with the help of equations (1.7):

$$J\mathrm{I}^S = J\frac{1}{\mathcal{V}^2}\begin{bmatrix} P^S & Q^S \\ -Q^S & P^S \end{bmatrix}\mathrm{V} = \frac{1}{\mathcal{V}^2}\begin{bmatrix} Q^S & 0 \\ 0 & Q^S \end{bmatrix}\mathrm{V} = [-B_C + B_L b]\mathrm{V}. \quad (2.29)$$

The latter two equations allow us to write

$$-\nabla_{\mathrm{V}} S^S_{pd}(\mathrm{V}) + J\mathrm{I}^S = B_L(b - k_P e)\mathrm{V} = B_L k_D \dot{e}\mathrm{V} = B_L k_D \dot{\mathcal{V}}\mathrm{V},$$

that concludes the proof. □□□

The cyclo-dissipativity of model (2.27) is stated in next proposition.

Proposition 4. *The operator $\Sigma^S_{pd}(\mathrm{I}^S, \mathrm{V})$ defined by the model (2.27) is cyclo–dissipative with respect to the supply rate $W(\mathrm{I}^S, \dot{\mathrm{V}})$ for all control action*

$$b(t) = k_P e(t) + k_D \dot{e}(t), \quad (2.30)$$

with $k_D \geq 0$. More precisely, the storage function S^S_{pd} satisfies

$$\frac{dS^S_{pd}(\mathrm{V})}{dt} = W(\mathrm{I}^S, \dot{\mathrm{V}}) - B_L k_D \dot{\mathcal{V}}^2 \mathcal{V} \leq W(\mathrm{I}^S, \dot{\mathrm{V}}). \quad (2.31)$$

The proof is straightforward from Fact 5, definition (2.3) and the identity

$$B_L k_D \dot{\mathcal{V}} \mathrm{V}^\top \dot{\mathrm{V}} = B_L k_D \dot{\mathcal{V}} \mathcal{V} \dot{\mathcal{V}} \leq 0.$$

Remark 9. Notice that the derivative action introduces a positive dissipation

$$d(\mathrm{V}, \dot{\mathrm{V}}) = B_L k_D \dot{\mathcal{V}}^2 \mathcal{V} \geq 0$$

which constitutes a noticeable difference with respect to classical (loss-less) energy function for these devices. This effect must not be confused with the additional damping signals that typically are added to the SVC control, see (Kundur, 1994).

Small signal properties Let us denote $\mathcal{V}^\star$ the equilibrium voltage for the model (2.25). This quantity is typically near $\mathcal{V}_{ref}$; the difference, if it exists, is due to finite controller gain. Let $b^\star$ be control action at the equilibrium. The linear model around the equilibrium, for a generic linear controller is

$$\begin{cases} p^S &= 0 \\ q^S &= 2[-B_C + 2B_L b^\star]\mathcal{V}^\star v + B_L(\mathcal{V}^\star)^2 \tilde{b} \\ \frac{d}{dt}x_k &= A_k x_k + B_k v \\ \tilde{b} &= C_k x_k + d_k v, \end{cases} \quad (2.32)$$

where x_k is the state vector of the regulator and $v := \mathcal{V} - \mathcal{V}^\star$. We denote $k(s) := C_k(sI - A_k)^{-1}B_k + d_k$ the transfer function of the regulator to get

$$\hat{b}(s) = k(s)\hat{v}(s) = k(s)k_v\hat{\mathrm{v}}(s) = k(s)\frac{\mathrm{V}^{\star\top}}{\mathcal{V}^\star}\hat{\mathrm{v}}(s),$$

where the small signal relation[9] $v = k_v\mathrm{v}$, and definition (4.1) were employed.

Recall equation (2.29) to write

$$I^S = -J[-B_C + B_L b]\mathrm{V},$$

and obtain the small signal model

$$\hat{\mathrm{i}}^S = J[B_C - B_L b^\star]\hat{\mathrm{v}} - JB_L\mathrm{V}^\star\hat{b}(s) = J[B_C - B_L b^\star]\hat{\mathrm{v}} - JB_L\mathrm{V}^\star k(s)k_v\hat{\mathrm{v}}(s).$$

Thus, the transfer function $\mathbf{Y}^S(s)$ such that $\hat{\mathrm{i}}(s) = \mathbf{Y}^S(s)\hat{\mathrm{v}}(s)$ is

$$\mathbf{Y}^S(s) = J[B_C - B_L b^\star] - \frac{B_L k(s)}{\mathcal{V}^\star}\mathrm{V}^\star\mathrm{V}^{\star\top}. \tag{2.33}$$

We now will state the conditions to be met by controller $k(s)$ in order to the SVC linear model (2.32) satisfies condition (2.21).

Proposition 5. *The transfer matrix $\mathbf{Y}^S(j\omega)$ satisfies*

$$\begin{bmatrix} I \\ \mathbf{Y}^S(j\omega) \end{bmatrix}^* \Pi_d(j\omega) \begin{bmatrix} I \\ \mathbf{Y}^S(j\omega) \end{bmatrix} \geq 0 \ \ \forall w \in \mathbb{R} \tag{2.34}$$

with Π_d given by (2.22) if and only if If $Im[k(j\omega)] \geq 0\ \forall\omega \geq 0$.

Proof: Condition (2.34) is equivalent to

$$j\omega[-\mathbf{Y}^S(j\omega)^\star J + J^\top\mathbf{Y}^S(j\omega)] \geq 0\ \forall\omega \in \mathbb{R} \Leftrightarrow$$

$$j\omega\frac{B_L}{\mathcal{V}^\star}\mathrm{V}^\star\mathrm{V}^{\star\top}(-k(j\omega) + k(j\omega)^*) = 2\omega\frac{B_L}{\mathcal{V}^\star}Im(k(j\omega)) \geq 0\ \forall\omega \in \mathbb{R} \Leftrightarrow$$

$$Im(k(j\omega)) \geq 0\ \forall\omega \geq 0.$$

□□□

Noticeably, any reasonable proper approximation of the PD control action $k(s) := \frac{k_P + sk_D}{Ts+1}$ satisfies $Im[k(j\omega)] \geq 0\ \forall\omega \geq 0$. Notice also that this condition is met by a broad class of controllers. The example studied in Section 3.2.1 includes a Nichols plot of this constraint on $k(j\omega)$ in Fig. 3.8.

[9] This relation is demonstrated in Section 4.1, see equations (4.1) and (4.8). It simply poses the linear dependence of the small variations of the module respect to the voltage phasor.

Chapter 3

Applications

Toda función de storage sueña con
ser de Lyapunov cuando sea grande...
... y por sí sola asegurar la estabilidad
del punto de equilibrio, de la región
y del universo.

The application of the dynamic properties discussed in Chapter 2 to the control and analysis of power systems is investigated in this chapter.

We know that, in absence of control and resistive elements, the power system admits a PCH formulation, equation (1.60) and the storage function S is non-increasing along the trajectories of the isolated power system, Proposition 2. A first question to investigate is the importance of these facts in the design of control laws ensuring performance and stability in spite of the presence of disturbance terms impeding the open loop cyclo-dissipativity. The chosen procedure is the synthesis of excitation controllers that suitably shape the storage function and ensure a damping of the closed loop modes. This method fits in a broader class of techniques, known generically as *energy–shaping*, that have been applied to several fields, see (Ortega et al., 2002; Ortega et al., 2001) and references therein. Applications to power systems has been reported e.g. in (Sun et al., 2000; Shen et al., 2003; Wang et al., 2003; Galaz et al., 2001; Ortega et al., 2005).

Section 3.2 studies the application of frequency domain quadratic constraints to the stability analysis of linear interconnected systems. An example involving the design of an SVC voltage regulator and the use of the IQC multipliers for robustness analysis is considered.

3.1 Controller design by energy shaping

In this section we consider an isolated power system given by equation (1.60) without external interactions:

$$\Sigma : \begin{cases} \dot{X} &= (K-R)\nabla_X S(X,\mathbf{V}) + B_u \mathbf{e}_{fd} \\ 0 &= -\nabla_{\mathbf{V}} S(X,\mathbf{V}) - \Psi(\mathbf{V}) + \Psi(\mathbf{V}^\star). \end{cases} \tag{3.1}$$

The control action $\mathbf{e}_{fd}$ is the vector of the incremental field voltages, see (1.15), of the synchronous machines, supposed to be described by simplified third order models. The system is supposed to be "lossy", i.e. the disturbance terms $\Psi(\mathbf{V})$ that impede the cyclo-dissipativity are assumed non zero.

We will investigate the design of excitation (decentralized) controllers that locally stabilize the desired equilibrium point. More precisely, we will prove that it is possible to assign to the overall *linearized* system a positive definite Lyapunov function, consisting of the sum of the storage function S plus a quadratic term in the rotor angle and speed deviations. This will be done by imposing some additional closed loop constraints on pole allocations and controller's structure. It is worth to mention that the non-linear version of this problem has been shown to be hard. In reference (Ortega et al., 2005) it is proved the existence of a nonlinear static state feedback law that ensures asymptotic stability for a general n–machine system including transfer conductances. Unfortunately, due to the computational complexity, an explicit expression of the controller can be derived only for the case $n \leq 3$.

We will establish asymptotic stability of the linearized system and, invoking Lyapunov's indirect method, we conclude that the original nonlinear system is also asymptotically stable. Section 3.1.1 includes the application of the proposed technique to a classical example.

As we know, when the simplifying Assumptions 4-6 are violated, the cyclo–dissipativity properties are lost, and the condition $\frac{dS(X,\mathbf{V})}{dt} \leq 0$ is not verified anymore. We will show that, with the addition of field control action $\mathbf{e}_{fd}$, it is possible to assign to the *non–ideal linearized* system a storage function that, under some conditions captured by an LMI, achieves a minimum at the desired equilibrium point hence qualifies as a *bona fide* Lyapunov function to assess stability of the equilibrium.

Let us denote[1] $g : \mathbb{R}^n \times \mathbb{R}^{2m} \to \mathbb{R}^{2m}$ the function

$$g(X, \mathbf{V}) := -\nabla_{\mathbf{V}} S(X, \mathbf{V}) - \Psi(\mathbf{V}) + \Psi(\mathbf{V}^\star).$$

In order to formulate the control problem we will suppose

Assumption 7. *There exists a set* $\mathcal{D}_g \in \mathbb{R}^n \times \mathbb{R}^{2m}$ *satisfying*

$$\mathcal{D}_g \triangleq \{(X, \mathbf{V}) \in \mathbb{R}^n \times \mathbb{R}^{2m} \mid g(X, \mathbf{V}) = 0 \text{ and } \nabla_{\mathbf{V}} g(X, \mathbf{V}) \text{ is non singular.}\}$$

where the solutions of the DAE are unique and well defined;

Assumption 8. *There exists an isolated* open loop equilibrium *of the system, that is, a point* $(X^\star, \mathbf{V}^\star) \in \mathcal{D}_g$ *where*

$$\begin{cases} 0 &= \nabla_X S(X^\star, \mathbf{V}^\star) \\ 0 &= \nabla_{\mathbf{V}} S(X^\star, \mathbf{V}^\star). \end{cases}$$

Assumptions 7-8 substitute the Assumptions 2-3 for our stand-alone case, see also equation (1.61). As a consequence of Assumption 7 and the Implicit Function Theorem there exists, locally around $(X^\star, \mathbf{V}^\star)$, a function $\hat{\mathbf{V}} : \mathbb{R}^n \to \mathbb{R}^{2m}$ such that $g(X, \hat{\mathbf{V}}(X)) = 0$. Consequently, we can write

$$\dot{\mathbf{V}} = M(X, \mathbf{V})\dot{X} \tag{3.2}$$

where $M(X, \mathbf{V}) \in \mathbb{R}^{2m \times n}$ is given by

$$M(X, \mathbf{V}) := -\nabla_{\mathbf{V}}^{-\top} g(X, \mathbf{V}) \nabla_X^\top g(X, \mathbf{V}).$$

Energy Shaping Problem: Consider the system (3.1) satisfying Assumptions 7-8. Find a control law $\mathbf{e}_{fd} = \hat{\mathbf{e}}_{fd}(X, \mathbf{V})$, and a function $S_a : \mathbb{R}^n \times \mathbb{R}^{2m} \to \mathbb{R}$, such that, for some set $\mathcal{D} \subset \mathbb{R}^n \times \mathbb{R}^{2m}$, with $(X^\star, \mathbf{V}^\star) \in \mathcal{D}$, the function

$$S_d(X^\star, \mathbf{V}^\star) := S(X^\star, \mathbf{V}^\star) + S_a(X^\star, \mathbf{V}^\star) \tag{3.3}$$

satisfies

C1. $(X^\star, \mathbf{V}^\star) = \arg\min_{(X,\mathbf{V}) \in \mathcal{D} \cap \mathcal{D}_g} S_d(X, \mathbf{V})$,

C2. $\frac{dS_d(X,\mathbf{V})}{dt} \leq 0, \quad \forall (X, \mathbf{V}) \in \mathcal{D} \cap \mathcal{D}_g.$

Consequently, $(X^\star, \mathbf{V}^\star)$ is a stable equilibrium of the closed–loop with Lyapunov function $S_d(X, \hat{\mathbf{V}}(X))$.

[1] We re-use the letter g to denote a slighly different function, see (1.46), but the context avoids any confusion.

For reasons that will become clear below, we select the added energy as a function of ω and δ only, that is, $S_a : \mathbb{R}^{2N} \to \mathbb{R}$, where $N = m_M$ denotes the number of machines in the system. We will take the control action as

$$\mathbf{e}_{fd} = L\nabla_X S(X, \mathbf{V}) \tag{3.4}$$

with $L \in \mathbb{R}^{N\times n}$ also to be determined. Let us compute

$$\begin{aligned}\frac{dS_d}{dt} &= \nabla_X^\top S\dot{X} + \nabla_{\mathbf{V}}^\top S\dot{\mathbf{V}} + \frac{dS_a}{dt} \\ &= \begin{bmatrix} \nabla_X S \\ \nabla_{\mathbf{V}} S \end{bmatrix}^\top \begin{bmatrix} K - R + B_u L \\ M(X,\mathbf{V})(K-R) + M(X,\mathbf{V})B_u L \end{bmatrix} \nabla_X S + \frac{dS_a}{dt}.\end{aligned}$$

where we have used (3.2). We will investigate the negativity of this function, in a neighborhood around the equilibrium point, when (3.4) is replaced by its linear approximation and we fix the added energy function as

$$S_a(\delta, \omega) = \frac{1}{2}\begin{bmatrix} \delta - \delta^\star \\ \omega \end{bmatrix}^\top P \begin{bmatrix} \delta - \delta^\star \\ \omega \end{bmatrix} \tag{3.5}$$

where $P = P^\top \in \mathbb{R}^{2N\times 2N}$ is a matrix to be computed. The question is then:

- Are there matrices P and L such that the conditions C1 and C2 of the problem formulation above are satisfied?

We will prove that the question can be recast as a *convex optimization* problem. More precisely, we show that the response is affirmative if an LMI, for P and L, is feasible. The LMI arises because we will analyze first the asymptotic stability of the linearized system. If this is ensured we establish, via Lyapunov's direct method, stability of the nonlinear system as well.

We define the matrices

$$\begin{aligned} M^\star &:= M(X^\star, \mathbf{V}^\star) \\ \mathcal{F} &:= \frac{\partial^2 S}{\partial X^2}(X^\star, \mathbf{V}^\star) + \frac{\partial^2 S}{\partial X \partial \mathbf{V}}(X^\star, \mathbf{V}^\star) M^\star \\ K_\psi &:= \frac{\partial \Psi}{\partial \mathbf{V}}(\mathbf{V}^\star), \end{aligned}$$

with which we obtain the first order approximations

$$\mathbf{v} \simeq M^\star x, \quad \nabla_X S(X, \mathbf{V}) \simeq \mathcal{F} x, \quad \nabla_{\mathbf{V}} S(X, \mathbf{V}) \simeq -K_\psi M^\star x,$$

where lowercases and $\tilde{\cdot}$ denote incremental variables. Now, for systems having only synchronous machines modeled with third order models, in view of the definition of X, equations (1.14) and (1.45), we have

$$\begin{aligned}\tilde{\delta} &= \mathrm{col}(\tilde{\delta}_i) = \mathrm{diag}([1\ 0\ 0])x =: \mathcal{U}_1 x \\ \tilde{\omega} &= \mathrm{col}(\tilde{\omega}_i) = \mathrm{diag}([0\ 1\ 0])x =: \mathcal{U}_2 x.\end{aligned}$$

Define $\mathcal{U} := \left[\begin{array}{cc} \mathcal{U}_1^\top & \mathcal{U}_2^\top \end{array}\right]^\top$. Using this notation we get

$$S_a(\delta,\omega) = \frac{1}{2}\left[\begin{array}{c}\tilde{\delta}\\ \omega\end{array}\right]^\top P \left[\begin{array}{c}\tilde{\delta}\\ \omega\end{array}\right] = \frac{1}{2}x^\top \mathcal{U}^\top P \mathcal{U} x,$$

and

$$\frac{dS_a}{dt} = x^\top \mathcal{U}^\top P \mathcal{U}\dot{x} = x^\top \mathcal{U}^\top P \mathcal{U}(K - R + B_u L)\mathcal{F}x = x^\top \mathcal{U}^\top P \mathcal{U}(K-R)\mathcal{F}x,$$

since $\mathcal{U}B_u = 0$, see (1.58). Thus

$$\frac{dS_d}{dt} \simeq x^\top [\mathcal{F}^\top [K-R+B_u L]\mathcal{F} - (M^\star)^\top K_\Psi^\top M^\star [(K-R)+B_u L]\mathcal{F} + \mathcal{U}^\top P \mathcal{U}(K-R)\mathcal{F}]x. \tag{3.6}$$

We also define the (fixed) matrices

$$\mathcal{W} := -M^\top K_\Psi^\top M(K-R)\mathcal{F},\ \mathcal{V} := \left[\begin{array}{c} B_u^\top M^\top K_\Psi M \\ \mathcal{F}\end{array}\right],\ \mathcal{Z} := \left[\begin{array}{c}\mathcal{U}\\ \mathcal{U}(K-R)\mathcal{F}\end{array}\right].$$

Using this notation (3.6) can be written as

$$\frac{dS_d}{dt} \simeq \frac{1}{2}x^\top Q(P,L)x,$$

where

$$Q(P,L) := \mathcal{F}^\top[-2R + B_u L + L^\top B_u^\top]\mathcal{F} + \mathcal{W} + \mathcal{W}^\top -$$

$$-\mathcal{V}^\top \left[\begin{array}{cc} 0_n & L \\ L^\top & 0_n\end{array}\right]\mathcal{V} + \mathcal{Z}^\top \left[\begin{array}{cc} 0_{2N} & P \\ P & 0_{2N}\end{array}\right]\mathcal{Z}, \tag{3.7}$$

and we have added the arguments on Q to make explicit the dependence on P and L—which is *linear*. Notice at this point that if the added energy S_a depended on the state variable E, the quadratic form will contain cross–products between P and L, destroying the linearity.

Let us check now positivity of the first order approximation of $S_d(X, \mathbf{V})$. By construction

$$\nabla_X S_d(X^\star, \mathbf{V}^\star) = 0,\ \ \nabla_{\mathbf{V}} S_d(X^\star, \mathbf{V}^\star) = 0.$$

On the other hand, the Hessian evaluated at the equilibrium is also a linear function of P that we denote $\mathcal{H}(P)$:

$$\frac{\partial^2 S_d(X, M^\star X)}{\partial X^2}|_{X^\star} = \frac{\partial^2 S(X, M^\star X)}{\partial X^2}|_{X^\star} + \mathcal{U}^\top P \mathcal{U} =: \mathcal{H}(P). \tag{3.8}$$

We are in position to present our main stabilization result whose proof follows immediately from the calculations above, and Lyapunov's direct method.

Proposition 6. *Assume the feasibility of the LMI*

$$Q(P, L) < 0, \quad \mathcal{H}(P) > 0,$$

for some $P = P^\top$ and L, where $Q(P, L)$ and $\mathcal{H}(P)$ are defined by (3.7) and (3.8), respectively. Then, a solution to the energy shaping problem is provided by the control $\mathbf{e}_{fd} = L\mathcal{F}x$ and the added energy function $S_a(\delta, \omega)$ given by (3.5).

Since the computation of a stabilizing control law is formulated as an LMI on P and the controller matrix L, several interesting performance requirements or conditions can be considered. We mention only two: pole allocation in a prescribed region in the complex plane and decentralized control action.

Pole placement The allocation of closed loop poles to a given region in the complex plane is an important performance requirement in power systems applications. There is a vast set of convex regions that admit an LMI formulation (Chilali and Gahinet, 1996). Consider the constants $r > 0, \alpha \geq 0$ and $\gamma \leq \pi/2$ and the region $R(\alpha, r, \gamma) \subset \mathbb{C}$ defined by

$$R(\alpha, r, \gamma) := \{\lambda = u + jw \in C |\ u < -\alpha < 0,\ |\lambda| < r,\ u \tan\gamma < -|w|\} \tag{3.9}$$

The region $R(\alpha, r, \gamma)$ is the intersection of the conic sector defined by r and γ with the half plane to the left side of the axis $\mathcal{R}e(\lambda) = -\alpha$. The requirement that all eigenvalues of a matrix $A \in R^{n\times n}$ belong to $R(\alpha, r, \gamma)$ is implied (see (Chilali and Gahinet, 1996)) by the existence of a symmetric matrix $X \in R^{n\times n}, X > 0$ such that

$$\begin{cases} L_1(X, A) := A'X + XA + 2\alpha X < 0 \\ L_2(X, A) := \begin{bmatrix} -rX & A'X \\ XA & -rX \end{bmatrix} < 0 \\ L_3(X, A) := \begin{bmatrix} \sin\gamma(A'X + XA) & \cos\gamma(A'X - XA) \\ \cos\gamma(XA - A'X) & \sin\gamma(A'X + XA) \end{bmatrix} < 0 \end{cases} \tag{3.10}$$

or, for brevity, $L(X, A) < 0$ if we denote $L(\cdot, \cdot) := \text{diag}(L_i(\cdot, \cdot))$.

If we fix X to be the Hessian of our Lyapunov function (3.8), i.e., $X = \mathcal{H}(P)$, and we write $A(L) := (K - R + B_u L)\mathcal{F}$, the stabilization with pole allocation in region R (3.9) can be stated as follows[2].

Corollary 1. *Assume there exist some $P = P^\top \in \mathbb{R}^{2N\times 2N}$ and $L \in \mathbb{R}^{N\times n}$ such that*

$$\mathcal{H}(P) > 0, \quad L(\mathcal{H}(P), A(L)) < 0,$$

where $Q(P, L)$, $\mathcal{H}(P)$ and $L(X, A)$ are defined by (3.7) and (3.8) and (3.10), respectively. Then, the solution to the energy shaping problem provided by the control $\mathbf{e}_{fd} = L\mathcal{F}x$, with the added energy function $S_a(\delta, \omega)$ given by (3.5), allocates all the closed loop eigenvalues in the region $R(\alpha, r, \gamma)$ defined in (3.9).

Decentralized control The implementation of the control law (3.4) requires the availability of full information of the overall system in each machine, which is not realistic in industrial applications. If we wish enforce the use of only local information X_i, V_i in the control law e_{fd_i} we must restrict our matrix L to be block diagonal. As our LMI conditions depend directly on L, this restriction can be easily added to Proposition 6 and Corollary 1 as follows.

In the decentralized case, it is convenient to define the control action as

$$E_{FD_i} = \begin{bmatrix} L_{\omega i} & L_{Pi} & L_{Vi} \end{bmatrix} \begin{bmatrix} \omega_i \\ P_{m_i} - P_i^M \\ \mathcal{V}_i^{ref} - \mathcal{V}_i \end{bmatrix}. \tag{3.11}$$

This can be interpreted as the action of an AVR plus a PSS modeled in a rough manner, see (Kundur, 1994), (Milano, 2005) for details. Since this feedback law is different from the one assumed in (3.4), the conditions to ensure stability must be slightly modified. Let us denote

$$z_i(x_i, \mathrm{V}_i) := \begin{bmatrix} \omega_i \\ P_{m_i} - P_i^M \\ \mathcal{V}_i^{ref} - \mathcal{V}_i \end{bmatrix}, \quad z(x, \mathbf{V}) := col(z_i(x_i, \mathrm{V}_i)), \quad L_{dec} := diag([L_{\omega i}\ L_{Pi}\ L_{Vi}]).$$

Straightforward computations allow us to conclude that Proposition 6 remains valid, if we substitute $Q(P, L)$ by the expression $\tilde{Q}(P, L_{dec})$ defined as

$$\tilde{Q}(P, L_{dec}) := -2\mathcal{F}^\top R\mathcal{F} + \mathcal{F}^\top B_u L_{dec}\mathcal{G} + \mathcal{G}^\top L_{dec}^\top B_u^\top \mathcal{F} + \mathcal{W} + \mathcal{W}^\top -$$

[2]It is worth to mention that it is not necessary to enforce all the Lyapunov matrices X in the $L_i(\cdot)$ functions to be the same. The formulation of Corollary 1, although correct, is not the best from a computational point of view.

$$-\tilde{\mathcal{V}}^\top \begin{bmatrix} 0_N & L_{dec} \\ L_{dec}^\top & 0_n \end{bmatrix} \tilde{\mathcal{V}} + \mathcal{Z}^\top \begin{bmatrix} 0_{2N} & P \\ P & 0_{2N} \end{bmatrix} \mathcal{Z},$$

where

$$\tilde{\mathcal{V}} := \begin{bmatrix} B_u^\top M^\top K_\Psi M \\ \mathcal{G} \end{bmatrix}, \; \mathcal{G} := \frac{\partial z}{\partial x}(x^\star, \mathbf{V}^\star) + \frac{\partial z}{\partial y}(x^\star, \mathbf{V}^\star) M^*.$$

Corollary 1 also remains valid if we substitute $Q(P, L)$ and $A(L)$ by $\tilde{Q}(P, L_{dec})$ and

$$\tilde{A}(L_{dec}) := (K - R)\mathcal{F} + B_u L_{dec} \mathcal{G},$$

respectively. Thus, the computation of the decentralized controller L_{dec} can be carried enforcing

$$\tilde{Q}(P, L_{dec}) < 0, \quad \mathcal{H}(P) > 0, \quad L(\mathcal{H}(P), \tilde{A}(L_{dec})) < 0,$$

and restricting the matrix L_{dec} to be *block diagonal*.

3.1.1 Example

We consider here the classical 3-machines, 9-buses WSCC system considered in the textbooks (Anderson and Fouad, 1993), (Sauer and Pai, 1998). The system is depicted in Figure 3.1. The synchronous machines are modelled with equations (1.13). We assume that the active components of the loads have constant power characteristics and the reactive components have constant impedance. Since this system has no infinite bus, the procedure we described in previous sections had to be slightly modified in order to cope with the non-isolated equilibrium point. The details are fairly standard, see (Willems, 1974), and they are omitted for brevity. Computations were done with the software package PSAT (Milano, 2005).

The network data can be seen in (Anderson and Fouad, 1993). The machine data are listed in Table 3.1 for reference.

The LMI condition in Corollary 1 was the tool for the synthesis of the controller gain L. The parameters of the desired region for the closed–loop poles, $R(\alpha, r, \gamma)$, were chosen as $\alpha = 0.008$, $\gamma = \frac{\pi}{2}$ and $r = 25$. An additional constraint on the controller gain, namely $\|L\| < 10$, was also imposed. The open and closed loop mode patterns are given in Table 3.2 and in Figure 3.2.

A decentralized control law was also computed following the procedure described in the previous section. No constraint on the norm of the controller was imposed in this case. The results are also listed in Table 3.2 and in Figure 3.2.

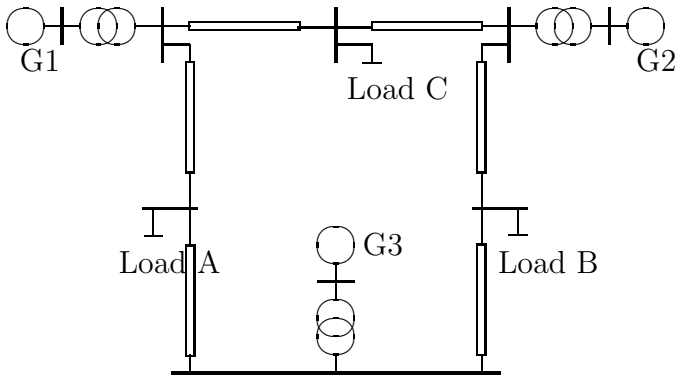

Figure 3.1: *Three-machines, nine-buses WSCC system.*

Table 3.1: Synchronous machines data.

	Generator ♯ 1	Generator ♯ 2	Generator ♯ 3
x_d	0.8958	1.3125	0.146
x'_d	0.1198	0.1813	0.0608
T'_{d0}	6.00	5.89	8.96
x_q	0.8645	1.2578	0.0969
x'_q	0.1969	0.25	0.0969
M	12.8	6.02	47.28
D	0.25	0.25	0.25

A mode at zero is present in all cases, and is associated with the existence of a manifold of equilibrium points (Willems, 1974). More precisely, the absence of an infinite bus implies that the right-hand side terms in the DAE (3.1) depend on the phasor angles only through their differences, see equations (1.13), (1.10). Thus, if $(X^\star, \mathbf{V}^\star)$ is an equilibrium point, so will be any point $(\bar{X}, \bar{\mathbf{V}})$ obtained by adding to all angles in $(X^\star, \mathbf{V}^\star)$ a fixed quantity. As our feedback laws (3.4) and (3.11) do not break this class of dependence on the angles, the equilibrium manifold is also preserved in the closed loop system.

Table 3.2: Mode patterns.

Open loop modes	Closed loop modes, full controller	Closed loop modes, decentralized controller
$-0.29 \pm j11.51$	$-2.23 \pm j10.86$	$-0.39 \pm j12.41$
$-0.13 \pm j8.18$	$-1.39 \pm j8.04$	$-0.24 \pm j8.58$
-0.19	-11.54	-0.18
-0.16	-1.71	-0.17
-0.01	-0.17	-0.04
-0.01	-0.01	-0.01
0.00	0.00	0.00

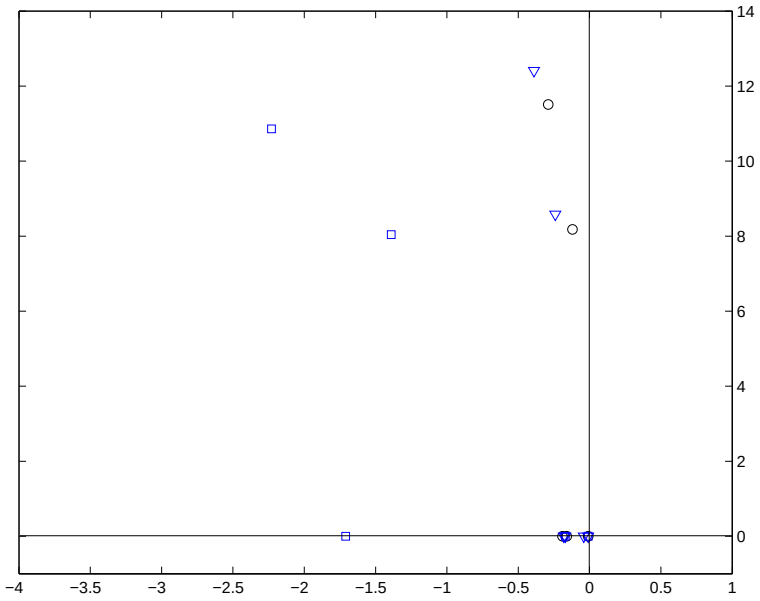

Figure 3.2: *Mode patterns. Open loop (O), Decentralized controller (▽), Full controller (□).*

Figures 3.3–3.5 depict the transient response of the open and closed–loop system to an initial condition $\omega_1(0) = 0.05$. All the transient responses shown were obtained from the respective linear models. Closed–loop responses for both full and decentralized controller are shown. As it can be seen from Table 3.2 and the transient responses, the full controller is able to significantly improve the system's stability and provide damping. The damping factors of the electromechanical modes were increased approximately 8 and 11 times.

The decentralized controller also improves the transient responses—increasing the damping of the electromechanical modes by 25 and 75 percent. However, if compared with the full controller, its performance is relatively modest. This is not unexpected because the decentralized scheme, although more realistic, has fewer degrees of freedom and exploits less dynamic information of the system.

A few comments on the feasibility of the technique are in order. The technique is based on the use of a family of Lyapunov functions which has at its core the function S, see (3.3). The positiveness of S around the equilibrium is not strictly necessary since there are some degrees of freedom (in the matrix P) to make S_d positive. However, these degrees of freedom are also necessary to ensure that S_d is non-increasing along the trajectories. Thus, the positiveness of S, albeit not necessary, is strongly correlated with the feasibility of the LMI (6).

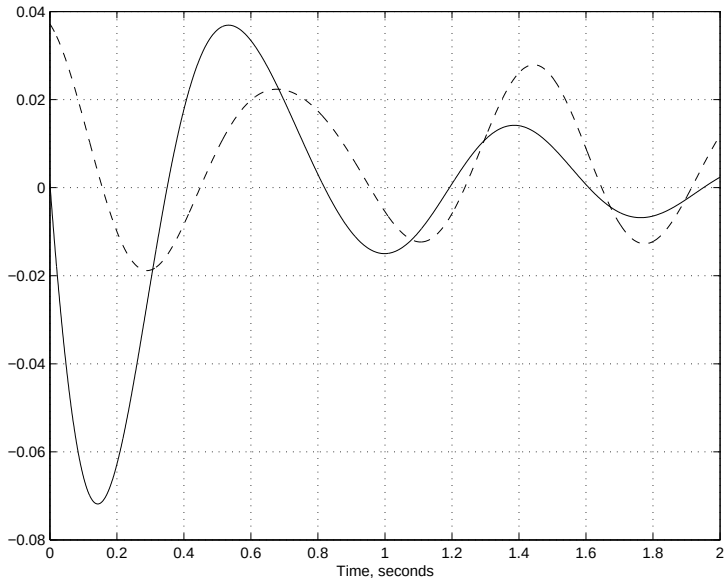

Figure 3.3: *Control action u_1. Decentralized controller (dashed), full controller (continuous).*

The function S was studied in detail in (Tsolas et al., 1985) and some conditions, valid for simpler models, were obtained to ensure its positiveness around a given equilibrium point.

Some concluding remarks are in order. We have provided a solution to the transient stabilization problem of power systems (3.1). The analysis is based on the linear approximation of the system and shows that a linear state feedback controller ensures stability of the desired equilibrium provided an LMI condition is feasible. The LMI is given in terms of the controller gain and the weighting matrix of the added energy function, which is quadratic in the increments. The usefulness of the technique for the controller synthesis was illustrated with its application to a classical example. The procedure is based on the *a priori* knowledge of a storage function S of the idealized open loop system that made way to the search of a closed loop Lyapunov function that allows us to avoid the nonlinear coupling between this and the feedback controller.

The technique described in this section does not take advantage of the linear model (2.14) introduced in Section 2.2. Its use would avoid the definition of several auxiliary matrix present in the text. The current version essentially preserves the original formulation in (Giusto et al., 2006a) as it was published and reviewed by peers.

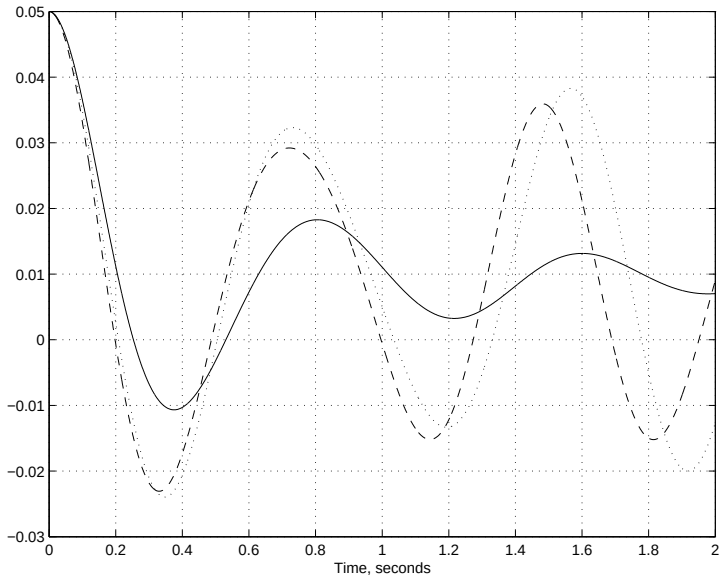

Figure 3.4: *Speed ω_1. Open loop (dotted), decentralized controller (dashed), full controller (continuous).*

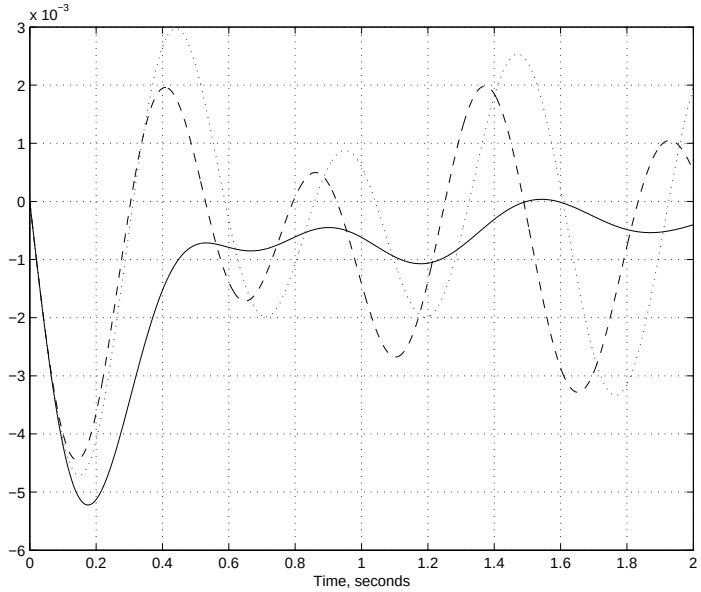

Figure 3.5: *Relative angle δ_{21}. Open loop (dotted), decentralized controller (dashed), full controller (continuous).*

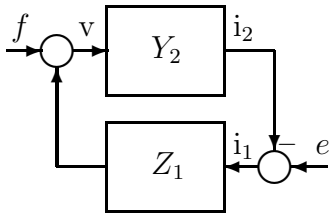

Figure 3.6: Feedback interconnection of systems Z_1, Y_2

3.2 Stability analysis of feedback interconnections

In Section 2.2 we showed the existence of a multiplier Π_d that satisfies conditions (2.20), (2.21) for the linearized models of a class of power system models. This Section is intended to examine the use of these properties for the stability analysis of feedback systems.

We briefly introduce the analysis of feedback systems through the use of multipliers and the IQC Theorem (Megretski and Rantzer, 1997). The discussion is restricted to linear models. The application of this technique to power systems models is illustrated in the example of Section 3.2.1.

The signals will be assumed belonging to the space $\mathcal{L}_2^e[0,\infty)$ and ensuring the existence of the respective Laplace transforms. We will refer as *map* or *operator* to any function $\mathcal{L}_2^e[0,\infty) \to \mathcal{L}_2^e[0,\infty)$ which, for linear systems, involves the transfer function and the Laplace transformation. Denote $\mathbf{Z}_1 \star \mathbf{Y}_2$ the operator $(e,f) \to (v,i_1)$ defined by the standard feedback interconnection depicted in Figure 3.2, given by

$$\begin{cases} v &= \mathbf{Z}_1 i_1 + f \\ i_1 &= -\mathbf{Y}_2 v + e \end{cases} . \tag{3.12}$$

The interconnection will be supposed *well posed*, i.e. the existence of the mentioned closed loop operator is assumed. The negative signal in the loop is completely conventional and it is intended to respect the current convention introduced in Section 4.1.

Assume $\mathbf{Z}_1$ and $\mathbf{Y}_2$ are linear, time-invariant operators with transfer functions $\mathbf{Z}_1(s), \mathbf{Y}_2(s) \in \mathbf{R}\mathcal{L}_\infty^{m\times m}$ and state space realizations:

$$\mathbf{Z}_1(s) = \left[\begin{array}{c|c} A_1 & B_1 \\ \hline C_1 & D_1 \end{array}\right], \ \mathbf{Y}_2(s) = \left[\begin{array}{c|c} A_2 & B_2 \\ \hline C_2 & D_2 \end{array}\right]. \tag{3.13}$$

We are interested in the closed loop *internal stability*, i.e. asymptotical stability of the equilibrium for the resulting state space representation. This

condition holds if and only if the dynamic closed loop matrix

$$A_{cl} = \begin{bmatrix} A_1 & 0 \\ 0 & A_2 \end{bmatrix} + \begin{bmatrix} B_1 & 0 \\ 0 & -B_2 \end{bmatrix} \begin{bmatrix} I_m & -D_1 \\ D_2 & I_m \end{bmatrix}^{-1} \begin{bmatrix} 0 & C_1 \\ C_2 & 0 \end{bmatrix}$$

is Hurwitz, see (Chen, 1984; Zhou et al., 1996) for a detailed exposition. We will refer as closed loop *modes* to the eigenvalues of the matrix A_{cl}. We also will use the word *mode*, in other sections, in its broader sense involving the physical nature of the dynamical response. Is in this sense that we will mention electromechanical modes, control modes, etc., when the object under study be the interconnection of power systems models.

We will work with the of maps $\mathbf{Z}_1, \mathbf{Y}_2$. As it is well known, the closed loop stability of feedback interconnections can be studied in the frequency domain if the involved open loop systems satisfy some basic requirements, stated in next assumption.

Assumption 9. *The state space realization of maps $\mathbf{Z}_1, \mathbf{Y}_2$ are stabilizable and detectable. In addition, the number of RHP poles of the cascade matrix $\mathbf{Y}_2(s)\mathbf{Z}_1(s)$ coincides with the sum of the RHP poles of $\mathbf{Y}_2(s)$ and $\mathbf{Z}_1(s)$.*

In a few words, Assumption 9 establishes the absence of unstable pole-zero cancelations in each system and in the cascade interconnection. In these conditions, we have the following basic lemma, see (Zhou et al., 1996):

Lemma 1. *The system $\mathbf{Z}_1 \star \mathbf{Y}_2$ with $\mathbf{Z}_1, \mathbf{Y}_2$ satisfying Assumption 9 is internally stable if and only if*

$$det(I + \mathbf{Y}_2(s)\mathbf{Z}_1(s))$$

has all the zeros in the open left-half plane.

Define the quadratic functions $\sigma_l, \sigma_u : \mathcal{C}^{m\times m} \times \mathcal{C}^{2m\times 2m} \to \mathcal{C}^{m\times m}$:

$$\begin{aligned} \sigma_l(X, \Pi) &:= \begin{bmatrix} I_m \\ X \end{bmatrix}^* \Pi \begin{bmatrix} I_m \\ X \end{bmatrix}, \\ \sigma_u(X, \Pi) &:= \begin{bmatrix} X \\ I_m \end{bmatrix}^* \Pi \begin{bmatrix} X \\ I_m \end{bmatrix}. \end{aligned} \tag{3.14}$$

Consider a Hermitian multiplier $\mathbf{\Pi} : \mathbb{R} \to \mathcal{C}^{2m\times 2m}$, $\mathbf{\Pi} \in \mathcal{L}_\infty^{2m\times 2m}$ and the following partition

$$\mathbf{\Pi} = \begin{bmatrix} \mathbf{Q} & \mathbf{R} \\ \mathbf{R}^* & \mathbf{V} \end{bmatrix}, \tag{3.15}$$

having each block dimensions $m \times m$. Define

$$\mathbf{S}_l(\mathbf{\Pi}) := \{\mathbf{X} \in \mathbf{R}\mathcal{H}_\infty^{m\times m} : \sigma_l(\mathbf{X}(\omega), \mathbf{\Pi}(\omega)) \geq 0 \ \forall \omega \in \mathbb{R}\}, \tag{3.16}$$

This notational conventions allow us, e.g., to write condition (2.20) as

$$\sigma_l(\mathbf{Z}(j\omega), \Pi_d(j\omega)) \geq 0 \ \forall \omega \in \mathbb{R},$$

and, if $\mathbf{Z}$ is stable,

$$\mathbf{Z} \in \mathbf{S}_l(\Pi_d).$$

The convexity of the set $\mathbf{S}_l$ have strong consequences on the stability analysis, and are determined by some algebraic properties of multiplier $\mathbf{\Pi}$. The following lemma, whose proof is included in the Appendix B, is a direct consequence of the quadratic nature of the frequential constraint in (3.16):

Lemma 2. *If the multiplier $\mathbf{\Pi} \in \mathcal{L}_\infty^{2m\times 2m}$ satisfies*

$$\begin{bmatrix} 0 \\ I_m \end{bmatrix}^* \mathbf{\Pi}(\omega) \begin{bmatrix} 0 \\ I_m \end{bmatrix} \leq 0 \ \forall \omega \in \mathbb{R}, \tag{3.17}$$

then the set $\mathbf{S}_l(\mathbf{\Pi})$ is convex.

The following proposition is a particular formulation of the IQC Theorem (Theorem 1 in (Megretski and Rantzer, 1997)), specialized for the linear case. It allows us to extend the stability of a nominal interconnection to a set of operators belonging to a suitably defined set $\mathbf{S}_l(\mathbf{\Pi})$. The well-posedness of the interconnection is assumed.

Proposition 7. *Let $\mathbf{Z}_1(s) \in \mathbf{R}\mathcal{L}_\infty^{m\times m}, \mathbf{Y}_2(s) \in \mathbf{R}\mathcal{H}_\infty^{m\times m}$ such that the operator $\mathbf{Z}_1 \star \mathbf{Y}_2$ is internally stable. Assume the existence of a Hermitian multiplier $\mathbf{\Pi}(\omega) \in \mathcal{L}_\infty^{2m\times 2m}$ and a scalar $\epsilon > 0$ such that the following conditions are met $\forall \omega \in \mathbb{R}$:*

$$i. \qquad \sigma_l(\mathbf{Y}_2(j\omega), \mathbf{\Pi}(\omega)) \geq 0, \tag{3.18}$$

$$ii. \qquad \sigma_u(-\mathbf{Z}_1(j\omega), \mathbf{\Pi}(\omega)) \leq -\epsilon I, \tag{3.19}$$

$$iii. \qquad \begin{bmatrix} 0 \\ I_m \end{bmatrix}^* \mathbf{\Pi}(\omega) \begin{bmatrix} 0 \\ I_m \end{bmatrix} \leq 0. \tag{3.20}$$

Then, the feedback interconnection $\mathbf{Z}_1 \star \mathcal{Y}_2$ is internally stable for all operator $\mathcal{Y}_2 \in \mathbf{S}_l(\mathbf{\Pi})$ such that the pair $\mathbf{Z}_1, \mathcal{Y}_2$ satisfies Assumption 9.

The demonstration of Proposition 7, included in the Appendix B, rests heavily on the IQC theory. The reader unfamiliar with this theory surely would appreciate an independent discussion of Proposition 7, intended to show the main ideas behind it.

The Proposition studies the stability of the interconnection $\mathbf{Z}_1 \star \mathcal{Y}_2$, with $\mathcal{Y}_2 \in \mathbf{S}_l(\mathbf{\Pi})$. This interconnection is supposed well possed and the Assumption 9 assures the equivalence between the input-output and internal stability.

We will show first that the belonging of $\mathcal{Y}_2$ to $\mathbf{S}_l(\mathbf{\Pi})$ and condition (3.19) imply the absence of closed loop modes on the imaginary axis. These conditions can be written

$$\begin{cases} \sigma_l(\mathcal{Y}_2(j\omega), \mathbf{\Pi}(\omega)) & \geq & 0 \ \forall \omega \in \mathbb{R} \\ \sigma_u(-\mathbf{Z}_1(j\omega), \mathbf{\Pi}(\omega)) & \leq & -\epsilon I \ \forall \omega \in \mathbb{R} \end{cases}$$

The first inequality is maintained if we left and right multiply it by $\mathbf{Z}_1^*, \mathbf{Z}_1$. We also invert the second inequality to get:

$$\begin{cases} \mathbf{Z}_1(j\omega)^* \sigma_l(\mathcal{Y}_2(j\omega), \mathbf{\Pi}(\omega)) \mathbf{Z}_1(j\omega) & \geq & 0 \ \forall \omega \in \mathbb{R} \\ -\sigma_u(-\mathbf{Z}_1(j\omega), \mathbf{\Pi}(\omega)) - \epsilon I & \geq & 0 \ \forall \omega \in \mathbb{R} \end{cases}$$

By addition, we obtain

$$-\epsilon I + \mathbf{Z}_1(j\omega)^* \sigma_l(\mathcal{Y}_2(j\omega), \mathbf{\Pi}(\omega)) \mathbf{Z}_1(j\omega) - \sigma_u(-\mathbf{Z}_1(j\omega), \mathbf{\Pi}(\omega)) \geq 0 \ \forall \omega \in \mathbb{R}.$$

If we operate with partition (3.15) and definitions (3.14) we can get

$$-\epsilon I + \mathbf{Z}_1^* \mathbf{R} (I + \mathcal{Y}_2 \mathbf{Z}_1) + (I + \mathcal{Y}_2 \mathbf{Z}_1)^* \mathbf{R}^* \mathbf{Z}_1 + \mathbf{Z}_1^* \mathcal{Y}_2^* \mathbf{V} \mathcal{Y}_2 \mathbf{Z}_1 - \mathbf{V} \geq 0 \ \forall \omega \in \mathbb{R},$$

where we have omitted the dependence on ω to avoid cluttering. If we suitably factorize the last two terms, we obtain

$$-\epsilon I + \mathbf{Z}_1^* \mathbf{R} (I + \mathcal{Y}_2 \mathbf{Z}_1) + (I + \mathcal{Y}_2 \mathbf{Z}_1)^* \mathbf{R}^* \mathbf{Z}_1 +$$

$$+ (I + \mathcal{Y}_2 \mathbf{Z}_1)^* \frac{\mathbf{V}}{2} (-I + \mathcal{Y}_2 \mathbf{Z}_1) + (-I + \mathcal{Y}_2 \mathbf{Z}_1)^* \frac{\mathbf{V}}{2} (I + \mathcal{Y}_2 \mathbf{Z}_1) \geq 0 \ \forall \omega \in \mathbb{R}.$$

If we right and left multiply this matrix inequality by an arbitrary vector $v \in \mathbb{C}^m$ and v^* we can conclude that

$$(I + \mathcal{Y}_2 \mathbf{Z}_1) v \neq 0 \ \forall \omega \in \mathbb{R},$$

or, equivalently,

$$det(I + \mathcal{Y}_2(j\omega) \mathbf{Z}_1(j\omega)) \neq 0 \ \forall \omega \in \mathbb{R}.$$

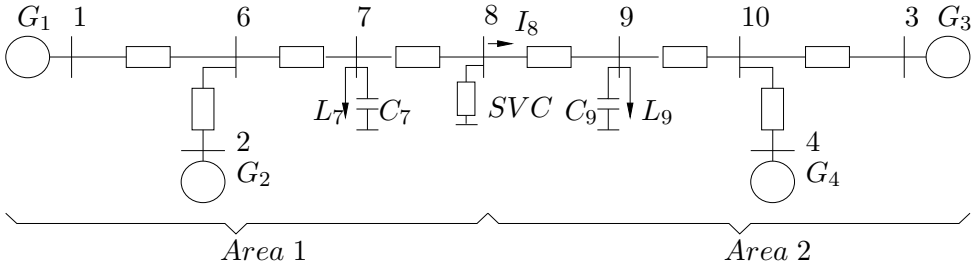

Figure 3.7: Two-area system.

This implies the absence of closed loop modes of $\mathbf{Z}_1 \star \mathcal{Y}_2$ on the imaginary axis.

So, the closed loop modes of $\mathbf{Z}_1 \star \mathcal{Y}_2$ do not cross the imaginary axis. The stability of $\mathbf{Z}_1 \star \mathbf{Y}_2$ locates the nominal modes on the left half plane. Notice that condition (3.20) and Lemma 2 ensure the convexity of the set $\mathbf{S}_l(\mathbf{\Pi})$. Thus, this set is *connected* and the map $\mathcal{Y}_2 \in \mathbf{S}_l(\mathbf{\Pi})$ can be reached by following a *continuous* path

$$\mathbf{Y}_2^{\mu} = (1-\mu)\mathbf{Y}_2 + \mu\mathcal{Y}_2, \mu \in [0,1],$$

that starts from the nominal, stable[3] system. In this way, the continuity of this transformation and the presence of the barrier on the imaginary axis for all $\mathcal{Y}_2 \in \mathbf{S}_l(\mathbf{\Pi})$ imply the stability of all interconnection $\mathbf{Z}_1 \star \mathcal{Y}_2$.

Remark 10. *Given $\mathbf{Z}_1, \mathbf{Y}_2$, the computation of a suitable multiplier Π satisfying conditions i-iii in Proposition 7 is a frequency dependent linear matrix inequality (FDLMI), i.e., a convex infinite dimensional problem. The problem, however, can be casted with the help of the Kalman-Yakubovic-Popov (KYP) lemma as a finite dimensional LMI problem, see (Megretski and Rantzer, 1997),(Rantzer, 1996).*

3.2.1 Example

This Section treats the application of the frequency domain properties derived in Section 2.2 to the robustness analysis with the help of Proposition 7. The analysis of a benchmark shows that the presence of excitation control and resistive elements does not completely destroy the dissipativity implications in the frequency domain, which remain valid in a significant frequency band associated to the electromechanical modes. The example includes a detailed robustness analysis showing the importance of the *a priori* knowledge of the dynamic properties of these models in the frequency band of interest.

[3]Notice that the assumption $\mathcal{Y}_2 \in \mathbf{R}\mathcal{H}_\infty$ is necessary. Otherwise, $\mathbf{Y}_2^{\mu=0}$ would have hidden unstable modes that will belong to RHP $\forall \mu \in [0,1]$.

Consider the system depicted in Fig. 3.7. It is based on the Example 12.6 in (Kundur, 1994) and includes a SVC. The system is split in two areas, with the bus 8 at the frontier. The SVC is associated to area 1. Linear models for both areas were computed with the program DSAT (Powertech Labs Inc., n.d.), by taking $\mathbf{v}_8$ and $\mathbf{i}_8$ as the interconnection variables.

The model of area 1 has the same parameters as (Kundur, 1994), included the non-zero machine resistances and transfer conductances. The excitation systems of machines G1 and G2, are given by the option iv) in (Kundur, 1994), i.e. high transient gain plus a standard setting for the PSS.

The SVC comprises a 200 MVAr fixed capacitor and a 0-200 MVAr thyristor-controlled reactor (TCR), see (Kundur, 1994), whose voltage regulator will be designed to ensure a proper voltage tracking and to improve the robust stability.

The area 2 is modeled fully in accordance with Assumptions 4-6, with $\mathbf{i}_8$ as output, see Fig. 3.7. The resistive losses in transmission lines and machines are neglected. Classical second order models are considered for generators G_3 and G_4. On the other hand, significant parametric variations are considered for the area 2, which are described below.

Design of the SVC voltage regulator The SVC is modeled as in Fig. 2.5 where the controller $k(s)$ includes a fixed time constant due to the converter. Notice that controller $k(s)$ must ensure the closed loop stability and the tracking requirements given by the slope of the voltage characteristic (set to 7 %) and a prescribed phase margin of approx. 45 degrees.

As area 2 satisfies Assumptions 4-6, by virtue of Proposition 3, $\mathbf{Y}_2$ satisfies

$$\sigma_l(\mathbf{Y}_2(j\omega), \Pi_d(j\omega)) \geq 0 \; \forall \omega \in \mathbb{R},$$

i.e. $\mathbf{Y}_2$ satisfies condition i in Proposition 7. It is convenient to mention that $\mathbf{Y}_2$ is stable and that condition iii in Proposition 7 is met by the multiplier Π_d, see definition (2.22). Thus, we will employ the SVC regulator $k(s)$ to ensure

$$\sigma_u(-\mathbf{Z}_1(j\omega), \Pi_d(j\omega)) \leq -\epsilon I, \forall \omega \in \Omega \tag{3.21}$$

for a set $\Omega \in \mathbb{R}$ as broad as possible. Notice that, by the structure of Π_d:

$$\sigma_u(-\mathbf{Z}_1(j\omega), \Pi_d(j\omega)) = \sigma_l(-\mathbf{Z}_1(j\omega), \Pi_d(j\omega)) =$$

$$= -\sigma_l(\mathbf{Z}_1(j\omega), \Pi_d(j\omega)).$$

Thus, in absence of control and resistive losses and because of Proposition 3, condition (3.21) would be true for $\epsilon = 0$ for all $\omega \in \mathbb{R}$. As it will be

shown below, the presence of excitation control, resistive loads and transmission losses restricts the band of frequencies where condition (3.21) is valid or feasible through the controller design. Thus, the multiplier Π_d will not be suitable to carry the robustness analysis via Proposition 7.

The constraints that (3.21) imposes on the gain $k(j\omega)$ for several frequencies are depicted in Fig. 3.8. The constraints were shown to be feasible for

$$\Omega = [\omega_l, \omega_h] = [0.38,\ 9.94].$$

This set can not be extended for lower frequencies due to voltage slope constraints nor for higher frequencies due to bandwidth limitations associated to the phase margin. However, this set Ω is, significantly, wide enough to include the system electromechanical local and interarea modes which range from 0.5 to 1.1 Hz (3.1 to 6.9 rad/sec). The SVC voltage regulator was obtained by loopshaping, see (Horowitz, 1993), and is given by

$$k(s) = \frac{6.5(s+1)}{(0.1s+1)(0.02s+1)}.$$

The plots in Figs. 3.9 and 3.10 show the resulting eigenvalues of the matrix $\sigma_l(-\mathbf{Z}_1(j\omega), \Pi_d(j\omega))$.

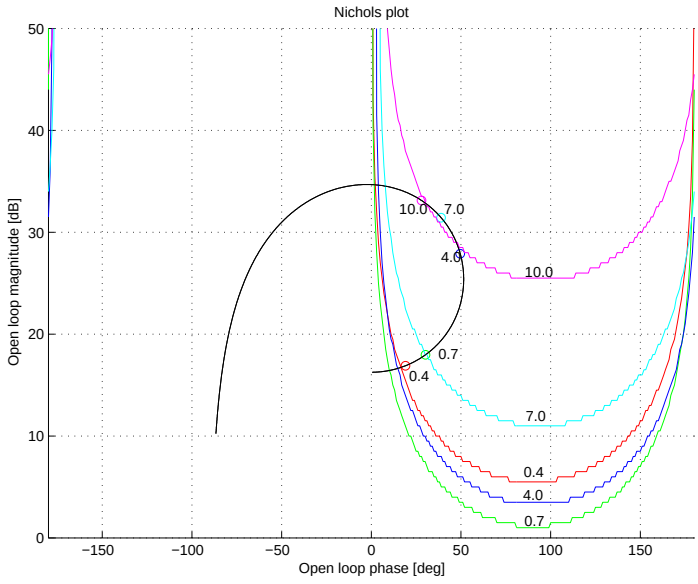

Figure 3.8: *SVC voltage regulator design. Nichols plot of* $k(j\omega)$ *and feasibility regions for* $\omega = \{0.4, 0.7, 4.0, 7.0, 10.0\}$ *rad/sec.*

Modeling of parametric uncertainty in area 2

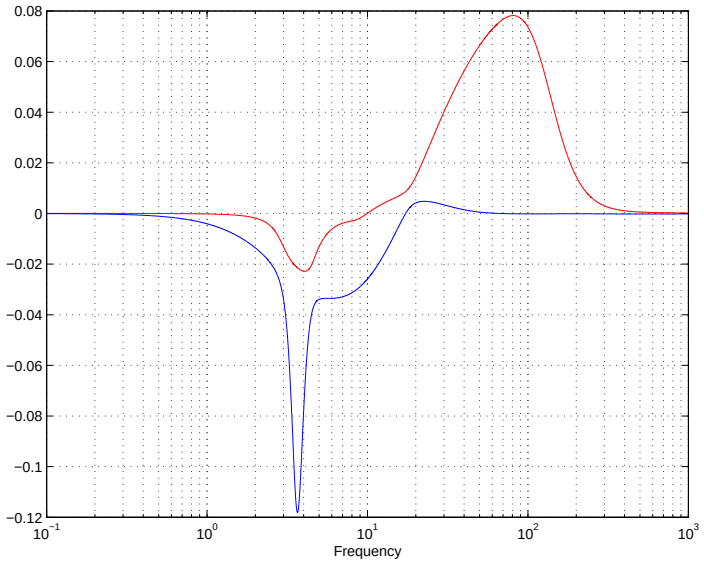

Figure 3.9: *Frequency domain condition for area 1. Eigenvalues of* $\sigma_l(-\mathbf{Z}_1(j\omega), \Pi_d(j\omega))$.

A set of scenarios for area 2 were considered, which are associated to two parameters: the voltage dependence of load L_9 and the transient reactance of machine G3. The reactive load $L9$ is supposed either constant impedance (case A), constant current (case B) or constant reactive power (case C). The transient reactance of generator G_3 is supposed to have values $X'_d \in [0.3, \lambda]$, being $\lambda \geq 0.3$ a figure of merit intended to compare some alternative approaches for the robustness analysis.

The choice of a set of eight values for the parameter X'_d and three for load L_9 results in $N = 24$ scenarios, each defined by the matrices (A_i, B_i, C_i, D_i) of the standard linear state space model. The corresponding matrices

$$M_i := \begin{bmatrix} A_i & B_i \\ C_i & D_i \end{bmatrix}, \ i = 1..N.$$

were approximated by the set

$$M_i = M_1 + \begin{bmatrix} P_1 \\ P_2 \end{bmatrix} \Delta [Q_1 \ Q_2]; i = 1..N$$

with M_1, P_1, P_2, Q_1, Q_2 fixed matrices and a variable block $\Delta_i \in R^{p \times p}, i = 1..N$. This approximation was carried with the help of an elementary singular value decomposition. The minimum size of blocks Δ_i for a good approximation is

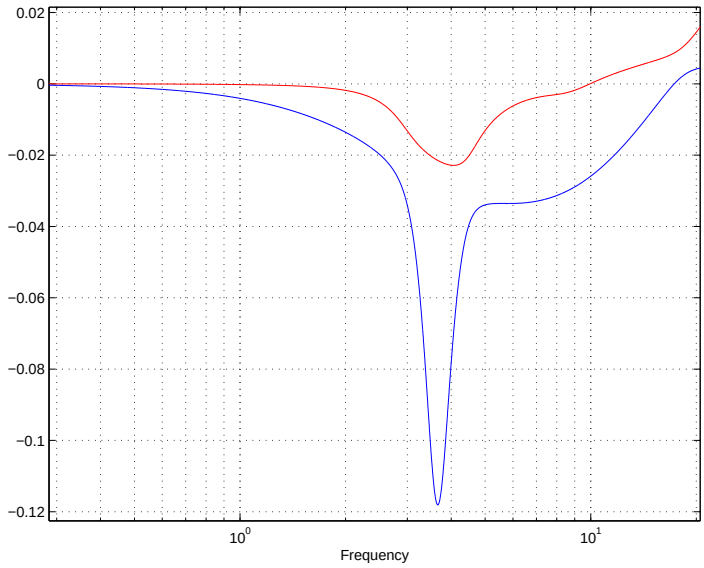

Figure 3.10: *Frequency domain condition for area 1. Detail.*

closely related with the number of independent parameters. In our case $p = 2$ was sufficient.

Finally, the area 2 is modeled as the polytope given by the N scenarios:

$$\begin{bmatrix} \dot{x} \\ \mathbf{i}_8 \end{bmatrix} = \left[M_1 + \begin{bmatrix} P_1 \\ P_2 \end{bmatrix} \Delta [Q_1 \; Q_2] \right] \begin{bmatrix} x \\ \mathbf{v}_8 \end{bmatrix}; \tag{3.22}$$

$$\Delta = \sum_{r=1}^{r=N} \alpha_r \Delta_r, \sum_r \alpha_r = 1, \alpha_r \geq 0. \tag{3.23}$$

that can also be written as the Linear Fractional Transformation[4] (LFT) of the nominal block $\mathbf{N}(s)$ and the uncertain block Δ depicted in Fig. 3.11, with

$$\mathbf{N}(s) = \left[\begin{array}{c|cc} A_1 & P_1 & B_1 \\ \hline Q_1 & 0 & Q_2 \\ C_1 & P_2 & D_1 \end{array}\right].$$

So, the overall uncertain system can be seen either as the interconnection of blocks Δ and $\mathcal{F}_l(\mathbf{N}, -\mathbf{Z}_1)$ at interface B, or the interconnection of $\mathcal{F}_u(\mathbf{N}, \Delta)$ with $(-\mathbf{Z}_1)$ at the interface A. It is necessary to highlight that model (3.23) considers all the continuous combinations of parameter X'_d and the ZIP model for load L_9.

[4]The reader is referred to (Zhou et al., 1996) for a detailed exposition of LFTs, that are briefly described in Appendix C.

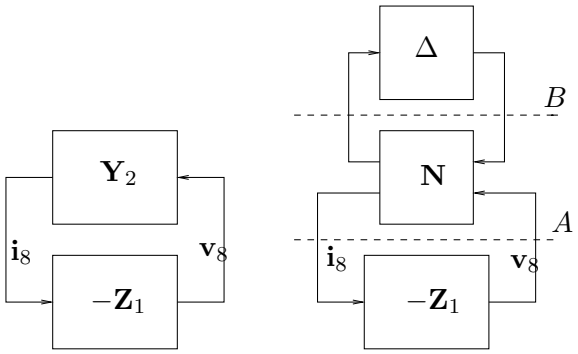

Figure 3.11: Feedback interconnections between subsystems $\mathbf{Z}_1$ and $\mathbf{Y}_2$.

The design of controller $k(s)$ of the SVC assures the nominal closed loop stability. The maps of area 1 and 2 are also nominally stable.

Robustness analysis

The stability of the feedback interconnection of area 1 and 2— given by equations (3.22),(3.23)—is analyzed with the help of Proposition 7. The problem is the computation of a suitable multiplier Π satisfying condition i) to iii).

The multiplier Π_d satisfies conditions i) and iii). However, it does not solve the problem since condition ii) is only satisfied for $\omega \in \Omega$.

Given the polytope description (3.23) for the area 2, it is convenient to consider the standard family of multipliers $\Pi_{pol} \in \mathbb{R}^{4\times 4}$, see (Megretski and Rantzer, 1997):

$$\Pi_{pol} = \left[\begin{array}{cc} Q & R \\ R^\top & V \end{array} \right]; Q = Q^\top; V = V^\top \tag{3.24}$$

such that

$$V \leq 0; \;\; Q + R\Delta_r + \Delta_r^\top R^\top + \Delta_r^\top V \Delta_r > 0, \forall r = 1..N. \tag{3.25}$$

This condition implies condition iii) for the multiplier Π_{pol} and

$$\sigma_l(\Delta, \Pi_{pol}) \geq 0,$$

i.e. condition ii) for all Δ satisfying (3.23). In a first instance the search for a suitable multiplier satisfying Proposition 7 were carried with multipliers of the family Π_{pol}. More precisely, the following computational problem was solved[5].

Problem 1 Find a multiplier $\Pi_{pol}^{\mathbb{R}}$ and $\epsilon > 0$ satisfying (3.24), (3.25) and

$$\sigma_u(\mathcal{F}_l(\mathbf{N}, -\mathbf{Z}_1)(j\omega), \Pi_{pol}^{\mathbb{R}}) \leq -\epsilon I, \forall \omega \in \mathbb{R}.$$

[5] $\mathcal{F}_l(\mathbf{N}, -\mathbf{Z}_1)$ denotes the lower linear fractional transformation between block $\mathbf{N}$ and $-\mathbf{Z}_1$, see Fig. 3.11

The existence of a solution for Problem 1 would allow us to apply Proposition 7–at interface B in Fig. 3.11–to establish the closed loop stability for all parametric variation. Problem 1 was formulated as a LMI via the KYP lemma, see (Megretski and Rantzer, 1997), and solved with the help of software package LMILAB (Gahinet et al., 1995). The extreme value of parameter λ for which the robust stability could be established is shown in Table 3.3. For comparison purposes, the stability of the interconnection was also studied by the computation of the eigenvalues of the dynamic matrix at a fine grid of scenarios. The extreme value, denote λ_{MAX} is also listed in Table 3.3.

Table 3.3: Extreme values of parameter λ for each technique of analysis

Problem 1 ($\Pi_{pol}^{\mathbb{R}}$)	Problem 2 (Π_{d+pol})	Problem 3 (Π_{pol}^{Ω})	Stability λ_{MAX}
0.32	2.53	0.32	2,548

As it can be observed, the analysis of robust stability based only with multiplier Π_{pol} is quite conservative. This is foreseeable, since the closed loop stability is also ensured for parameters α_r in equation (3.23) having an arbitrary temporal dependence $\alpha_r(t)$, see (Megretski and Rantzer, 1997).

In a second instance the search was confined to the frequency weighted sum of two members $\Pi_{pol}^{lf}, \Pi_{pol}^{hf}$ of the family Π_{pol}, trying to exploit the fact that the multiplier Π_d satisfies condition i), ii) and iii) of Proposition 7 in a significant band Ω. So, the structure of the multiplier Π was chosen

$$\Pi_{d+pol} = \mathbf{w}_{lf}(\omega)\Pi_{pol}^{lf} + \mathbf{w}_{hf}(\omega)\Pi_{pol}^{hf} \tag{3.26}$$

with the weights $\mathbf{w}_{lf}, \mathbf{w}_{hf}$ given by

$$\mathbf{w}_{lf} = \begin{cases} 1 & if\ |\omega| < \omega_l \\ 0 & otherwise \end{cases} ;\ \mathbf{w}_{hf} = \begin{cases} 1 & if\ |\omega| > \omega_h \\ 0 & otherwise \end{cases} .$$

In this way, the computation of the multiplier can now be relaxed to:

Problem 2 Find $\Pi_{pol}^{lf}, \Pi_{pol}^{hf}$ and $\epsilon > 0$ satisfying (3.24), (3.25), and

$$\sigma_u(\mathcal{F}_l(\mathbf{N}, -\mathbf{Z}_1)(j\omega), \Pi_{pol}^{lf}) \leq -\epsilon I, \forall |\omega| < \omega_l,$$

$$\sigma_u(\mathcal{F}_l(\mathbf{N}, -\mathbf{Z}_1)(j\omega), \Pi_{pol}^{hf}) \leq -\epsilon I, \forall |\omega| > \omega_h.$$

Problem 2 was also formulated as a LMI, by following the lines of the Generalized Kalman-Yakubovic-Popov lemma (GKYP), see reference (Iwasaki and

Hara, 2005). The maximum λ for which Problem 2 is feasible is also listed in Table 3.3. The solution of Problem 2 ensures the existence of multiplier Π_{d+pol} as in (3.26) that satisfies the hypotheses of Proposition 7–at the interface B of Fig.3.11–for all $\omega \notin \Omega$. As we know, the multiplier Π_d meets these conditions in Ω at the interface A. So, the Proposition 7 is not directly applicable. However, this does not constitute an essential obstacle. As we know, the Proposition 7 is based on three basic conditions: the nominal stability, the convexity of the set $\mathbf{S}_l$ and the existence of a barrier at the imaginary axis for the closed loop modes. In our example we simply conclude the existence of this barrier, by examining the interconnection at two different interfaces[6].

As it can be seen from Table 3.3, the procedure of splitting the frequency domain in three regions and taking into account the multiplier Π_d improved noticeably the results of the analysis. However, it is convenient to know if the improvement is due to the splitting in regions or to the use of multiplier Π_d. So, only for comparison purposes, it was computed the maximum λ such that the following problem remains feasible:

Problem 3 Find the multiplier Π_{pol}^{Ω} and $\epsilon > 0$ satisfying (3.24), (3.25) and

$$\sigma_u(\mathcal{F}_l(\mathbf{N}, -\mathbf{Z}_1)(j\omega), \Pi_{pol}^{\Omega}) \leq -\epsilon I, \forall \omega \in \Omega.$$

The result also can be read in Table 3.3 and seems to indicate that the difficulties in the assessment of robust stability with multipliers $\Pi_{pol}^{\mathbb{R}}$ resides precisely in the band Ω associated to the electromechanical modes and the associated resonances. The exploitation of multiplier Π_d, derived by analytical methods and valid in a sensible frequency band, allows to significantly improve the results of the analysis.

Figure 3.12 displays the stability regions able to be predicted by each choice of multiplier. The oblique region was determined by a careful choice of parameters once the stability boundary was computed directly. Significantly, the gap between the hard stability limit and the region able to be predicted by the simultaneous use of multiplier Π_{pol} and Π_d is very small.

Figure 3.13 depicts the loci of the most significant modes of the interconnection when the load L_9 is modeled with constant reactive power and x'_d varies in the interval $[0.3, 2.8]$ (notice that the maximum value exceeds λ_{MAX}). The local mode of area 1 remains unchanged as expected. The local mode of area 2

[6]The statements in this paragraph can be formally formulated and demonstrated. It is not done here because is beyond the scope of this thesis

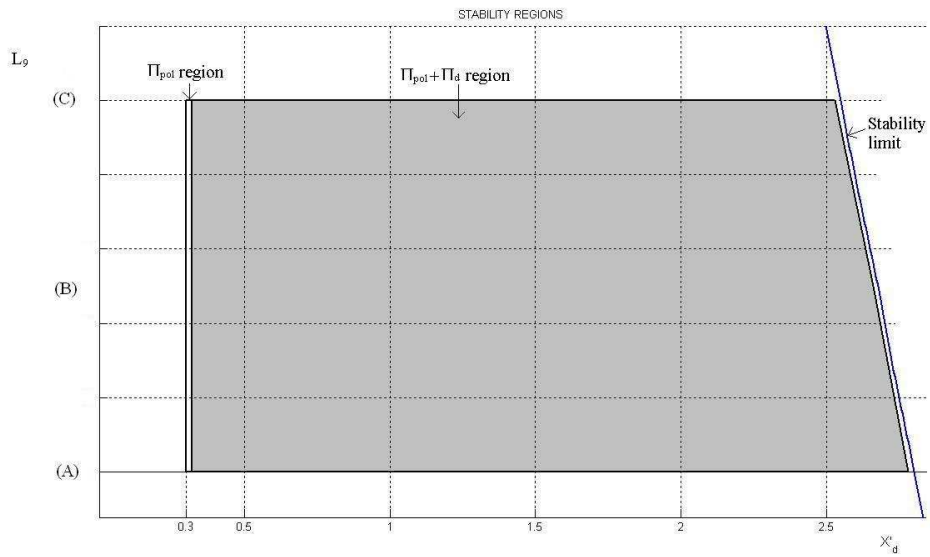

Figure 3.12: Stability regions. Space of parameter $X'_d - L_9$.

and the inter-area mode vary significantly but without crossing the imaginary axis because the barrier at the imaginary axis is valid even for greater values of λ for a suitable frequency band Ω. In this case, the stability is lost at frequency zero when a real mode turns unstable.

3.3 Some primary concluding remarks

These lines close in some sense a first part of this thesis. The analysis done up to this point is based on a class of power system models given mainly by Assumptions 4-6. We have shown in Chapter 2 that some important dynamic properties are valid for this class of power system. We indeed extended this class to include detailed models of synchronous machines and a class of controlled SVCs. We also have seen that these properties are not completely destroyed when some of the above-mentioned assumptions are not valid, see the example of Section 2.2.1.

We also have seen that the excitation control can be used to exploit the open loop cyclo-dissipativity of idealized models to ensure stability and improve performance even in the presence of resistive elements, Section 3.1. The articulation of the phase constraint in Proposition 3 with the IQC framework, Section 3.2, enables its use for robustness analysis and controller synthesis, as

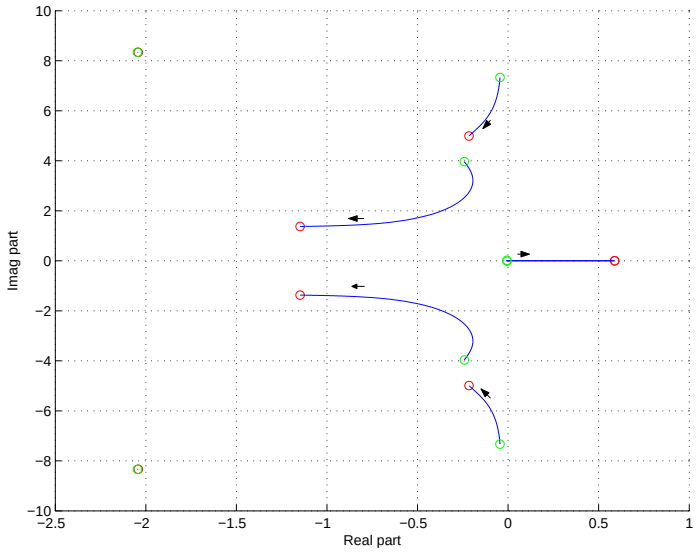

Figure 3.13: *Eigenvalue loci for power flow C,* $X'_d \in [0.3, 2.8]$. *Local, interarea and real modes.*

done in the previous example.

As it was already mentioned, the inclusion of resistive components and realistic models of voltage regulation compromises the cyclo–dissipativity. It is possible to appreciate that the frequency domain constraint, Proposition 3, is however preserved at the frequency band associated to the electromechanical modes. In addition, the stabilizing signals injected to the system at generators and FACTS act by *enforcing* the phase constraint on the frequency channel.

These observations and the will to study power system models closer to the real ones open the question on whether this concept of dissipativity can be modified to cope with classical control actions as voltage regulation and damping injection.

So, we will proceed to

abandon Assumptions 4-6,

restrict our analysis to linear models,

consider frequency constraints valid on a subset of the imaginary axis,

and characterize classical control actions of power systems,

with the objective of understand the mechanisms and effects of these control strategies on the system dynamic behavior. This is the content of the following chapter.

Chapter 4

Effects of damping and voltage regulation

The dynamic behavior of power systems is complex due, among other factors, to the interactions of multiple control actions, necessary to ensure proper performance and operation. However, in spite of their complexity, the controlled power systems typically exhibit a dynamic behavior relatively robust which allows them to keep stability when extreme conditions are not present. This fact is, of course, consequence of engineering control practices that have taken into account the underlying physical structure of the system. One example is the synthesis of control actions intended to improve the inherent damping behavior, see e.g. (Cigré, 1996; Commitee, 2004; Klein et al., 1992; Kundur, 1994; Stankovic et al., 1999). On the other hand the voltage regulation, although necessary to proper operation, introduces a new dynamics, absent in the open loop system.

This chapter examines some structural properties of realistic models of power systems that in certain conditions explain its robust properties. More precisely, the effect of the classical control actions on the robustness of electromechanical modes of power systems is examined. The analysis is done with independence of modeling details of the different controlled devices, by focusing on the effects of the classical control actions on the input-output maps of small signal models of power systems.

A first contribution is a generic, frequency domain characterization of the performance of voltage regulation and damping injection, which are discussed with the help of both numerical and analytical examples. These measures of control performance constitute quadratic constraints–on a finite band of frequencies–that have links with the phase constraint derived in Section 2.2,

and also with some familiar concepts in power system community.

The implications of these control actions on the system stability are then investigated through a procedure that, although based on IQCs, has some particularities. The chosen approach has the virtue of keeping direct links with the well known power system concepts mentioned above. In this way, it is shown that a certain balance between damping, voltage regulation and voltage sensitivity constitutes a sufficient condition for the robust stability of the electromechanical modes. This result is validated through the analysis of a classical example.

The control theory provides us with a valuable set of concepts and techniques that allows us to analyze the robustness of dynamic systems with respect to a broad class of uncertainties (Fan et al., 1991; Megretski and Rantzer, 1997). The power systems literature possesses significant contributions on the application of these tools, related modeling procedures and case studies (Abdel-Magid et al., 2000; Boukarim et al., 2000; Castellanos et al., 2006; Djukanovic et al., 1999; Pal and Chaudhuri, 2005). However, the above-mentioned vocation of linking the analysis with the classical control actions requires a specialized framework which constitutes an original contribution of this work. Four important observations are in order:

O1 The approach has no modeling limitations beyond the consideration of the small signal model around a stable equilibrium.

O2 Despite the use of concepts of the robust control theory strongly related with IQCs and real μ, (Fan et al., 1991; Megretski and Rantzer, 1997), the theoretical treatment is mostly self-contained.

O3 The quadratic constraints are satisfied only on a finite range of frequencies, strongly related with the validity range of the models used for transient stability analysis.

O4 The use of numerical optimization is purposely avoided, leading to results expressed in familiar terms to power systems community.

Section 4.1 presents some basic assumptions on power system modeling and basic notation. In Section 4.2 we introduce a characterization of the performance of voltage regulation and damping injection in terms of frequency domain properties of the input-output maps of generic devices, along with some

small examples intended to clarify the main ideas. These concepts are employed in Section 4.3 to derive sufficient conditions for the robust stability of electromechanical modes. Section 4.4 illustrates the application of these results to an example. Section 4.5 wraps up the chapter with some concluding remarks.

4.1 Power System Modeling

Variables at the equilibrium will be denoted with a supra-index $\star$: $\mathrm{V}^\star, \mathrm{I}^{d\star}$, etc. Lowercase will denote small signal variables:

$$\mathrm{v} := \mathrm{V} - \mathrm{V}^\star; v := \mathcal{V} - \mathcal{V}^\star; p^d := P^d - P^{d\star}; q^d := Q^d - Q^{d\star}.$$

The angle and frequency deviations of the bus voltage will be denoted $\vartheta := \theta - \theta^\star$ and $\lambda := \dot{\theta} = \dot{\vartheta}$. Given the equilibrium value for the bus voltage $\mathrm{V}^\star$, define the row vectors $k_v, k_\theta \in \mathbb{R}^2$

$$k_v := \frac{\mathrm{V}^{\star\top}}{\mathcal{V}^\star}, k_\theta := \frac{(J\mathrm{V}^\star)^\top}{\mathcal{V}^\star}. \tag{4.1}$$

Notice that the pair $k_v^\top, k_\theta^\top$ constitutes an orthonormal basis of $\mathbb{R}^2$, since $|k_v| = |k_\theta| = 1, k_v k_\theta^\top = 0$. So, if we define the matrix $U_\theta \in \mathbb{R}^{2\times 2}$

$$U_\theta := \begin{bmatrix} k_v \\ k_\theta \end{bmatrix} = \frac{1}{\mathcal{V}^\star} \begin{bmatrix} \mathrm{V}^{\star\top} \\ (J\mathrm{V}^\star)^\top \end{bmatrix} = \begin{bmatrix} \cos\theta^\star & \sin\theta^\star \\ -\sin\theta^\star & \cos\theta^\star \end{bmatrix}, \tag{4.2}$$

it follows

$$U_\theta^\top U_\theta = \begin{bmatrix} k_v^\top & k_\theta^\top \end{bmatrix} \begin{bmatrix} k_v \\ k_\theta \end{bmatrix} = \begin{bmatrix} k_v \\ k_\theta \end{bmatrix} \begin{bmatrix} k_v^\top & k_\theta^\top \end{bmatrix} = U_\theta U_\theta^\top = I_2. \tag{4.3}$$

Notice that U_θ is the matrix corresponding to the clockwise rotation by an angle θ in $\mathbb{R}^2$.

Our object of study is a generic shunt device given by the dynamic relation between the respective electrical variables at its terminal bus $e \in \mathbb{B}$, i.e. the phasors V_e and I_e^d. The word *device* is used here either to mean a power system component (a generator, a load, etc.) or a subsystem composed by the interconnection of several components through transmission lines. The input signals will be assumed belonging to the space $\mathcal{L}_2^e[0,\infty)$ and also ensuring the existence of the respective Laplace transforms. We will refer as *map* or *operator* to any function $\mathcal{L}_2^e[0,\infty) \to \mathcal{L}_2^e[0,\infty)$ which, for linear systems, involves

the transfer function and the Laplace transformation. The dynamic relation between the electrical variables is given by

$$\Sigma(\mathrm{I}_e^d, \mathrm{V}_e) : \begin{cases} \dot{X} &= f(X, \mathbf{V}) \\ 0 &= g(X, \mathbf{V}, \mathrm{I}_e^d), \end{cases} \tag{4.4}$$

where $X \in \mathbb{R}^n$ is the state vector and $\mathbf{V} := col_{j\in\mathbb{B}}\mathrm{V}_j$ is the voltage vector of all the buses in the subsystem, $e \in \mathbb{B}$ included. The functions $f : \mathbb{R}^n \times \mathbb{R}^{2m} \to \mathbb{R}^n$ and $g : \mathbb{R}^n \times \mathbb{R}^{2m} \times \mathbb{R}^2 \to \mathbb{R}^{2m}$ are supposed smooth enough to ensure, along with Assumptions 2-3, the existence and uniqueness of the solutions.

The above-mentioned assumptions ensure the existence of the small signal dynamical model

$$\begin{cases} \dot{x} &= Ax + B\mathrm{i}_e^d \\ 0 &= Cx + D\mathrm{i}_e^d - \mathrm{v}_e, \end{cases} \tag{4.5}$$

where the link variables were eliminated with the help of Assumption 2. The small signal dynamics can also be described in the Laplace domain by

$$\hat{\mathrm{v}}_e(s) = \mathbf{Z}(s)\hat{\mathrm{i}}_e^d(s) \ \forall \mathrm{i}_e^d \in \mathcal{L}_2^e, \tag{4.6}$$

$$Z(s) = \left[\begin{array}{c|c} A & B \\ \hline C & D \end{array}\right] := C(sI_n - A)^{-1}B + D.$$

The choice of currents as inputs and voltages as outputs is completely arbitrary, since that, except for some special cases that need be treated separately, the following assumption is fairly generic[1].

Assumption 10. *Given the map $Z(s)$ meeting (4.6), there exists a map $\mathbf{Y}(s) = \mathbf{Z}(s)^{-1}$ such that*

$$\hat{\mathrm{i}}_e^d(s) = \mathbf{Y}(s)\hat{\mathrm{v}}_e(s) \ \forall \mathrm{v}_e \in \mathcal{L}_2^e. \tag{4.7}$$

Classical studies of power systems stability often are based on simplified models where some variables are supposed constant. These models result in individual devices not having one of the linear maps $\mathbf{Z}, \mathbf{Y}$. This difficulty disappears when more complex systems are considered or when simple modeling modifications are done. The following assumptions establishes the non existence of poles of $\mathbf{Z}$ and $\mathbf{Y}$ on the set $j\Omega$.

Assumption 11. $\mathbf{Z} \in \mathbf{R}\mathcal{L}_\infty(\Omega)$.

Assumption 12. $\mathbf{Y} \in \mathbf{R}\mathcal{L}_\infty(\Omega)$.

[1]The existence of the inverse map is equivalent to the existence of matrix D^{-1} in (4.5).

4.2 Frequency domain characterization

This section is devoted to characterize the small signal response of power systems through three frequential functions directly related to voltage regulation, damping injection and voltage sensitivity. The analysis of the voltage regulation and damping is done with independence of modeling details, by focusing on the effects of these control actions on the map of the generic device. The power systems dynamics is composed by phenomena of different time scales, each related with different models and analysis tools. We will focus our attention on a certain subset of frequencies $\Omega \subset \mathbb{R}$ satisfying

Assumption 13. $\Omega \subset \mathbb{R}$ *is non empty, compact, bounded, and* $0 \notin \Omega$.

All future mention to set Ω supposes valid Assumption 13.

4.2.1 Voltage regulation

The primary objective of voltage regulation is to keep the variable $\mathcal{V} = |\tilde{V}|$ as constant as possible[2]. Since $\mathcal{V}^2 = V_R^2 + V_I^2$, we have

$$2\mathcal{V}^\star v = 2V_R^\star \mathrm{v}_R + 2V_I^\star \mathrm{v}_I,$$

and, if we use definition (4.1):

$$v = \frac{1}{\mathcal{V}^\star}(\mathrm{V}_R^\star \mathrm{v}_R + \mathrm{V}_I^\star \mathrm{v}_I) = \frac{\mathrm{V}^{\star T}}{\mathcal{V}^\star}\mathrm{v} = k_v \mathrm{v}. \tag{4.8}$$

We will introduce an auxiliary set of matrices. Be

$$\mathbb{U} := \{U \in \mathbb{C}^{2\times 2} \textit{invertible and } |\bar{\sigma}(U)| = 1\}, \tag{4.9}$$

and, given two invertible matrices $Z \in \mathbb{C}^{2\times 2}, U \in \mathbb{U}$ define the *regulation index* $g_r : \mathcal{C}^{2\times 2} \times \mathbb{U} \to \mathbb{R}$:

$$g_r(Z,U) := \frac{1}{||k_v Z U^{-1}||}. \tag{4.10}$$

The assumptions on Z, U implies that ZU^{-1} is invertible and hence g_r is well defined.

Let us define a set of matrix functions that will be used as spatial and frequency weights for the voltage regulation. Consider a set $\Omega \subset \mathbb{R}$ and define

$$\mathcal{U} := \{\mathbf{U} : \mathbb{R} \to \mathbb{C}^{2\times 2} \textit{ such that } \mathbf{U} \in \mathcal{L}_\infty(\Omega), \mathbf{U}(\omega) \in \mathbb{U} \ \ \forall \omega \in \Omega.\} \tag{4.11}$$

[2]Often, the variable to be controlled is $\mathcal{V}_c = |\tilde{V}_c| := |\tilde{V} - Z_c \tilde{I}^d|$ due to a control action known as load compensation (Kundur, 1994). The explicit consideration of this control action has no theoretical inconveniences.

Definition 2. Voltage regulation performance function *Given the set* Ω*, the map* $\mathbf{Z}$ *satisfying Assumptions* 10-13*, and a matrix function* $\mathbf{U} \in \mathcal{U}$*, we define the function* $\gamma_r : \mathbf{RL}_\infty^{2\times 2}(\Omega) \times \mathcal{U} \times \Omega \to \mathbb{R}^+$*:*

$$\gamma_r(\mathbf{Z}, \mathbf{U}; \omega) := g_r(\mathbf{Z}(j\omega), \mathbf{U}(\omega)), \forall\ \omega \in \Omega \tag{4.12}$$

which will be denoted Voltage regulation performance function *of the map* $\mathbf{Z}$ *(weighted by* $\mathbf{U}$*).*

The assumptions on $\mathbf{Z}$ and $\mathbf{U}$, along with the comment following the definition of function g_r imply that the function γ_r is well defined. The following lines are intended to illustrate the relation of the function γ_r with the concept of voltage regulation. We will omit the dependence of γ_r on $\mathbf{Z}$ and $\mathbf{U}$, in order to keep the notation as simple as possible. So, we will use the brief notation

$$\gamma_r(\omega) := \gamma_r(\mathbf{Z}, \mathbf{U}; \omega).$$

Definition (4.12) implies

$$\gamma_r^{-2}(\omega) = ||k_v \mathbf{Z}(j\omega)\mathbf{U}(\omega)^{-1}||^2 = \max_{y\in\mathbb{C}^2, ||y||\neq 0} \frac{||k_v \mathbf{Z}(j\omega)\mathbf{U}(\omega)^{-1} y||^2}{||y||^2} =$$

$$= \max_{x\in\mathcal{C}^2, ||\mathbf{U}x||\neq 0} \frac{||k_v \mathbf{Z}(j\omega)x||^2}{||\mathbf{U}(\omega)x||^2}.$$

Thus, for all vector $x \in \mathbb{C}^2$

$$|k_v \mathbf{Z}(j\omega)x|^2 \leq \gamma_r(\omega)^{-2} ||\mathbf{U}(\omega)x||^2 \forall \omega \in \Omega.$$

So, if we chose $x = \hat{\mathrm{i}}^d(j\omega)$ with $\mathrm{i}^d \in \mathcal{L}_2^e$ arbitrary, and we recall equations (4.6) and (4.8), we get

$$|k_v \mathbf{Z}(j\omega)x|^2 = |k_v \mathbf{Z}(j\omega)\hat{\mathrm{i}}^d(j\omega)|^2 = |k_v \hat{\mathrm{v}}(j\omega)|^2 = |\hat{v}(j\omega)|^2,$$

and thus

$$|\hat{v}(j\omega)| \leq \frac{1}{\gamma_r(\omega)} ||\mathbf{U}(\omega)\hat{\mathrm{i}}^d(j\omega)||\ \ \forall \omega \in \Omega,\ \forall \mathrm{i}^d \in \mathcal{L}_2^e. \tag{4.13}$$

This inequality describes the role of the current as the disturbance for the voltage regulation. For a power system device having voltage regulation, e.g. a generator, the function γ_r and the matrix $\mathbf{U}(\cdot)$ capture the frequential and spatial nature of the action of current i^d on the voltage v. Slow variations of the current deviations should be easily compensated by the control action, which results in a weight $\gamma_r(\omega)$ relatively big at lower frequencies. On the other hand, small deviations of the current $\tilde{I}_d$ in phase with voltage $\tilde{V}^\star$ should have a minor

influence on the voltage magnitude. This fact can be taken into account with the help of the weight $\mathbf{U}$. The function γ_r can be seen as a figure of merit of the control action: γ_r gets bigger as the voltage tracking performance gets better.

The function $U(\cdot)$ provides a spatial characterization of the voltage regulation, able to be exploited[3] for robustness analysis in Section 4.3. The following example shows the analytical calculation of γ_r of a typical Static Var Compensator (SVC).

Voltage regulation performance of a SVC

Consider the model introduced in the Section 2.3, depicted in Figs. 2.4 and 2.5. The small signal model is given by its admittance transfer matrix $\mathbf{Y}^S(s)$, equation (2.33). The impedance transfer matrix $\mathbf{Z}^S$ can be computed

$$\mathbf{Z}^S(s) = \mathbf{Y}^S(s)^{-1} = \{J[B_C - B_L b^\star] - \frac{B_L k(s)}{\mathcal{V}^\star} \mathrm{V}^\star \mathrm{V}^{\star\top}\}^{-1}.$$

Denoting $B_S^\star := [B_C - B_L b^\star]$, recalling definitions (4.1), and doing some algebraic computations, we obtain

$$\mathbf{Z}^S = -\frac{1}{\Delta(s)}[B_S^\star I_2 + \frac{B_L}{\mathcal{V}^\star} k(s)(J\mathrm{V}^\star)(J\mathrm{V}^\star)^\top]J,$$

with

$$\Delta(s) := B_S^\star [B_S^\star + \frac{B_l}{\mathcal{V}^\star} k(s)].$$

Compute

$$k_v \mathbf{Z}^S = -\frac{B_S^\star}{\Delta(s)} k_v J = -\frac{1}{[B_S^\star + \frac{B_l}{\mathcal{V}^\star} k(s)]} k_v J.$$

So, if we take $U = I_2$, it follows

$$\gamma_r(\mathbf{Z}^S, I_2; \omega) = ||k_v \mathbf{Z}^S(j\omega)||^{-1} = |B_S^\star + \frac{B_l}{\mathcal{V}^\star} k(j\omega)|,$$

which evidences the direct effect of the controller $k(s)$ on the voltage regulation.

4.2.2 Stabilizing control actions

We consider now those control actions typically used in power systems to improve the damping of the electromechanical modes. Examples of these control actions are the *Power System Stabilizers* (PSS), the stabilizing signals at SVC, and also the rotorical damping circuits of the synchronous machines, see (Anderson and Fouad, 1993; Kundur, 1994). By abstracting technical details about each device, it is possible to conclude that all these control actions are

[3] When such spatial weighting is not of interest, it can be taken $\mathbf{U} = I_2$.

intended to provide an incremental generated active power opposite in phase with the frequency deviations at least in a certain frequency band Ω, see e.g. (Kundur et al., 1989; Lee et al., 1981).

Our objective is to obtain a definition of damping able to be characterized as a constraint on the map $\mathbf{Z}$. The main difficulty is that the damping is normally expressed in terms of active power p^d and voltage angle θ, variables whose dependence on $\mathbf{Z}$ is not direct.

By reasons that will be clear later, we focus our attention on the set of input vectors $\hat{\mathrm{i}}^d$ that cause no small signal variation in voltage magnitude v. Define

$$\mathcal{I}_{v=0} = \{\hat{\mathrm{i}}^d \in \mathcal{L}_2^e : \hat{v}(s) = k_v \mathbf{Z}(s)\hat{\mathrm{i}}^d(s) \equiv 0\}. \tag{4.14}$$

It is necessary to consider the polar description of the small signal voltage $\tilde{v}$. With the help of equations (1.4), (1.5), (1.6), and (4.1) compute

$$\mathcal{V}^\star \vartheta = \mathcal{V}^\star \frac{\partial \theta}{\partial \mathrm{V}_R}\mathrm{v}_R + \mathcal{V}^\star \frac{\partial \theta}{\partial \mathrm{V}_I}\mathrm{v}_I = \frac{1}{\mathcal{V}^\star}[-\mathrm{V}_I^\star \;\; \mathrm{V}_R^\star]\mathrm{v} = \frac{(J\mathrm{V}^\star)^\top}{\mathcal{V}^\star}\mathrm{v} = k_\theta \mathrm{v}. \tag{4.15}$$

Let us denote u the small signal polar description of phasor $\tilde{V}$:

$$u := \begin{bmatrix} v \\ \mathcal{V}^\star \vartheta \end{bmatrix} = \begin{bmatrix} k_v \\ k_\theta \end{bmatrix} \mathrm{v} = U_\theta \mathrm{v}, \tag{4.16}$$

where definitions (4.1) and (4.2) were employed. The inverse relationship between u and v is given by

$$\mathrm{v} = \begin{bmatrix} k_v^\top & k_\theta^\top \end{bmatrix} u = U_\theta^\top u. \tag{4.17}$$

Thus, the map $u \to i^d$ is given by

$$\hat{\mathrm{i}}^d = \mathbf{Y}\hat{\mathrm{v}} = \mathbf{Y}U_\theta^\top \hat{u} = \mathbf{Y}\begin{bmatrix} k_v^\top & k_\theta^\top \end{bmatrix}\hat{u} = \mathbf{Y}k_v^\top \hat{v} + \mathbf{Y}k_\theta^\top \mathcal{V}^\star \hat{\vartheta}. \tag{4.18}$$

We define an auxiliary function $g_d : \mathbb{C}^{2\times 2} \times \Omega \to \mathbb{R}$:

$$g_d(Y, \omega) := \frac{j\omega}{\omega^2}[-k_v Y k_\theta^\top + k_\theta Y^* k_v^\top] = \frac{2}{\omega} Im(k_v Y k_\theta^\top), \tag{4.19}$$

that enable us to define the

Definition 3. Damping performance function *Given the set Ω and the maps $\mathbf{Z}, \mathbf{Y}$ satisfying Assumptions* 10-13*, we define the function $\gamma_d : \mathbf{R}\mathcal{L}_\infty^{2\times 2}(\Omega) \times \Omega \to \mathbb{R}$:*

$$\gamma_d(\mathbf{Y}; \omega) := g_d(\mathbf{Y}(j\omega), \omega) \;\forall \omega \in \Omega. \tag{4.20}$$

The function γ_d will be denoted Damping performance function *of the map $\mathbf{Y}$.*

Notice that the assumptions on $\mathbf{Y}$ and Ω ensure $\gamma_d \in \mathcal{L}_\infty(\Omega)$. The reason for considering γ_d to describe the damping performance is clarified in next lemma. We denote $\gamma_d(\omega) := \gamma_d(\mathbf{Y};\omega)$ by brevity and recall that the frequency λ of the voltage phasor was defined at the beginning of Section 4.1.

Lemma 3. Damping performance *Given the set Ω and the map $\mathbf{Y}$ satisfying Assumptions* 10-13*, it is satisfied*

$$Re[(\hat{p}^d(j\omega))^*\hat{\lambda}(j\omega)] = \frac{1}{2}\mathcal{V}^{\star 2}\gamma_d(\omega)|\hat{\lambda}(j\omega)|^2 \ \forall\omega\in\Omega, \forall\hat{\mathrm{i}}^d \in \mathcal{I}_{v=0}. \tag{4.21}$$

Proof. Equation (1.5) allows us to compute the small signal component of the active power:

$$p^d = \mathrm{V}^{\star\top}\mathrm{i}^d + (\mathrm{I}^{d\star})^\top \mathrm{v}.$$

By invoking equations (4.16) and (4.17),

$$p^d = \mathrm{V}^{\star\top}\mathrm{i}^d + (\mathrm{I}^{d\star})^\top \begin{bmatrix} k_\theta^\top & k_v^\top \end{bmatrix} \begin{bmatrix} \mathcal{V}^\star\vartheta \\ v \end{bmatrix} = \mathrm{V}^{\star\top}\mathrm{i}^d + (\mathrm{I}^{d\star})^\top[J\mathrm{V}^\star\vartheta + \frac{\mathrm{V}^\star}{\mathcal{V}^\star}v].$$

If we recall equations (4.1) and (1.5), we can write

$$p^d = \mathrm{V}^{\star\top}\mathrm{i}^d + Q^d\vartheta + \frac{P^d}{\mathcal{V}^\star}v \ \forall\mathrm{i}^d \in \mathcal{L}_2^e.$$

The same relation can be written in a more compact way with the help of equations (4.16) and (4.18):

$$\hat{p}^d = \mathrm{V}^{\star\top}\hat{\mathrm{i}}^d + Q^{d\star}\hat{\vartheta} + \frac{P^{d\star}}{\mathcal{V}^\star}\hat{v} = \mathrm{V}^{\star\top}\mathbf{Y}U_\theta^\top\hat{u} + \frac{1}{\mathcal{V}^\star}\begin{bmatrix} P^{d\star} & Q^{d\star} \end{bmatrix}\hat{u}, \ \forall\mathrm{i}^d \in \mathcal{L}_2^e, \tag{4.22}$$

or, equivalently

$$\hat{p}^d = [\mathrm{V}^{\star\top}\mathbf{Y}k_v^\top + \frac{P^{d\star}}{\mathcal{V}^\star}]\hat{v} + [\mathrm{V}^{\star\top}\mathbf{Y}k_\theta^\top\mathcal{V}^\star + Q^{d\star}]\hat{\vartheta}, \ \forall\mathrm{i}^d \in \mathcal{L}_2^e, \tag{4.23}$$

If we focus on the case $\hat{\mathrm{i}}^d \in \mathcal{I}_{v=0}$, we have $\hat{v} \equiv 0$ and

$$\hat{p}^d = \mathrm{V}^{\star\top}\mathbf{Y}(j\omega)k_\theta^\top\mathcal{V}^\star\hat{\vartheta} + Q^{d\star}\hat{\vartheta} = [\mathrm{V}^{\star\top}\mathbf{Y}(j\omega)k_\theta^\top\mathcal{V}^\star + Q^{d\star}]\frac{\hat{\lambda}}{j\omega}, \forall\hat{\mathrm{i}}^d \in \mathcal{I}_{v=0},$$

since $\hat{\lambda} = j\omega\hat{\vartheta}$. Thus

$$Re[\hat{p}^{d*}\hat{\lambda}] = Re[\hat{p}^d\hat{\lambda}^*] = Re[\frac{1}{j\omega}\mathrm{V}^{\star\top}\mathbf{Y}(j\omega)k_\theta^\top\mathcal{V}^\star]|\hat{\lambda}|^2, \forall\hat{\mathrm{i}}^d \in \mathcal{I}_{v=0}.$$

By recalling definitions (4.1), we have

$$Re[\hat{p}^{d*}\hat{\lambda}] = \mathcal{V}^{\star 2}Re[\frac{1}{j\omega}k_v\mathbf{Y}(j\omega)k_\theta^\top]|\hat{\lambda}|^2 = \frac{\mathcal{V}^{\star 2}}{\omega}Im[k_v\mathbf{Y}(j\omega)k_\theta^\top]|\hat{\lambda}|^2 \forall\hat{\mathrm{i}}^d \in \mathcal{I}_{v=0}.$$

The proof concludes recalling the definition of γ_d, equations (4.19),(4.20). □□□

Notice that, for all complex numbers $v, w \in C,$, the expression $Re[v^* w] = |v||w|\cos(\theta_v - \theta_w)$, weights the projection of the complex v on the direction of w. Notice also that the influence of voltage variations v on the quantity $Re[(\hat{p}^d)^* \hat{\lambda}]$ is specifically avoided in the definition since all variables in equation (4.21) are computed for the case $v = 0$. The function γ_d allows us to quantify the component of the active power p^d in phase with the frequency deviations λ.

It is a common practice to assume constant bus voltage in certain controlled devices to perform some simplified analysis. In such cases, the maps that describe the device have less dimension and the procedures above employed do not apply directly. The classical synchronous machine model is one of these cases, since it establishes only the relation between p^d and λ, see (Anderson and Fouad, 1993; Kundur, 1994). We consider this case next to clarify the main ideas behind the definition of γ_d, albeit it is not directly applicable.

Classical generator model Consider the classical model with constant e.m.f. behind the transient reactance:

$$\begin{cases} \dot{\delta} = \lambda \\ \frac{2H}{\Omega_0}\dot{\lambda} + \frac{K_D}{\Omega_0}\lambda = P_m + P^d. \end{cases}$$

In the small signal setting, the angle dynamics can be written

$$\hat{p}^d = j\omega\frac{2H}{\Omega_0}\hat{\lambda} + \frac{K_D}{\Omega_0}\hat{\lambda}.$$

Compute

$$Re[(\hat{p}^d)^*\hat{\lambda}] = Re[(-j\omega\frac{2H}{\Omega_0}|\hat{\lambda}|^2 + \frac{K_D}{\Omega_0}|\hat{\lambda}|^2)] = \frac{K_D}{\Omega_0}|\hat{\lambda}|^2. \tag{4.24}$$

Examine the previous equation and Lemma 3. The idea behind the damping performance function γ_d is to capture the classical concept of damping even for complex, controlled devices. So, beyond some constant factors, the function γ_d plays the role of the classical damping coefficient k_D. Its usefulness for a realistic synchronous machine model will be illustrated in section 4.2.4 with a numerical example.

4.2.3 Voltage sensitivity of active power

The small signal deviations of active power around the equilibrium can be computed with the help of equation (4.23). Recall definition (4.1) and write, for the case $\vartheta \equiv 0$:

$$\hat{p}^d = [\mathcal{V}^\star k_v Y k_v^\top + \frac{P^{d\star}}{\mathcal{V}^\star}]\hat{v}. \tag{4.25}$$

We define the auxiliary function $g_g : \mathbb{C}^{2\times 2} \to \mathbb{R}$:

$$g_g(Y) := |k_v Y k_v^\top + \frac{P^{d\star}}{\mathcal{V}^{\star 2}}|, \tag{4.26}$$

that enable us to define the

Definition 4. Voltage sensitivity function *Given the set* Ω *and the maps* $\mathbf{Z}, \mathbf{Y}$ *satisfying Assumptions* 10-13*, we define the function* $\gamma_g : \mathbf{R}\mathcal{L}_\infty^{2\times 2}(\Omega)\times\Omega \to \mathbb{R}$*:*

$$\gamma_g(\mathbf{Y};\omega) := g_g(\mathbf{Y}(j\omega)) \; \forall \omega \in \Omega, \tag{4.27}$$

that will be denoted Voltage sensitivity function *of the map* $\mathbf{Y}$ *.*

The reasons for such denomination are clear from equation (4.25): γ_g is proportional to the module of the transfer function between the voltage deviations v and the active power p^d. The voltage sensitivity of the power system loads has a very significant effect on the damping of power system oscillations, see e.g. (Klein et al., 1992).

Remark 11. *Notice that the sensitivity depends directly on the equilibrium value of the active power. However, when all subsystems interconnected at a single bus are considered jointly, it is satisfied* $\sum_d P_j^{d\star} = 0$*. If we denote* $\mathbf{Y}_j^d$ *the respective input-output maps of each device, we have*

$$\gamma_g(\sum_d \mathbf{Y}_j^d) := |k_v \sum_d \mathbf{Y}_j^d k_v^\top + \sum_d P_j^{d\star}| = |k_v \sum_d \mathbf{Y}_j^d k_v^\top|,$$

and the effect of the individual active powers $P_j^{d\star}$ *is canceled.*

4.2.4 Some examples

The Figure 4.1 displays the function γ_r for the generator G_1 of the Example 12.6 in (Kundur, 1994) in three cases: constant excitation, AVR gain $K_A = 20$, and $K_A = 200$. As it can be seen, γ_r is essentially proportional to the gain at low frequencies and converges to the open loop response at high frequencies. The addition of a PSS, not shown, has little effect.

The analysis of the function γ_d in Figure 4.2 evidences the effect of the damping windings at frequencies about 10 rad/sec. The damping of the synchronous machine with constant excitation is always positive, with small values at low frequency. The inclusion of a positive value for the damping parameter $K_D = 1$ is very noticeable at low frequencies, where γ_d exhibits an almost constant value that coincides with (4.24). The effect of the AVR with gain

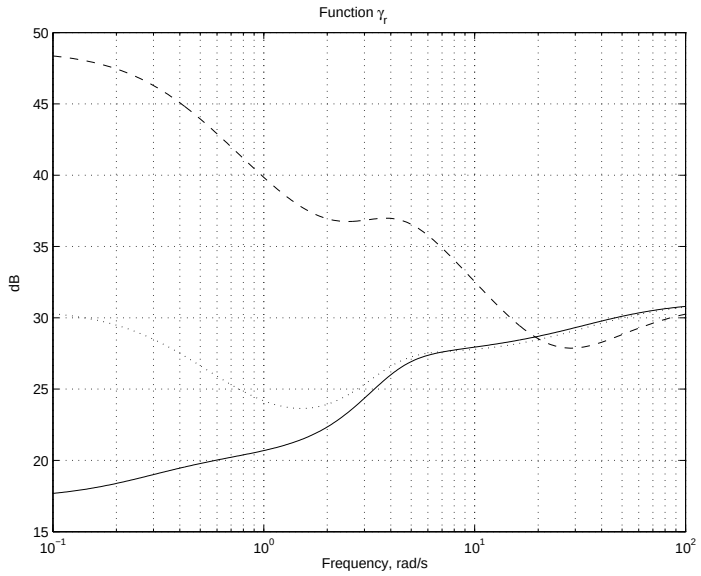

Figure 4.1: *Function γ_r, in dB, for different excitation systems: constant excitation (solid), $K_A = 200$ (dashed), $K_A = 20$ (dotted).*

$K_A = 200$ in absence of PSS (case $K_S = 0$) exhibits a worsening of the damping at low frequencies where it take negative values[4]. This effect of the AVR on the function γ_d can be interpreted in a similar way to the conclusions of the classical paper (DeMello and Concordia, 1969) about the effect of the AVR on the equivalent damping coefficient. The effect of increasing values of the PSS gain on the function γ_d is clearly positive. It is also possible to appreciate a moderate effect of the PSS on the synchronizing factor, see (DeMello and Concordia, 1969), that is evidenced here by the shifting to higher frequencies of the electromechanical resonance. From the standpoint of the control technology, it is noticeable that, while the AVR has a positive effect on the regulation and one negative on the damping, the PSS improves the damping with no appreciable effect on the voltage regulation.

The similarities of our analysis with the conclusions of the reference (DeMello and Concordia, 1969) must not be misunderstood since our definition of damping is different and has other objectives. The comments above are intended to provide links with concepts well known in the power system community.

The role of the static loads is also interesting for this analysis. Consider the

[4]Although the plot is logarithmic, the change of signal is evidenced by the zero crossing at $\omega \approx 0.08$ rad/sec.

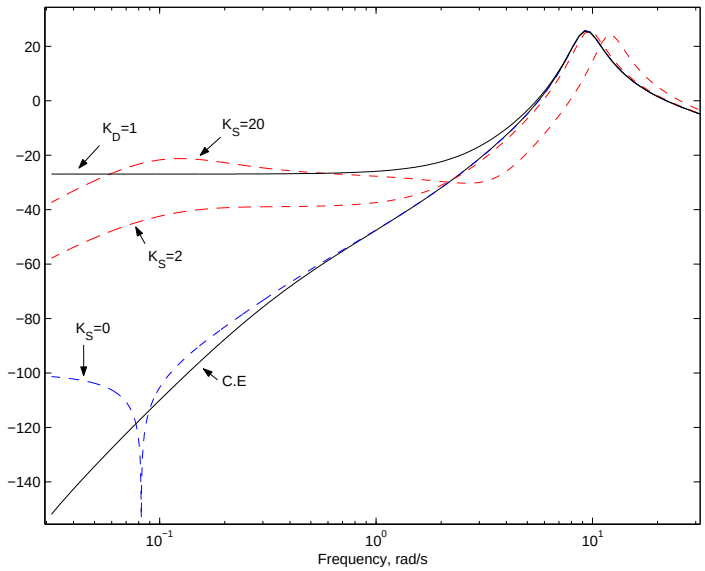

Figure 4.2: *Function γ_d, in dB, for different excitation systems: constant excitation (CE); constant excitation with $K_D = 1$; PSS gain $K_S = 20, 2, 0$.*

generic, standard model (Kundur, 1994)

$$\begin{aligned} P^d &= P^\star[p_1(\tfrac{V}{V^\star})^2 + p_2\tfrac{V}{V^\star} + p_3][1 + k_{pf}\Delta f] \\ Q^d &= Q^\star[q_1(\tfrac{V}{V^\star})^2 + q_2\tfrac{V}{V^\star} + q_3][1 + k_{qf}\Delta f] \end{aligned},$$

with Δf the frequency deviations, in p.u., of the bus voltage. The respective portions of constant impedance, current and power satisfy

$$\sum_{i=1}^{3} p_i = 1, \sum_{i=1}^{3} q_i = 1, p_i \geq 0, q_i \geq 0 \; \forall i = 1..3.$$

The coefficients k_{pf} and k_{qf} are the respective sensitivities of active and reactive power loads to frequency deviations. In the Appendix D the small signal model

$$Y_{ZIP} = \frac{1}{V^{\star 2}} U_\theta^\top \{ \begin{bmatrix} P^\star(p_1 - p_3) & Q^\star \\ -Q^\star(q_1 - q_3) & P^\star \end{bmatrix} + \frac{j\omega}{2\Pi f_0} \begin{bmatrix} 0 & P^\star k_{pf} \\ 0 & -Q^\star k_{qf} \end{bmatrix} \} U_\theta,$$

is computed. The application of Definitions 3, 4 allows us to determine the damping and voltage sensitivity functions

$$\gamma_d(Y_{ZIP}; \omega) = \frac{2}{\omega} Im[k_v Y_{ZIP} k_\theta^\top] = \frac{P^\star}{\Pi f_0 V^{\star 2}} k_{pf}, \tag{4.28}$$

$$\gamma_g(Y_{ZIP}) = |k_v Y_{ZIP} k_v^\top + \frac{P^\star}{V^{\star 2}}| = |\frac{P^\star}{V^{\star 2}}(p_1 - p_3) + \frac{P^\star}{V^{\star 2}}|. \tag{4.29}$$

Remark 12. *As it can be appreciated from equations (4.28) and (4.29), the damping performance is only affected by the term k_{pf}, i.e. the sensitivity of the active power load to frequency deviations. On the other hand, the effect of the constant impedance term on the voltage sensitivity is equal and opposite to the one due to the constant power. So, the quantity $|k_v Y_{ZIP} k_v^\top|$–that, by the reasons mentioned in Remark 11, is the one really significant in our analysis–reaches its minimum, vanishes, for $p_1 = p_3$.*

4.3 Stability analysis

In this section we examine the use of the functions defined in Section 4.2 for the stability analysis of interconnections of power systems models. The approach is based on the use of multipliers and quadratic constraints in the frequency domain, (Doyle, 1982; Fan et al., 1991; Megretski and Rantzer, 1997). Although the control theory is fairly mature in these topics, we adopt a specialized approach because of the following reasons:

R1 We are focusing on a specialized set of linear systems: square, invertible and having a dynamic behavior strongly affected by damping injection and voltage regulation.

R2 The conventional approach via IQCs requires a set of conditions to be met for all frequency $\omega \in \mathbb{R}$, while our interest is focused on the frequency band associated to the electromechanical modes.

R3 We will try to limit the use of generic multipliers as optimization variables in order to keep a direct link with variables having a direct engineering meaning, like those introduced in Section 4.2.

The object under study is the interconnection of linear systems $\mathbf{Z}_1, \mathbf{Y}_2$ depicted in Fig. 3.2 and given by equation 3.12.

Albeit we are studying the same interconnection that in Section 3.2, in this chapter we are interested in weaker dynamic properties–the stability of a given set of closed loop modes–, departing from laxer conditions to be met by the open loop maps. So, we will work with a set $\Omega \subset \mathbb{R}$ satisfying Assumption 13, and with $\mathbf{Z}_1$ and $\mathbf{Y}_2$ linear, time-invariant operators with transfer functions[5] $\mathbf{Z}_1(s), \mathbf{Y}_2(s) \in \mathbf{R}\mathcal{L}_\infty^{m\times m}(\Omega)$.

[5]Sections 4.1 and 4.2 were focused on the case $m = 2$. The results in this section are nevertheless valid for the general case.

Assumption 9 is a very reasonable hypothesis that we will suppose valid, which implies Lemma 1.

Consider a Hermitian multiplier $\mathbf{\Pi} : \mathbb{R} \to \mathcal{C}^{2m\times 2m}$ bounded on $j\Omega$, i.e. $\mathbf{\Pi} \in \mathcal{L}_\infty(\Omega)$. Consider also a constant matrix $\Pi \in \mathbb{C}^{2m\times 2m}$, and define the sets

$$\mathcal{S}_l(\Pi) := \{X \in \mathbb{C}^{m\times m} : \sigma_l(X, \Pi) \geq 0\}, \tag{4.30}$$

$$\mathbf{S}_l(\mathbf{\Pi}, \Omega) := \{\mathbf{X} \in \mathbf{R}\mathcal{L}_\infty^{m\times m}(\Omega) : \ \mathbf{X}(j\omega) \in \mathcal{S}_l(\mathbf{\Pi}(\omega)) \ \forall \omega \in \Omega\}, \tag{4.31}$$

with the function σ_l defined in (3.14). Notice that, while $\mathcal{S}_l(\cdot)$ is a subset of $\mathbb{C}^{m\times m}$, $\mathbf{S}_l(\mathbf{\Pi}, \Omega)$ is a set of frequency dependent functions. Notice also two important differences between this set and $\mathbf{S}_l(\mathbf{\Pi})$ defined in equation (3.16): the quadratic constraint is only met on $j\Omega$ and the stability is not required.

The following Lemma can be demonstrated in a similar way to Lemma 2, see Appendix B:

Lemma 4. *The set* $\mathbf{S}_l(\mathbf{\Pi}, \Omega)$ *is convex if* $\mathbf{\Pi} \in \mathcal{L}_\infty^{2m\times 2m}(\Omega)$ *satisfies*

$$\begin{bmatrix} 0 \\ I_m \end{bmatrix}^* \mathbf{\Pi}(\omega) \begin{bmatrix} 0 \\ I_m \end{bmatrix} \leq 0 \ \forall \omega \in \Omega. \tag{4.32}$$

In a first instance, we will consider some properties of the interconnection of constant matrices. So, $Z_1, Y_2 \in \mathbb{C}^{m\times m}$ are constant, invertible matrices whose respective inverses are denoted Y_1, Z_2. Define the auxiliary function $\Gamma : \mathbb{C}^{m\times m} \times \mathbb{C}^{m\times m} \times \mathbb{C}^{m\times m} \times \mathbb{R} \to \mathbb{C}^{2m\times 2m}$:

$$\Gamma(Q, R, Y, \epsilon) := \begin{bmatrix} Y^*QY + Y^*R + R^*Y - \epsilon I_m & R^* \\ R & -Q \end{bmatrix}, \tag{4.33}$$

whose domain will be later extended to include also matrix functions as arguments. Notice the identity

$$\sigma_l(Y_2, \Gamma(Q, R, Y_1, \epsilon)) = Y_1^*QY_1 - Y_2^*QY_2 + (Y_1+Y_2)^*R + R^*(Y_1+Y_2) - \epsilon I_m, \tag{4.34}$$

and that

$$\sigma_l(Y_2, \Gamma(Q, R, Y_1, \epsilon)) \geq 0 \iff Y_1^*QY_1 - Y_2^*QY_2 + (Y_1+Y_2)^*R + R^*(Y_1+Y_2) \geq \epsilon I_m. \tag{4.35}$$

Consider the following lemma:

Lemma 5. *Be $Z_1, Y_2 \in C^{m\times m}$ and the respective inverse $Y_1 := Z_1^{-1}$. Assume the existence of two matrices $Q = Q^*, R \in C^{m\times m}$ and a real $\epsilon > 0$ such that*

$$Q \geq 0, \tag{4.36}$$

$$Y_1^* Q Y_1 - Y_2^* Q Y_2 + (Y_1 + Y_2)^* R + R^*(Y_1 + Y_2) \geq \epsilon I_m, \tag{4.37}$$

Then

$$\det(I_m + Z_1 \mathcal{Y}_2) \neq 0 \tag{4.38}$$

for all $\mathcal{Y}_2 \in \mathcal{S}_l(\Pi) \subset \mathbb{C}^{m\times m}$, with $\Pi \in \mathbb{C}^{2m\times 2m}$ given by

$$\Pi = \Gamma(Q, R, Y_1, \epsilon). \tag{4.39}$$

Furthermore, the set $\mathcal{S}_l(\Pi)$ is convex.

Proof: The condition (4.37) can be written–see the equivalence (4.35)–:

$$\sigma_l(Y_2, \Pi) \geq 0, \tag{4.40}$$

with Π given by (4.39). By virtue of Lemma 4, $Q \geq 0$ implies the convexity of $\mathcal{S}_l(\Pi)$. Furthermore, by definition, all $\mathcal{Y}_2 \in \mathcal{S}_l(\Pi)$, satisfies

$$\sigma_l(\mathcal{Y}_2, \Pi) \geq 0,$$

or equivalently

$$Y_1^* Q Y_1 - \mathcal{Y}_2^* Q \mathcal{Y}_2 + (Y_1 + \mathcal{Y}_2)^* R + R^*(Y_1 + \mathcal{Y}_2) \geq \epsilon I_m, \ \forall \mathcal{Y}_2 \in \mathcal{S}_l(\Pi). \tag{4.41}$$

As a consequence of the identity

$$Y_1^* Q Y_1 - \mathcal{Y}_2^* Q \mathcal{Y}_2 + (Y_1 + \mathcal{Y}_2)^* R + R^*(Y_1 + \mathcal{Y}_2) =$$
$$= (Y_1 + \mathcal{Y}_2)^*[R + \frac{Q}{2}(Y_1 - \mathcal{Y}_2)] + [(Y_1 - \mathcal{Y}_2)^* \frac{Q}{2} + R^*](Y_1 + \mathcal{Y}_2),$$

the condition (4.41) is equivalent to

$$(Y_1 + \mathcal{Y}_2)^*[R + \frac{Q}{2}(Y_1 - \mathcal{Y}_2)] + [(Y_1 - \mathcal{Y}_2)^* \frac{Q}{2} + R^*](Y_1 + \mathcal{Y}_2) \geq \epsilon I_m \ \forall \mathcal{Y}_2 \in \mathcal{S}_l(\Pi),$$

that is equivalent to

$$v^*(Y_1+\mathcal{Y}_2)^*[R+\frac{Q}{2}(Y_1-\mathcal{Y}_2)]v+v^*[(Y_1-\mathcal{Y}_2)^*\frac{Q}{2}+R^*](Y_1+\mathcal{Y}_2)v \geq \epsilon||v||^2, \ \forall v \in \mathbb{C}^m, v \neq 0.$$

This implies

$$(Y_1 + \mathcal{Y}_2)v \neq 0 \ \forall v \in \mathbb{C}^m, v \neq 0, \ \forall \mathcal{Y}_2 \in \mathcal{S}_l(\Pi)$$

and

$$det(Y_1 + \mathcal{Y}_2) = det(Y_1) det(I_m + Z_1 \mathcal{Y}_2) \neq 0,$$

that implies the thesis. □□□

The previous lemma establishes conditions that ensure $det(I+Z_1\mathcal{Y}_2) \neq 0$ for a convex set of matrices $\mathcal{Y}_2$, for a fixed Z_1. We will introduce now a proposition that allows us to check the presence of closed loop modes on the set $j\Omega$ for the system $\mathbf{Z}_1 \star \mathbf{Y}_2$ and for an extended, convex set of systems around it.

Proposition 8. *Consider the feedback interconnection (3.12) for two linear, time-invariant systems $\mathbf{Z}_1$ and $\mathbf{Y}_2$ satisfying Assumptions 9-12 for Ω satisfying Assumption 13. Assume the existence of a scalar $\epsilon > 0$ and two matrices $\mathbf{Q}, \mathbf{R} : \mathbb{R} \to C^{m\times m}, \mathbf{Q}, \mathbf{R} \in \mathcal{L}_\infty^{m\times m}(\Omega)$ such that $\mathbf{Q} = \mathbf{Q}^*$ and*

$$\mathbf{Q}(\omega) \geq 0 \; \forall \omega \in \Omega, \tag{4.42}$$

$$\begin{array}{c} \mathbf{Y}_1(j\omega)^*\mathbf{Q}(\omega)\mathbf{Y}_1(j\omega) - \mathbf{Y}_2(j\omega)^*\mathbf{Q}(\omega)\mathbf{Y}_2(j\omega) + \\ +[\mathbf{Y}_1(j\omega)+\mathbf{Y}_2(j\omega)]^*\mathbf{R}(\omega) + \mathbf{R}(\omega)^*[\mathbf{Y}_1(j\omega)+\mathbf{Y}_2(j\omega)] \geq \epsilon I_m \; \forall \omega \in \Omega. \end{array} \tag{4.43}$$

Then, the operator $\mathbf{Z}_1 \star \mathbf{Y}_2$ has no modes on $j\Omega$. Therefore, there are no modes of $\mathbf{Z}_1 \star \mathcal{Y}_2$ on $j\Omega$ for all stabilizable and detectable realization of $\mathcal{Y}_2 \in \mathbf{S}_l(\mathbf{\Pi}, \Omega)$, with $\mathbf{\Pi} = \Gamma(\mathbf{Q}, \mathbf{R}, \mathbf{Y}_1, \epsilon)$. Furthermore, the set $\mathbf{S}_l(\mathbf{\Pi}, \Omega)$ is convex.

Proof The hypotheses on the systems $\mathbf{Z}_1, \mathbf{Y}_1, \mathbf{Y}_2$ imply the existence of uniform bounds for these maps on $j\Omega$. So, we can apply the Lemma 5 for the matrices $\mathbf{Z}_1(j\omega), \mathbf{Y}_1(j\omega), \mathbf{Y}_2(j\omega) \; \forall \omega \in \Omega$. Thus, the condition (4.43) allows us to conclude

$$det(I_m + \mathbf{Z}_1(j\omega)\mathbf{Y}_2(j\omega)) \neq 0 \; \forall \omega \in \Omega,$$

which implies, due to Assumption 9 and Lemma 1, the absence of closed loop modes of $\mathbf{Z}_1 \star \mathbf{Y}_2$ on the set $j\Omega$.

The extension of this property for any $\mathcal{Y}_2 \in \mathbf{S}_l(\mathbf{\Pi}, \Omega)$ is as follows. Since both $\mathcal{Y}_2$ and $\mathbf{Z}_1$ are bounded on $j\Omega$ there is no pole-zero cancellation on $j\Omega$ in the cascade system $\mathbf{Z}_1\mathcal{Y}_2$. As the realizations of both systems are stabilizable and detectable, the closed loop modes on $j\Omega$, if any, must make $det(I_m + \mathbf{Z}_1(j\omega)\mathcal{Y}_2(j\omega)) = 0$. This is not possible since $\mathcal{Y}_2 \in \mathbf{S}_l(\mathbf{\Pi}, \Omega)$ implies $\sigma_l(\mathcal{Y}_2(j\omega), \Pi(\omega)) \geq 0, \; \forall \omega \in \Omega$, and, by virtue of equivalence (4.35), this constraint makes way to the application of Lemma 5 for $\mathbf{Z}_1(j\omega), \mathcal{Y}_2(j\omega), \forall \omega \in \Omega$.

The convexity of the set $\mathbf{S}_l(\mathbf{\Pi}, \Omega)$ is ensured by (4.42), the existence of a uniform bound for $\mathbf{\Pi}$, and Lemma 4. □□□

Remark 13. *The condition (4.43) is a Frequency Dependent Linear Matrix Inequality (FDLMI) and constitutes an infinite dimensional constraint on $\mathbf{Q}, \mathbf{R}$. Notice that the finite domain Ω impedes the application of the classical KYP Lemma, see e.g. (Megretski and Rantzer, 1997; Rantzer, 1996). However, if*

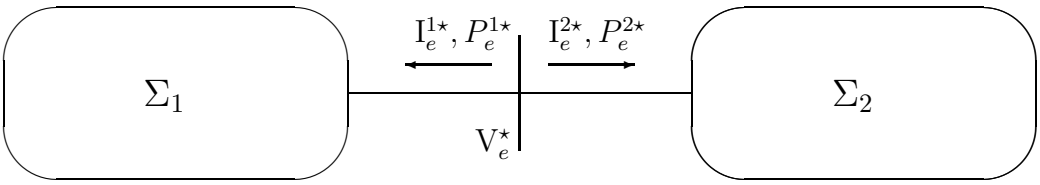

Figure 4.3: Interconnection of power systems.

finite state space realizations are supposed for $\mathbf{Q}, \mathbf{R}$*, the FDLMI can be formulated as an LMI, by applying the Generalized KYP Lemma, see reference (Iwasaki and Hara, 2005).*

The set $\mathbf{S}_l(\mathbf{\Pi}, \Omega)$ is infinite dimensional since its elements are frequential functions satisfying a quadratic constraint. Thus, its usefulness to describe a family of models of a physical system– subject e.g. to parametrical variations–is not direct. In the next section we again consider power systems to exploit the frequential characterization described in Section 4.2, to later build a family of models able to be linked with Proposition 8.

4.3.1 Interconnections of small signal models of power systems

This section is intended to apply the previous results to small signal models of power systems, taking advantage of the functions introduced in Section 4.2. The object under study is the interconnection of two power system as depicted in Fig. 4.3.1. It can be modeled, in small signal, as the interconnection described by equation (3.12), once we model the subsystems Σ_1, Σ_2 respectively through its impedance and admittance models, $\mathbf{Z}_1, \mathbf{Y}_2$, given by equations (4.6), (4.7). Notice also that, as a consequence of Kirchoff laws,

$$P_e^{1\star} + P_e^{2\star} = 0, \tag{4.44}$$

that enables the application of Remark 11, relative to function γ_g.

In the present case $\mathbf{Z}_1, \mathbf{Y}_2$ are square, 2×2 maps. We suppose valid the Assumptions 10, 11, 12 that imply the existence of uniform bounds of these maps and their inverses on the set $j\Omega$.

We will consider in first instance, constant, complex matrices $Z_1, Y_2 \in \mathbb{C}^{2\times 2}, Y_1 := Z_1^{-1}$ that coincide with the evaluation of the respective transfer function at one frequency $\omega \in \Omega$:

$$Z_1 = \mathbf{Z}_1(j\omega), Y_1 = \mathbf{Y}_1(j\omega), Y_2 = \mathbf{Y}_2(j\omega). \tag{4.45}$$

Consider the definition of the orthogonal versors $k_v^\top, k_\theta^\top \in \mathbb{R}^2$, equation (4.1), taking the bus e in Fig 4.3.1 as reference. All mention to the subindex $e \in \mathbb{B}$ will be omitted, by brevity, in the sequel.

Consider a matrix $R \in \mathbb{C}^{2\times 2}$ given by

$$R := j\omega k_v^\top k_\theta, \omega \in \Omega, \tag{4.46}$$

Recall definitions (4.1) and (4.2), and property (4.3). Thus, for R given by (4.46) and a constant matrix $Y \in \mathbb{C}^{2\times 2}$, it can be computed

$$U_\theta(Y^*R + R^*Y)U_\theta^\top = j\omega \begin{bmatrix} k_v \\ k_\theta \end{bmatrix} (Y^* k_v^\top k_\theta - k_\theta^\top k_v Y) \begin{bmatrix} k_v^T & k_\theta^T \end{bmatrix} =$$

$$= \begin{bmatrix} 0 & j\omega k_v Y^* k_v^\top \\ -j\omega k_v Y k_v^\top & j\omega(k_\theta Y^* k_v^\top - k_v Y k_\theta^\top) \end{bmatrix}. \tag{4.47}$$

Recall the definition of the function g_d, equation (4.19). Thus, the equation (4.47) can be written

$$U_\theta(Y^*R + R^*Y)U_\theta^\top = \begin{bmatrix} 0 & j\omega k_v Y k_v^\top \\ -j\omega k_v Y k_v^\top & \omega^2 g_d(Y,\omega) \end{bmatrix}. \tag{4.48}$$

The following fact is a direct consequence of definition (4.10):

Lemma 6. *For all invertible matrix $Z \in \mathbb{C}^{2\times 2}$, and $U \in \mathbb{U}$, it is satisfied*

$$Y^*U^*UY - k_v^\top k_v g_r^2(Z,U) \geq 0, \tag{4.49}$$

being $Y = Z^{-1}$.

Proof. By definition (4.10):

$$g_r(Z,U)^2 ||k_v Z U^{-1}||^2 = g_r(Z,U)^2 \bar{\sigma}^2(k_v Z U^{-1}) = 1.$$

A standard property of the maximum singular value[6] allow us to write

$$I_2 - g_r^2(Z,U)\bar{U}^{-*} Z^* k_v^\top k_v Z U^{-1} \geq 0.$$

Left and right multiplying by Y^*U^* and UY, we get

$$Y^*U^*UY - g_r^2(Z,U) k_v^\top k_v \geq 0.$$

□□□

[6] $\bar{\sigma}^2(A) = 1 \Longrightarrow A^*A \leq I$.

For a given matrix $Z_2 \in \mathbb{C}^{2\times 2}$, let us choose a particular weighting matrix :

$$U_2 := \frac{Z_2}{||Z_2||}. \tag{4.50}$$

It is immediate to verify that $U_2 \in \mathbb{U}$, recall definition (4.9), and

$$g_r(Z_2, U_2) = ||Z_2||^{-1}. \tag{4.51}$$

Next lemma proposes a particular choice for Q that, along with R given by (4.46), allows us to satisfy conditions (4.36) and (4.37) in Lemma 5:

Lemma 7. *Suppose valid the assumptions* 10- 13 *for the set* Ω *and maps* $\mathbf{Z}_1, \mathbf{Y}_2$ *describing the small signal model of interconnection depicted in Figure* 4.3.1. *Denote* Z_1, Y_2, Y_1 *as in (*4.45*) for an arbitrary* $\omega \in \Omega$. *The existence of a real* $\epsilon > 0$ *such that*

$$\begin{bmatrix} \frac{\omega^2||Z_2||^2}{2} g_d(Y_1+Y_2,\omega)[g_r^2(Z_1,U_2) - g_r^2(Z_2,U_2)] & \omega g_g(Y_1+Y_2) \\ \omega g_g(Y_1+Y_2) & \frac{\omega^2}{2} g_d(Y_1+Y_2,\omega) \end{bmatrix} \geq \epsilon I_2, \tag{4.52}$$

implies the existence of $Q, R \in \mathbb{C}^{2\times 2}$ *such that* $Q \geq 0$ *and*

$$Y_1^* Q Y_1 - Y_2^* Q Y_2 + (Y_1+Y_2)^* R + R^*(Y_1+Y_2) \geq \epsilon I_m, \tag{4.53}$$

Proof: Take $Q = xU_2^* U_2$, with $x \in \mathbb{R}, x \geq 0$, a degree of freedom to be exploited to optimize feasibility. Notice that $Q \geq 0$ and compute

$$U_\theta[Y_1^* Q Y_1 - Y_2^* Q Y_2] U_\theta^\top = xU_\theta[Y_1^* U_2^* U_2 Y_1 - Y_2^* U_2^* U_2 Y_2] U_\theta^\top =$$

$$= xU_\theta[Y_1^* U_2^* U_2 Y_1 - ||Z_2||^{-2} I_2] U_\theta^\top \geq xU_\theta[g_r^2(Z_1,U_2) k_v^\top k_v - ||Z_2||^{-2} I_2] U_\theta^\top =$$

$$= x \begin{bmatrix} g_r^2(Z_1,U_2) - g_r^2(Z_2,U_2) & 0 \\ 0 & -||Z_2||^{-2} \end{bmatrix}, \tag{4.54}$$

where equations (4.49) , (4.50), and (4.51) were employed. Thus, take R as in (4.46), and recall (4.48),(4.54) to get

$$U_\theta[Y_1^* Q Y_1 - Y_2^* Q Y_2 + (Y_1+Y_2)^* R + R^*(Y_1+Y_2)] U_\theta^\top \geq$$

$$\geq x \begin{bmatrix} g_r^2(Z_1,U_2) - g_r^2(Z_2,U_2) & 0 \\ 0 & -||Z_2||^{-2} \end{bmatrix} + \begin{bmatrix} 0 & j\omega k_v (Y_1+Y_2) k_v^\top \\ -j\omega k_v (Y_1+Y_2) k_v^\top & \omega^2 g_d(Y_1+Y_2,\omega)) \end{bmatrix}.$$

By hypothesis, the net active power entering both subsystems is zero, equation (4.44), and hence $|k_v(Y_1+Y_2)k_v^\top| = g_g(Y_1+Y_2)$, see Remark 11. Thus, if we introduce $\psi_{12} := \angle k_v(Y_1+Y_2)k_v^\top$, we have

$$U_\theta[Y_1^* Q Y_1 - Y_2^* Q Y_2 + (Y_1+Y_2)^* R + R^*(Y_1+Y_2)] U_\theta^\top \geq$$

$$= \begin{bmatrix} x[g_r^2(Z_1,U_2) - g_r^2(Z_2,U_2)] & j\omega g_g(Y_1+Y_2)e^{j\psi_{12}} \\ -j\omega g_g(Y_1+Y_2)e^{-j\psi_{12}} & \omega^2 g_d(Y_1+Y_2,\omega) - x||Z_2||^{-2} \end{bmatrix}. \quad (4.55)$$

Now, we will determine x such that

$$\begin{bmatrix} x[g_r^2(Z_1,U_2) - g_r^2(Z_2,U_2)] & j\omega g_g(Y_1+Y_2)e^{j\psi_{12}} \\ -j\omega g_g(Y_1+Y_2)e^{-j\psi_{12}} & \omega^2 g_d(Y_1+Y_2,\omega) - x||Z_2||^{-2} \end{bmatrix} \geq \epsilon I_2, \quad (4.56)$$

which is equivalent to

$$\begin{cases} x[g_r^2(Z_1,U_2) - g_r^2(Z_2,U_2)] & \geq \epsilon \\ \omega^2 g_d(Y_1+Y_2,\omega) - x||Z_2||^{-2} & \geq \epsilon \\ \{x[g_r^2(Z_1,U_2) - g_r^2(Z_2,U_2)] - \epsilon\}\{\omega^2 g_d(Y_1+Y_2,\omega) - x||Z_2||^{-2} - \epsilon\} & \geq \omega^2 g_g^2(Y_1+Y_2) \end{cases}$$

For ϵ sufficiently small, the optimum x to ensure the previous conditions is

$$x_{opt} = \arg\max_{x\geq 0}\{x[\omega^2 g_d(Y_1+Y_2,\omega) - x||Z_2||^{-2}]\} = \frac{\omega^2||Z_2||^2 g_d(Y_1+Y_2,\omega)}{2}.$$

If we take $x = x_{opt}$ in (4.56) and omit the phase factor $je^{j\Psi_{12}}$ in the non diagonal terms–with no significance for the signal definition–we recover the inequality (4.52). Thus, this hypothesis implies the inequality (4.56) that, due to inequality (4.55), yields condition (4.53) that concludes the proof. □□□

As consequence of the previous development, we have built a pair of multipliers $\tilde{\mathbf{Q}}, \tilde{\mathbf{R}}$ given by

$$\tilde{\mathbf{Q}}(\omega) := \frac{\omega^2}{2}\gamma_d(\mathbf{Y}_1+\mathbf{Y}_2;\omega)\mathbf{Z}_2(j\omega)^*\mathbf{Z}_2(j\omega); \quad \tilde{\mathbf{R}}(\omega) := j\omega k_v^\top k_\theta \ \ \forall\omega\in\Omega. \quad (4.57)$$

These functions are bounded on $j\Omega$ since this set is bounded and excludes the origin. Define the function $\tilde{\mathbf{U}}_2 : \mathbb{R} \to \mathbb{U}$:

$$\tilde{\mathbf{U}}_2 := \frac{\mathbf{Z}_2(j\omega)}{||\mathbf{Z}_2(j\omega)||}, \ \forall\omega\in\Omega. \quad (4.58)$$

Since $\mathbf{Z}_2 \in \mathbf{R}\mathcal{L}_\infty(\Omega)$, it is easy to check that $\tilde{\mathbf{U}}_2 \in \mathbf{U}$, see definition (4.11).

The following proposition extends the previous lemma for all $\omega \in \Omega$, setting the additional conditions to be met by the involved maps. Its proof is straightforward from Lemma 7, definitions (4.57-4.58), and the previous discussion.

Proposition 9. *Consider the feedback interconnection (*3.12*) for two linear, time-invariant systems* $\mathbf{Z}_1$ *and* $\mathbf{Y}_2$ *satisfying Assumptions* 10-12 *for* Ω *meeting*

Assumption 13. *Assume that equation (*4.44*) holds for the equilibrium and that a scalar* $\epsilon > 0$ *exists such that*[7]

$$\begin{bmatrix} \frac{\omega^2||\mathbf{Z}_2||^2}{2}\gamma_d(\mathbf{Y}_1+\mathbf{Y}_2)[\gamma_r^2(\mathbf{Z}_1,\tilde{\mathbf{U}}_2)-\gamma_r^2(\mathbf{Z}_2,\tilde{\mathbf{U}}_2)] & \omega\gamma_g(\mathbf{Y}_1+\mathbf{Y}_2) \\ \omega\gamma_g(\mathbf{Y}_1+\mathbf{Y}_2) & \frac{\omega^2}{2}\gamma_d(\mathbf{Y}_1+\mathbf{Y}_2) \end{bmatrix} \geq \epsilon I_2, \ ,\forall\omega\in\Omega \tag{4.59}$$

Then, there exist $\tilde{\mathbf{Q}},\tilde{\mathbf{R}}$ *defined in (*4.57*) satisfying*

$$\tilde{\mathbf{Q}}(\omega)\geq 0 \ \ \forall\omega\in\Omega, \tag{4.60}$$

$$\begin{gathered}\mathbf{Y}_1(j\omega)^*\tilde{\mathbf{Q}}(\omega)\mathbf{Y}_1(j\omega)-\mathbf{Y}_2(j\omega)^*\tilde{\mathbf{Q}}(\omega)\mathbf{Y}_2(j\omega)+ \\ +[\mathbf{Y}_1(j\omega)+\mathbf{Y}_2(j\omega)]^*\tilde{\mathbf{R}}(\omega)+\tilde{\mathbf{R}}(\omega)^*[\mathbf{Y}_1(j\omega)+\mathbf{Y}_2(j\omega)]\geq\epsilon I_m \ \forall\omega\in\Omega.\end{gathered} \tag{4.61}$$

Let us examine some key quantities in inequality (4.59). To meet this inequality it is necessary that

$$||\mathbf{Z}_2(j\omega)||^2[\gamma_r^2(\mathbf{Z}_1,\tilde{\mathbf{U}_2})-\gamma_r^2(\mathbf{Z}_2,\tilde{\mathbf{U}_2})]=||k_v\mathbf{Z}_1\mathbf{Y}_2(j\omega)||^{-2}-1>0,\forall\omega\in\Omega,$$

where equations (4.10), (4.58) and (4.51) were employed. This inequality is equivalent to

$$||k_v\mathbf{Z}_1(j\omega)\mathbf{Y}_2(j\omega)||<1, \ \forall\omega\in\Omega,$$

which is an $\mathcal{H}_\infty$-like condition on the loop gain $\mathbf{Z}_1\mathbf{Y}_2$ on one of the two output channels, the one associated to the voltage module. Other necessary condition implicit in (4.59) is

$$\gamma_d(\mathbf{Y}_1+\mathbf{Y}_2;\omega)>0 \ \forall\omega\in\Omega,$$

which is a damping requirement on the angle (or frequency) channel: the power system must have, at the bus considered, a positive damping. Provided these two conditions, (4.59) requires

$$\gamma_g(\mathbf{Y}_1+\mathbf{Y}_2;\omega)^2<\frac{\omega^2||\mathbf{Z}_2||^2}{4}\gamma_d(\mathbf{Y}_1+\mathbf{Y}_2;\omega)^2[\gamma_r^2(\mathbf{Z}_1,\tilde{\mathbf{U}_2})-\gamma_r^2(\mathbf{Z}_2,\tilde{\mathbf{U}_2})$$

that can be interpreted as a *low voltage sensitivity* condition.

Remark 14. *Condition (*4.59*) imposes thus a* balance *between damping and voltage regulation on the one hand, and the voltage sensitivity on the other. The classical control actions and the load static characteristic play a direct role on each parameter in this inequality. The inequalities (*4.60*) and (*4.61*) also imply an implicit, less restrictive,* balance *between these variables. Due to these reasons, in the sequel, we will refer generically to condition (*4.59*) (or the pair (*4.60*) - (*4.61*)) as* balance conditions.

[7] *The dependence of the functions* $\gamma_r,\gamma_d,\gamma_g$ *on* ω *is omitted to facilitate the reading.*

4.3.2 Robustness analysis

The main results in the preceding sections of this chapter allow us to check the presence of closed loop modes on the set $j\Omega$ and the extension of this property to a convex set that includes the nominal system. To progress with the stability analysis of small signal models of power systems, it is necessary to build a family of models for which some relevant dynamic property is guaranteed.

The robust control theory provides us many ways to describe families of dynamical systems, each one accompanied by its corresponding robustness analysis tool, see e.g. (Megretski and Rantzer, 1997).

Our development has followed, in some sense, an inverse way. We have defined three frequency domain functions with direct meanings in the power system community. We assume a given balance between these functions, Proposition 9, to later examine its consequences on the dynamic behavior of the interconnection. To advance to this objective, we will define a family of small signal models of power systems.

We will follow partially the lines of references (Doyle, 1982; Doyle, 1985; Fan et al., 1991) to propose a Linear Fractional Transformation (LFT) model. Consider a given, fix, matrix function $N(s) \in \mathbf{RL}_{\infty}^{4\times 4}(\Omega)$ with a partition of four square blocks

$$N(s) = \begin{bmatrix} N_{11}(s) & N_{12}(s) \\ N_{21}(s) & N_{22}(s) \end{bmatrix}. \tag{4.62}$$

We will assume that N_{12} is invertible, and that N_{12}^{-1} is bounded on $j\Omega$. So, the matrix function $\tilde{N} : j\Omega \to \mathbb{C}^{4\times 4}$:

$$\tilde{N}(j\omega) := \begin{bmatrix} N_{12}^{-1} & -N_{12}^{-1}N_{11} \\ N_{22}N_{12}^{-1} & N_{21} - N_{22}N_{12}^{-1}N_{11} \end{bmatrix}(j\omega) \tag{4.63}$$

exists and it is bounded on $j\Omega$. Consider also a convex, compact set $\mathcal{D}_{\Delta} \subset \mathbb{R}^{2\times 2}$ with $0_{2\times 2} \in \mathcal{D}_{\Delta}$, and the family of systems

$$\mathbf{Y}_{N,\Delta} := \{\mathcal{Y} : \mathcal{Y}(s) = \mathcal{F}_u(N(s), \Delta), \forall \Delta \in \mathcal{D}_{\Delta}\} \tag{4.64}$$

The family $\mathbf{Y}_{N,\Delta}$, depicted in Figure 4.3.2, is parameterized by $\Delta \in \mathcal{D}_{\Delta}$, and its members are supposed to have stabilizable and detectable state space realization. The case $\Delta = 0_{2\times 2}$ constitutes the so-called nominal system $\mathbf{Y} = \mathcal{F}_u(N(s), 0) = N_{22}(s)$, see Appendix C.

This family of systems can be used directly to model uncertain systems where Δ collects some real parameters varying in a certain domain. A significant

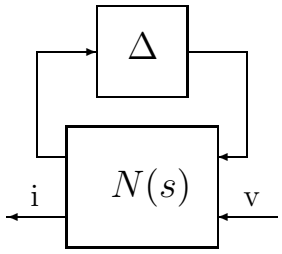

Figure 4.4: Description of the family of power systems models.

case is the use of Δ to *exactly* capture the variations of a static load with a ZIP model, see Appendix D.

Lemma 8. *Be* $\mathbf{\Pi} : \mathbb{R} \to \mathbb{C}^{4\times 4}$ *an Hermitian multiplier* $\mathbf{\Pi} \in \mathcal{L}_\infty(\Omega)$ *and* $N(s) \in \mathbf{R}\mathcal{L}_\infty^{4\times 4}(\Omega)$ *partitioned as in (4.62). $N_{12}^{-1}(s)$ exists and $N_{12}^{-1} \in \mathbf{R}\mathcal{L}_\infty(\Omega)$. Assume $\Delta \in \mathcal{D}_\Delta$ given and $\mathcal{F}_u(N,\Delta) \in R\mathcal{L}_\infty^{2\times 2}(\Omega)$. Then the following two statements are equivalent*

1. $\mathcal{F}_u(N,\Delta) \in \mathbf{S}_l(\mathbf{\Pi},\Omega)$
2. $\Delta \in \mathbf{S}_l(\tilde{N}^*\mathbf{\Pi}\tilde{N},\Omega)$.

Proof: The hypotheses ensure that the functions $N_{12}(j\omega)^{-1}$ and $[I_m - N_{11}(j\omega)\Delta]^{-1}$ are bounded on Ω. Thus, the Lemma 10 in Appendix C allows us to conclude the equivalence between

$$\mathcal{F}_u(N(j\omega),\Delta) \in \mathcal{S}_l(\mathbf{\Pi}(\omega),\epsilon)\ \forall\omega \in \Omega,$$

and

$$\Delta \in \mathcal{S}_l(\tilde{N}(j\omega)^*\mathbf{\Pi}(\omega)\tilde{N}(j\omega),\epsilon)\ \forall\omega \in \Omega.$$

So, the thesis results directly from the definition (4.31). □□□

A very important characteristic of the power systems dynamics is the presence of electromechanical modes. They are typically studied in the state space where the modal analysis allows us to link each mode with a set of state variables (rotor angles, speeds, etc.) which evidences its physical meaning. However, it is not simple to capture the physical nature of these modes in an input-output setting. However, the electromechanical modes are typically characterized by their frequency range. These modes typically ranges from 0.2 to 2Hz, see (Kundur, 1994). This range–one decade–may be even smaller when a concrete case and certain parameter variations are under study. Thus, we will characterize the set of electromechanical modes through their frequency range and also through their continuity with respect to parametrical variation.

We will assume that a balance condition holds for our nominal system $\mathbf{Z}_1 \star \mathbf{Y}_2$, and we will study the consequences on the stability of the electromechanical modes facing parametrical variations. The results are precisely stated in the next Proposition.

Theorem 1. *Consider a set Ω satisfying Assumption 13, and the interconnection $\mathbf{Z}_1 \star \mathcal{Y}_2$ with $\mathcal{Y}_2 \in \mathbf{Y}_{N,\Delta}$ with $\Delta \in \mathcal{D}_\Delta \subset \mathbb{R}^{2\times 2}$ and $\mathcal{D}_\Delta$ compact and convex. $N(s) \in \mathbf{R}\mathcal{L}_\infty^{4\times 4}(\Omega)$, partitioned as in (4.62) satisfies that $N_{12}(j\omega)$ has a bounded inverse en $j\Omega$. Assume state space realizations for both $\mathbf{Z}_1$ and $\mathcal{Y}_2$ for all $\Delta \in \mathcal{D}_\Delta$ satisfying Assumptions 9-12. Denote $\mathbf{Y}_2 = \mathcal{F}_u(N, 0)$ and $\mathbf{Z}_1 \star \mathbf{Y}_2$ the nominal interconnection. Assume that the equation (4.44) holds for the equilibrium. Assume also*

A1. the existence of a scalar $\epsilon > 0$ such that $\tilde{\mathbf{Q}}$,$\tilde{\mathbf{R}}$ given by (4.57) satisfy

$$\tilde{\mathbf{Q}}(\omega) \geq 0 \ \ \forall \omega \in \Omega, \tag{4.65}$$

$$\begin{array}{c} \mathbf{Y}_1(j\omega)^*\tilde{\mathbf{Q}}(\omega)\mathbf{Y}_1(j\omega) - \mathbf{Y}_2(j\omega)^*\tilde{\mathbf{Q}}(\omega)\mathbf{Y}_2(j\omega)+ \\ +[\mathbf{Y}_1(j\omega)+\mathbf{Y}_2(j\omega)]^*\tilde{\mathbf{R}}(\omega)+\tilde{\mathbf{R}}(\omega)^*[\mathbf{Y}_1(j\omega)+\mathbf{Y}_2(j\omega)] \geq \epsilon I_m \ \forall \omega \in \Omega; \end{array} \tag{4.66}$$

A2. that the uncertain model satisfies

$$\begin{bmatrix} 0 \\ I_2 \end{bmatrix}^* \tilde{N}(j\omega)^*\tilde{\mathbf{\Pi}}(\omega)\tilde{N}(j\omega) \begin{bmatrix} 0 \\ I_2 \end{bmatrix} \leq 0 \ \forall \omega \in \Omega$$

with $\tilde{\mathbf{\Pi}} = \Gamma(\tilde{\mathbf{Q}}, \tilde{\mathbf{R}}, \mathbf{Y}_1, \epsilon)$;

A3. that $\mathbf{Z}_1 \star \mathcal{Y}_2$ has a set of closed loop modes $m_i : \mathcal{D}_\Delta \to \mathbb{C}, i \in \mathcal{M} \subset \mathbb{N}$ satisfying

$$Im(m_i(\Delta)) \in \Omega \ \forall \Delta \in \mathcal{D}_\Delta,$$

that are continuous, bounded functions on $\mathcal{D}_\Delta$;

A4. that the nominal interconnection satisfies $Re(m_i(0)) < 0 \ \forall i \in \mathcal{M}$.

Then

$$Re(m_i(\Delta)) < 0 \ \forall i \in \mathcal{M} \ \forall \Delta \in \mathbf{\Delta}$$

with

$$\mathbf{\Delta} := \mathcal{D}_\Delta \cap \mathbf{S}_l(\tilde{N}(j\omega)^*\tilde{\mathbf{\Pi}}(\omega)\tilde{N}(j\omega), \Omega). \tag{4.67}$$

Proof The inequality (4.66) can be written, in compact notation, $\mathbf{Y}_2 \in \mathbf{S}_l(\tilde{\mathbf{\Pi}}, \Omega)$. Since $\mathbf{Y}_2 = \mathcal{F}_u(N, 0)$, the assumptions on the boundedness of N_{12}^{-1} and $\mathcal{F}_u(N, \Delta)$ and Lemma 8 implies that

$$\mathbf{0}_{2\times 2} \in \mathbf{S}_l(\tilde{N}(j\omega)^*\tilde{\mathbf{\Pi}}(\omega)\tilde{N}(j\omega), \Omega)$$

and this set is thus nonempty. Consider an arbitrary matrix $\Delta_0 \in \mathbf{\Delta}$.

Notice that Assumption A2 and Lemma 4 imply that the set $\mathbf{S}_l(\tilde{N}^*\tilde{\mathbf{\Pi}}\tilde{N}, \Omega)$ is convex. $\mathbf{\Delta}$ is thus convex since it is the intersection of two convex sets, see (4.67). Both $0_{2\times 2}, \Delta_0 \in \mathbf{\Delta}$, then

$$\Delta(\mu) := \mu\Delta_0 \in \mathbf{\Delta}\ \forall \mu \in [0,1].$$

As $\Delta(\mu) \in \mathcal{D}_\Delta$ it is ensured that $\mathcal{Y}_\mu := \mathcal{F}_u(N, \Delta_\mu) \in \mathbb{R}\mathcal{L}_\infty(\Omega)$. Since $\Delta_\mu \in \mathbf{S}_l(\tilde{N}(j\omega)^*\tilde{\mathbf{\Pi}}(\omega)\tilde{N}(j\omega), \Omega$, the Lemma 8 implies that

$$\mathcal{Y}_\mu \in \mathbf{S}_l(\mathbf{\Pi}, \Omega),$$

and, due to Proposition 8, the interconnection $\mathbf{Z}_1 \star \mathcal{Y}_\mu$ has no closed loop modes on the set $j\Omega$.

Suppose, reasoning by the absurd, that there exists a closed loop mode $k \in \mathcal{M}$ such that

$$Re[m_k(\Delta_0)] >= 0.$$

Then, we have a continuous, bounded function $m_k(\mu\Delta_0)$ whose real part is negative for $\mu = 0$ and non negative for $\mu = 1$. This implies that there exists an intermediate $\mu^\star$ such that $Re[m_k(\mu^\star\Delta_0)] = 0$. Due to Assumption A3 $Im[m_k(\mu^\star\Delta_0)] \in \Omega$ which violates the absence of closed loop modes of $\mathbf{Z}_1 \star \mathcal{Y}_\mu$ on $j\Omega$. Thus, the absurd hypothesis is not correct and the thesis is demonstrated. □□□

Theorem 1 constitutes a robust stability test for a set of closed loop modes characterized by its frequency range Ω and its continuity. The balance condition, assumption A1, determines the existence of a barrier at the set $j\Omega$. The continuity and frequency domain characterization of the modes and the convexity of the domain impede the modes to cross this barrier. So, the nominal stability of these modes determines their robust stability for all $\Delta \in \mathbf{\Delta}$. Figure 4.5 represents the complex plane and schematically depicts the mode loci when the parameter moves along a given curve $\Delta(\mu) \in \mathbf{\Delta}$. Notice that Theorem 1 does not exclude the possibility that other modes can cross the imaginary axis avoiding the mentioned barrier.

Remark 15. *Notice that the Theorem* 1 *is also valid if we substitute the pair* $\tilde{\mathbf{Q}}, \tilde{\mathbf{R}}$ *in Assumption A1 for any pair* $\mathbf{Q}, \mathbf{R}$ *satisfying the assumptions of Proposition* 8. *It is also true that we can adopt a more general uncertainty model and that a convex optimization algorithm can be used to improve feasibility of condition A1. However, as it was mentioned before, we are not interested in that,*

but in investigating the links between the classical power system control actions and the robust stability of the electromechanical modes. Notice also that, by virtue of Proposition 9*, the Theorem* 1 *is also valid when A1 is substituted by the other, more explicit, balance condition (*4.59*).*

A few words on assumption A2 are necessary. This condition is needed to ensure the convexity of $\mathbf{\Delta}$ and thus its connectedness, essential to demonstrate the theorem. Assumption A2 can be written

$$\begin{bmatrix} -N_{12}^{-1}N_{11} \\ N_{21} - N_{22}N_{12}^{-1}N_{11} \end{bmatrix}^* \tilde{\mathbf{\Pi}} \begin{bmatrix} -N_{12}^{-1}N_{11} \\ N_{21} - N_{22}N_{12}^{-1}N_{11} \end{bmatrix} (j\omega) \geq 0 \; \forall \omega \in \Omega,$$

i.e., an inequality that depends quadratically on N_{11}, of the type:

$$[A + BN_{11} + N_{11}^* B^* + N_{11}^* C N_{11}](j\omega) \leq 0.$$

The independent term, that we denoted A above, is given by the expression

$$A = N_{21}^* \begin{bmatrix} 0 \\ I_2 \end{bmatrix}^* \tilde{\mathbf{\Pi}} \begin{bmatrix} 0 \\ I_2 \end{bmatrix} N_{21}.$$

The condition (4.65) implies $A \leq 0$. Thus, the Assumption A2 can be viewed as a constraint on the maximum $||N_{11}(j\omega)||$. In particular, Assumption A2 is met for all uncertain models of the type

$$\mathbf{Y}_{N,\Delta} := \{\mathcal{Y} : \mathcal{Y}(s) = \mathbf{Y}(s) + N_{21}(s)\Delta N_{12}(s), \forall \Delta \in \mathcal{D}_\Delta\},$$

which is known in the robust control literature as multiplicative model, see (Doyle et al., 1992). The choice of the LFT model (4.64) is justified by its generality–this model allows us to capture the dependence of the modes of $\mathcal{Y}_2$ on the parameter–albeit it turns Assumption A2 necessary.

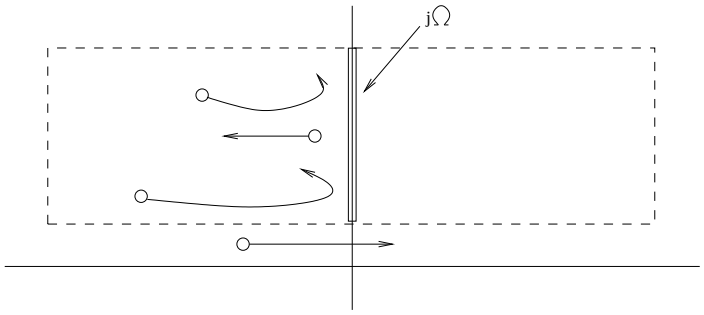

Figure 4.5: *Closed loop modes behavior for* $\Delta(\mu) \in \mathbf{\Delta}$.

The application of Theorem 1 to the stability analysis of the electromechanical modes of power system rests, in first instance, on the reasonableness of

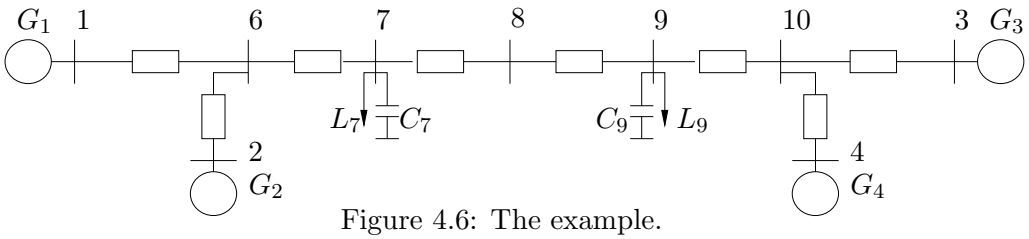

Figure 4.6: The example.

Assumption A3 as characterization of these modes. However, it is also required Assumption A1 and its balance between damping, voltage regulation and voltage sensitivity. In next section we will examine a well known classical example to check this condition and validate the theorem.

4.4 Example

Consider the system depicted in Fig. 4.6, see (Kundur, 1994), pg. 813. The parameters are in complete accordance with the reference and the excitation control is modeled as a thyristor exciter with high transient gain and PSS, option (iv) in (Kundur, 1994). The interconnection at the bus 7 is studied, by denoting $\mathbf{Y}_2$ the small signal admittance model of load L_7 and $\mathbf{Z}_1$ the impedance model for the rest of the system, including the four machines and load L_9.

The objective of the study is the use of Theorem 1 for the analysis of the electromechanical modes when the parameters of the ZIP model of L_7 are varied in certain domain. The nominal system corresponds to a ZIP model for L_7 with active and reactive components with constant power. Since the subsystem $\mathbf{Y}_2$ consists exclusively of a static load, it can be modeled as in Appendix D, equation (D.5), with the set $\mathcal{D}_\Delta$ given by (D.6) with the parameters $k_{pf} \in [0, 3], k_{qf} = 0$. The modeling and computation of small signal system were done with the software DSAT, (Powertech Labs Inc., n.d.).

Figure 4.7 depicts the functions involved in the balance conditions for the nominal system. Observe the significance of the damping function mainly restricted to the frequency band associated to electromechanical modes. The term associated to the voltage regulation remains approximately constant, and the voltage sensitivity has in this case a behavior similar to γ_d. To check the balance conditions, the minimum eigenvalues of the corresponding matrices are displayed. Balance conditions (4.59) and (4.61) are respectively satisfied[8] in the ranges $\omega \in [1.3, 12.3]\ rad/sec$ and $\omega \in [1, 20.8]$. Since left hand side of condition

[8]Since no numerical optimization is involved, these conditions were checked on a fine grid of frequency points, taking advantage of the continuity of these functions.

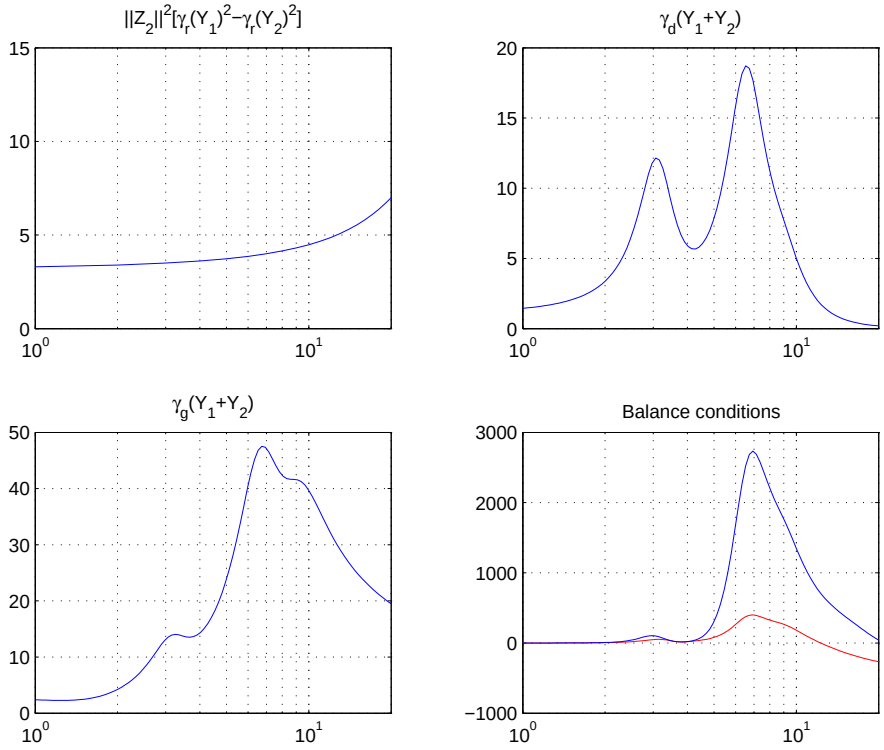

Figure 4.7: Voltage regulation function (top left), damping function (top right), voltage sensitivity function (bottom left) and balance conditions (bottom right).

(4.61) is always greater than the left hand side of (4.59), see Proposition 9, it is not necessary to identify each plot. The analysis of several cases allows us to chose $\Omega = [2.1, 10]$, which seems to be reasonable with the results known for this example en several scenarios, see (Klein et al., 1992; Kundur, 1994; Stankovic et al., 1999).

The robust stability of the electromechanical modes was assessed with the help of Theorem 1. The balance condition of the nominal interconnection, hypothesis A1, is satisfied in a suitable frequency range. The hypothesis A2 is trivially satisfied by the uncertainty model (D.5). We studied the extent of the uncertainty set $\mathbf{\Delta}$ by checking the belonging of the vertices of $\mathcal{D}_\Delta$ to the set $\mathbf{S}_u(\tilde{N}(j\omega)^*\tilde{\mathbf{\Pi}}(\omega)\tilde{N}(j\omega), \Omega)$, the convexity ensures that this procedure is sufficient.

The results of this procedure are the domains $\mathbf{\Delta}$ plotted in Figure 4.8. Notice that the stability of the electromechanical modes is ensured for most of the domain, and it is improved by a positive frequency coefficient k_{pf} of the load.

The stability of the electromechanical modes for the extreme values of $\mathbf{\Delta}$

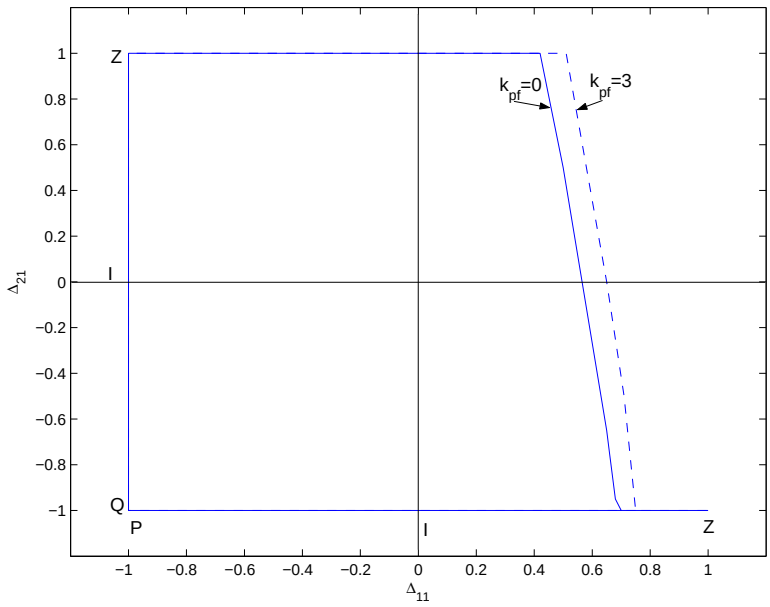

Figure 4.8: Space of parameters for load L_7, cases $k_{pf} = \{0, 3\}$. $\Delta_{11} = p_1 - p_3$ at the horizontal axis, $\Delta_{21} = q_1 - q_3$ at the vertical axis. The labels P,Q,I,Z indicate the points of pure constant power, current or impedance for each axis.

was verified directly and the corresponding loci are depicted in Figure 4.9.

Fig. 4.9 also remember us that Theorem 1 is a *sufficient* condition: some scenarios whose stability could not be ensured by Theorem 1 are nevertheless stable.

4.5 Some concluding remarks

The objective of this chapter was to study the consequences, at the system level, of the classical control actions in power systems. Voltage regulation and damping injection are done everywhere in the networks at generators, FACTS and some controlled loads. We have provided a way to quantify these control actions with the help of two suitably defined frequency functions. The ideas behind these functions were illustrated with the help of several examples involving either analytical or numerical computation. With these functions in mind, a pair of frequency dependent multipliers was obtained that allow us quantify the amount of damping and voltage regulation necessary to guarantee some robust closed loop properties. It was shown that if a balance is ensured between damping, voltage regulation and voltage sensitivity, a set of closed loop modes is kept stable in spite of model uncertainty. The robust stability condition derived in this work does not require the numerical computation of multipliers or

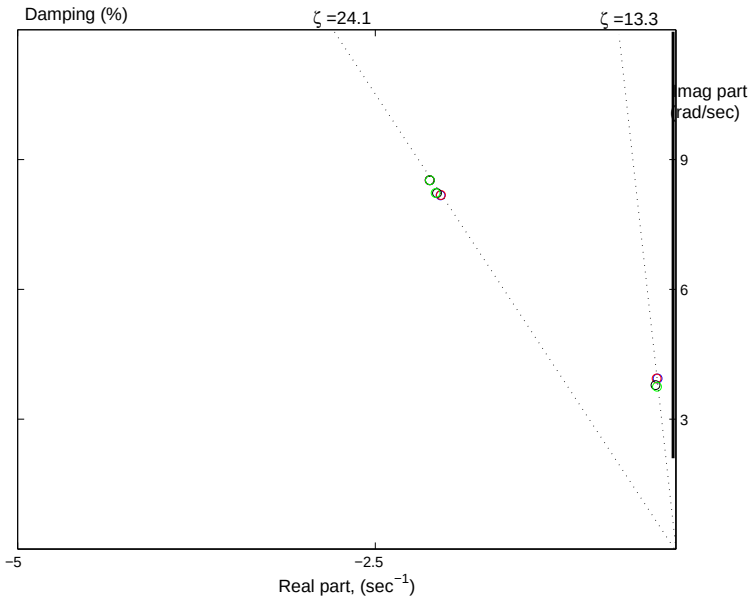

Figure 4.9: Loci of the electromechanical modes for the extreme points shown in Fig. 4.8 for $k_{pf} = 0$. The damping factors and the $j\Omega$ barrier are also depicted.

scalings, and it provides an interesting insight since it is directly formulated in well known terms in power system community. The feasibility of the robustness test and the extent of the parametric variations supported by the method was assessed with the help of a classical benchmark.

Chapter 5

Conclusions and future work

The main original contributions presented in this thesis are commented next.

- Section 2.1 introduces an extension of the classical concept of dissipativity, intended to cope with differential–algebraic descriptions of power systems. A specific power supply rate function W is proposed that enables the establishment of dissipative properties for a class of power system models. The dissipativity also holds for the incremental dynamics around the equilibrium which is shown to have direct consequences for the small signal dynamics.

- Detailed non linear full order models of synchronous machines are shown to be cyclo-dissipative in the above-mentioned sense. This fact allows us to include these models into the classical energy function for power systems, avoiding the use of oversimplified models. Section 1.3.2 and Chapter 2.

- The small signal models of the above-mentioned class of power systems are shown to meet a convex constraint in the frequency domain, more precisely on the phase of the transfer function. This constraint is even satisfied in a significant frequency band in the presence of non-dissipative terms. Section 2.2.

- A standard non linear model of SVC with PD voltage control is shown to be cyclo–dissipative. It is shown that the control law can add dissipation to the device. A complete characterization of the linear controllers preserving this property for the small signal is provided. Section 2.3.

- The simplifying modeling assumptions mentioned above are abandoned in Chapter 4, to treat generic small signal models of power systems. A first

contribution of this chapter is a precise definition of the performance of voltage regulation and damping injection that have direct links with the phase constraint mentioned above and also with some classical concepts. It is shown that a certain balance, precisely established, between damping, voltage regulation and voltage sensitivity on a suitable frequency band constitutes a sufficient condition for the robust stability of the electromechanical modes. Definitions 2-4 and Theorem 1.

The methodology has been quite *eclectic*, since the analysis includes so diverse tools as differential-algebraic equations, dissipativity, Lyapunov stability analysis, IQCs, LMI optimization and quadratic constraints on a finite frequency band.

Seen from a certain distance, it can be said that the analysis tools followed a way inverse to the assumptions taken on the model. Global statements valid for nonlinear models in the whole state space are only possible for a restricted class of systems that–it worths to emphasize it–was a bit extended in this thesis. The consideration of small signal models made possible to quantify the modest effect of some parameters that nevertheless obstruct the establishment of the dissipativity for non linear models. The further inclusion of realistic features of power systems into the model restricted us first to the consideration of linear models, and finally to the study of certain properties in a given frequency band.

The work reported in this thesis opens some opportunities for future research:

- The results in Chapter 4 can be better illustrated with a bigger example, closer to the common practices of power system community.
- The new terms, associated to detailed models of synchronous machines and SVCs, that are now admitted by the classical energy function can be tested on a benchmark to improve the accuracy of the existing direct methods to compute critical clearing times.
- The relation between the dissipativity of AC-modulated electrical networks, the classical passivity of electrical circuits and the role of the phasorial models perhaps deserves more attention.

Appendix

Appendix A

A brief introduction to dissipative systems

A deep treatment of the classical concepts of dissipativity, passivity and their links with stability and performance of feedback systems is beyond the scope of this thesis. This appendix is intended to offer a brief presentation including the Willems' definition of dissipativity, a definition of passivity and some links between these concepts and Lyapunov stability.

Reference (Willems, 1972) presents a general theory of dissipative dynamic systems, oriented to the state space description of these systems. The concept of dissipativity generalizes the idea of *passivity* as the storage functions generalizes the concept of energy stored. Although these concepts are classical, e.g., in thermodynamics and circuit theory, different formulations co-exist that are not equivalent. The interested reader can find in reference (Wyatt et al., 1981) several alternative definitions of passivity along with some examples showing the respective flaws.

We will follow the lines of reference (Willems, 1972) to define dissipativity, but we will purposely restrict the class of dynamical systems under study to those given by the differential formulation

$$\Sigma(u,v): \begin{cases} \dot{x} &= f(x,u) \\ v &= r(x,u) \end{cases} \tag{A.1}$$

where $x \in \mathbb{R}^n$ is the state and $(u,v) \in \mathbb{R}^p \times \mathbb{R}^p$ are the port variables. The function $r : \mathbb{R}^n \times \mathbb{R}^p \to \mathbb{R}^p$ is the read-out function. $f : \mathbb{R}^n \times \mathbb{R}^p \to \mathbb{R}^n$ and r are functions smooth enough to ensure the existence and uniqueness of the solutions on a set $\mathcal{D} \subset \mathbb{R}^n \times \mathbb{R}^p$.

Definition 5. *Consider the dynamical system* Σ *(*A.1*). Let* $w : \mathbb{R}^p \times \mathbb{R}^p \to \mathbb{R}$ *be locally integrable along trajectories of* Σ*, i.e.*

$$\int_{t_1}^{t_2} w(u(t), v(t))dt < \infty, \quad \forall\, t_1, t_2 \in \mathbb{R}.$$

We say that Σ *is* dissipative *with respect to the supply rate* $w(u, v)$ *if and only if there exists a non-negative differentiable function* $S : \mathbb{R}^n \to \mathbb{R}$*, called storage function, such that all solution* $(x(t), u(t)) \in \mathcal{D}$ *satisfies*

$$S(x(t_2)) - S(x(t_1)) \leq \int_{t_1}^{t_2} w(u(t), v(t))dt \quad \forall t_2 \geq t_1. \tag{A.2}$$

We also define the dissipation function $d : \mathbb{R}^n \times \mathbb{R}^p \to \mathbb{R}$

$$\int_{t_1}^{t_2} d(x(t), u(t))dt = S(x(t_2)) - S(x(t_1)) - \int_{t_1}^{t_2} w(u(t), v(t))dt \quad \forall t_2 \geq t_1.$$

The system is lossless *if the dissipation inequality (*A.2*) holds with identity, the same to say* $d \equiv 0$*.*

Finally, if the storage function is not bounded from below, we say that Σ is *cyclo-dissipative* with respect to the supply rate w. See references (Willems, 1972; Hill and Moylan, 1980) for a detailed discussion about the consequences of the non-negativeness of the storage functions and the dissipativity along closed trajectories.

The definition above is very general. An engineering standpoint requires the establishment of some dynamic properties as the existence of equilibrium points, the boundedness of trajectories, among others. So, additional requirements either on the storage function S or the supply rate function w are needed.

Reference (Hill and Moylan, 1980), in an input-output setting for the system description, focuses its attention on quadratic supply rate function. This class of functions are rich enough to capture passivity and bounds on the $\mathcal{L}_2$ gain.

To highlight the links between dissipativity and the better known concept of passivity we will reproduce the definition in (Khalil, 1996) due, among other reasons, to its formulation in the state space. So, suppose that

Assumption 14. *The system* Σ*, equation (*A.1*) satisfies*

$$\begin{cases} f(0,0) &= 0 \\ h(0,0) &= 0. \end{cases}$$

This assumption implies that the origin is an equilibrium point when the system is not subject to external inputs.

Definition 6. *The system Σ satisfying Assumption* 14 *is said to be* passive *if there exists a continuously differerentiable positive semidefinite function $V(x)$ (called the storage function) such that*

$$\frac{d}{dt}V(x) \leq u^\top v - (\epsilon u^\top u + \delta v^\top v + \rho\Psi(x)) \;\; \forall (x,u) \in \mathbb{R}^n \times \mathbb{R}^p \tag{A.3}$$

where ϵ, δ and ρ are nonnegative constants, and $\Psi(x)$ is a positive semidefinite function such that

$$\Psi(x(t)) \equiv 0 \Rightarrow x(t) \equiv 0$$

for all the solutions $(x(t), u(t))$ of Σ. The system is said to be

- *lossless if (*A.3*) is satisfied with equality and $\epsilon = \delta = \rho = 0$:*

$$\frac{d}{dt}V(x) = u^\top v.$$

- *input strictly passive if $\epsilon > 0$.*
- *output strictly passive if $\delta > 0$.*
- *state strictly passive if $\rho > 0$.*

The definition of these several types of of passivity opens very direct links with Lyapunov stability when some additional conditions hold, see Lemma 10.6 in (Khalil, 1996):

Lemma 9. *If the system Σ satisfying Assumption* 14

is passive with a definite positive storage function $V(x)$, then the origin of $\dot{x} = f(x, 0)$ is stable;

is state strictly passive with a definite positive storage function $V(x)$, then the origin of $\dot{x} = f(x, 0)$ is asymptotically stable.

The interested reader is referred to the above-mentioned references and to (Van der Schaft, 2000) for a deep discussion of these topics in a general setting.

Appendix B

Some demonstrations of Chapters 1 and 3

B.1 Demonstrations of Chapter 1

We reproduce the Fact 3 of Section 1.3.2, omitting the indices associated to the specific bus to facilitate the reading. Later we proceed to demonstrate it.

Fact 3 *The synchronous machine model (*1.30*) defines an operator* Σ^{M_6} : $(\mathrm{I}^M, \mathrm{V}; e_{fd}, i_{fd})$ *described by the implicit PCH system*

$$\Sigma^{M_6} : (\mathrm{I}^M, \mathrm{V}; e_{fd}, i_{fd}) \begin{cases} \dot{X} &= (K-R)\nabla_X S^{M_6}(X, \mathrm{V}) + B_{fd} e_{fd} \\ 0 &= -\nabla_{\mathrm{V}} S^{M_6}(X, \mathrm{V}) + J\mathrm{I}^M \end{cases} \tag{B.1}$$

with storage function $S^{M_6} : R^6 \times R^2 \to R$*:*

$$S^{M_6}(X, \mathrm{V}) := \frac{1}{2}\Omega_0 h(\omega_r - 1)^2 + \frac{1}{2}\Phi^\top L^{-1}\Phi - T_m\delta - I^\star_{fd}\Phi_{fd}. \tag{B.2}$$

with the matrices K, R *defined in (*1.33*),(*1.34*).*

Proof First, notice that the stator flux Φ_s is not a state variable, but a function on δ and V. In effect, from equations (1.28) and (1.22), we have

$$\Phi_s = J^{-1}\mathrm{E}_s = -J\mathrm{E}_s = -J[JU_\delta \mathrm{V}] = U_\delta \mathrm{V}. \tag{B.3}$$

As a consequence, the flux vector Φ, see equation (1.26), is a function of the state vector X and the link variables V. With the help of the auxiliary matrices

$$T_s = \begin{bmatrix} I_2 \\ 0_{4\times 2} \end{bmatrix}, T_r = \begin{bmatrix} 0_{2\times 4} \\ I_4 \end{bmatrix},$$

we write

$$\Phi = \begin{bmatrix} \Phi_s \\ \Phi_{fd} \\ \Phi_r \end{bmatrix} = T_s\Phi_s + T_r \begin{bmatrix} \Phi_{fd} \\ \Phi_r \end{bmatrix}, \quad -I_s = T_s^\top I. \tag{B.4}$$

By invoking equations (B.3) and (B.4), we can compute

$$\frac{\partial \Phi}{\partial \mathrm{V}} = \frac{\partial \Phi}{\partial \Phi_s}\frac{\partial \Phi_s}{\partial \mathrm{V}} = T_s U_\delta, \tag{B.5}$$

and, with the help of property (1.23):

$$\frac{\partial \Phi}{\partial \delta} = \frac{\partial \Phi}{\partial \Phi_s}\frac{\partial \Phi_s}{\partial \delta} = T_s \frac{dU_\delta}{d\delta}\mathrm{V} = T_s[-JU_\delta]\mathrm{V} = -T_s E_s. \tag{B.6}$$

Define the function $S_0^M : R^6 \times R^2 \to R$:

$$S_0^M(X, \mathrm{V}) := \frac{1}{2}\Omega_0 h(\omega_r - 1)^2 + \frac{1}{2}\Phi^\top L^{-1}\Phi - T_m\delta. \tag{B.7}$$

From definition (B.7) and equation (1.26), we get

$$\frac{\partial S_0^M}{\partial \Phi} = (L^{-1}\Phi)^\top = I^\top, \tag{B.8}$$

and, from (B.6) and (1.29):

$$\frac{\partial S_0^M}{\partial \Phi}\frac{\partial \Phi}{\partial \delta} = I^\top[-T_s E_s] = I_s^\top E_s = -P^M. \tag{B.9}$$

The partial derivative $\frac{\partial S_0^M}{\partial \mathrm{V}}$ can be computed with the help of equations (B.8), (B.5), (B.4) and (1.24):

$$\frac{\partial S_0^M}{\partial \mathrm{V}} = \frac{\partial S_0^M}{\partial \Phi}\frac{\partial \Phi}{\partial \mathrm{V}} = I^\top[T_s T(\delta)] = -I_s^\top T(\delta) = -[T(\delta)^\top I_s]^\top.$$

Equation (1.22) allows us to conclude

$$\frac{\partial S_0^M}{\partial \mathrm{V}} = [T(\delta)^\top J T(\delta)\mathrm{I}^M]^\top = [J\mathrm{I}^M]^\top.$$

Definition (B.7) and equation (B.9) imply:

$$\frac{\partial S_0^M}{\partial X} = \begin{bmatrix} -T_m + \frac{\partial S}{\partial \Phi}\frac{\partial \Phi}{\partial \delta} \\ h\Omega_0(\omega_r - 1) \\ T_r^\top L^{-1}\Phi \end{bmatrix}^\top = \begin{bmatrix} -T_m - P^M \\ h\Omega_0(\omega_r - 1) \\ T_r^\top I \end{bmatrix}^\top. \tag{B.10}$$

Thus, from the definition (B.2) and equation (B.10), we get the gradients of function S^M:

$$\nabla_X S^M(X, \mathrm{V}) = \begin{bmatrix} -T_m - P^M \\ h\Omega_0(\omega_r - 1) \\ T_r^\top I \end{bmatrix} - B_{fd} I_{fd}^\star; \;\; \nabla_{\mathrm{V}} S^M(X, \mathrm{V}) = J\mathrm{I}^M. \tag{B.11}$$

with the matrix B_{fd} defined as

$$B_{fd} = \begin{bmatrix} 0 & 0 & 1 & 0 & 0 & 0 \end{bmatrix}^\top.$$

B.2 Demonstrations of Chapter 3

We will demonstrate here both lemma 2 and Proposition 7 of Section 3.2. As the proof of Proposition 7 is based on the IQC Theorem in (Megretski and Rantzer, 1997), it is worth to briefly repeat this Theorem here, after mention some basic definition.

So, we will said that two signals $v, w \in \mathcal{L}_2$ *satisfy the IQC defined by* $\mathbf{\Pi} \in \mathcal{L}_\infty$ if

$$\int_{-\infty}^{+\infty} \begin{bmatrix} \hat{v}(j\omega) \\ \hat{w}(j\omega) \end{bmatrix}^* \mathbf{\Pi}(\omega) \begin{bmatrix} \hat{v}(j\omega) \\ \hat{w}(j\omega) \end{bmatrix} d\omega \geq 0. \tag{B.12}$$

The definition is extended for operators $\mathcal{L}_e^2 \to \mathcal{L}_e^2$ in the following way: A bounded operator Δ is said to *satisfy the IQC defined by* Π if (B.12) holds for all $w = \Delta v$, $\forall v \in \mathcal{L}_2$.

Consider two operators G and Δ. The standard feedback interconnection is given by

$$\begin{cases} v &= Gw + f \\ w &= \Delta v + e \end{cases}. \tag{B.13}$$

The closed loop stability is defined in (Megretski and Rantzer, 1997) in the $\mathcal{L}_2$ sense, see reference (Vidyasagar, 1993) for a deep discussion.

Next, we reproduced the Theorem 1 in (Megretski and Rantzer, 1997):

IQC Theorem *Let* $G(s) \in \mathbf{R}\mathcal{L}_\infty$*, and let* Δ *be a bounded causal operator. Assume that:*

1. for every $\tau \in [0, 1]$, the interconnection of G and $\tau\Delta$ is well-possed;
2. for every $\tau \in [0, 1]$ the IQC defined by Π is satisfied by $\tau\Delta$;
3. there exists $\epsilon > 0$ such that

$$\begin{bmatrix} G(j\omega) \\ I \end{bmatrix}^* \Pi(\omega) \begin{bmatrix} G(j\omega) \\ I \end{bmatrix} \leq -\epsilon I, \ \forall \omega \in \mathbb{R}.$$

Then, the feedback interconnection of G *and* Δ *is stable.*

As it can be seen, the object of study of (Megretski and Rantzer, 1997) is the interconnection of a linear time invariant operator G and a generic operator Δ. When only linear time-invariant systems are considered, the Integral Quadratic Constraint (B.12) is equivalent to a quadratic constraint to be met

for all frequency. In fact, if Δ is a time invariant linear system $\Delta \in \mathbf{R}\mathcal{H}_\infty$, we have that all signal w defined by

$$\hat{w} := \Delta\hat{v}, v \in \mathcal{L}_2$$

meets $w \in \mathcal{L}_2$. If $\Delta \in \mathbf{S}_l(\mathbf{\Pi})$, we have

$$\begin{bmatrix} I_m \\ \Delta(j\omega) \end{bmatrix}^* \mathbf{\Pi}(\omega) \begin{bmatrix} I_m \\ \Delta(j\omega) \end{bmatrix} \geq 0; \forall\omega \in \mathbb{R}. \tag{B.14}$$

If we right and left multiply this inequality respectively by $\hat{v}(j\omega)$ and $\hat{v}(j\omega)^*$ we have

$$\begin{bmatrix} \hat{v}(j\omega) \\ \hat{w}(j\omega) \end{bmatrix}^* \mathbf{\Pi}(\omega) \begin{bmatrix} \hat{v}(j\omega) \\ \hat{w}(j\omega) \end{bmatrix} \geq 0; \forall\omega \in \mathbb{R}, \tag{B.15}$$

where we introduced the definition of signal w. Since $v, w \in \mathcal{L}_2$ and $\mathbf{\Pi}$ is bounded, we can integrate on $j\mathbb{R}$ to obtain

$$\int_{-\infty}^{+\infty} \begin{bmatrix} \hat{v}(j\omega) \\ \hat{w}(j\omega) \end{bmatrix}^* \mathbf{\Pi}(\omega) \begin{bmatrix} \hat{v}(j\omega) \\ \hat{w}(j\omega) \end{bmatrix} d\omega \geq 0, \tag{B.16}$$

i.e. the block Δ satisfies the IQC defined by multiplier $\mathbf{\Pi}$, recall definition (B.12). The converse also can be shown to be true. Hence

$$\Delta \in \mathbf{S}_l(\mathbf{\Pi}) \Longleftrightarrow \Delta \in \mathbf{R}\mathcal{H}_\infty \; satisfies \; the \; IQC \; defined \; by \; \mathbf{\Pi}. \tag{B.17}$$

Next we will demonstrate the Lemma 2:

Lemma 2 *If the multiplier* $\mathbf{\Pi} \in \mathcal{L}_\infty^{2m\times 2m}$ *satisfies*

$$\begin{bmatrix} 0 \\ I_m \end{bmatrix}^* \mathbf{\Pi}(\omega) \begin{bmatrix} 0 \\ I_m \end{bmatrix} \leq 0 \; \forall\omega \in \mathbb{R}, \tag{B.18}$$

then the set $\mathbf{S}_l(\mathbf{\Pi})$ *is convex.*

Proof: If we recall the partition (3.15) for $\mathbf{\Pi}$, we can write the quadratic constraint in definition (3.16) and assumption B.18 respectively as

$$\sigma_l(\mathbf{X}(j\omega), \mathbf{\Pi}(\omega)) = \mathbf{Q}(\omega)+\mathbf{R}(\omega)\mathbf{X}(j\omega)+\mathbf{X}(j\omega)^*\mathbf{R}(\omega)^*+\mathbf{X}(j\omega)^*\mathbf{V}(\omega)\mathbf{X}(j\omega) \geq 0 \; \forall\omega \in \mathbb{R},$$

and

$$\mathbf{V}(\omega) \leq 0 \; \forall\omega \in \mathbb{R}.$$

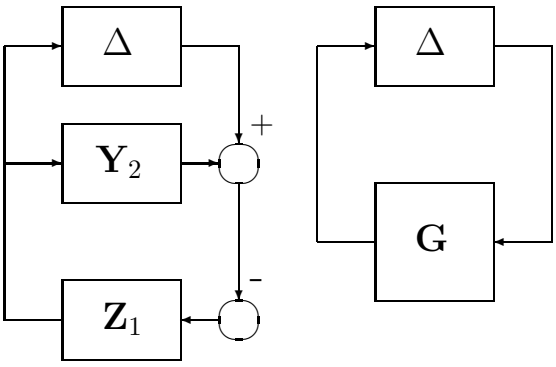

Figure B.1: Feedback interconnection of systems $\mathbf{Z}_1, \mathcal{Y}_2$

Consider two maps $\mathbf{X}_1, \mathbf{X}_2 \in \mathbf{S}_l(\mathbf{\Pi})$. So, both are stable and bounded on $j\mathbb{R}$ and satisfy[1]

$$\begin{aligned} \mathbf{Q} + \mathbf{R}\mathbf{X}_1 + \mathbf{X}_1^*\mathbf{R}^* + \mathbf{X}_1^*\mathbf{V}\mathbf{X}_1 &\geq 0 \ \forall \omega \in \mathbb{R} \\ \mathbf{Q} + \mathbf{R}\mathbf{X}_2 + \mathbf{X}_2^*\mathbf{R}^* + \mathbf{X}_2^*\mathbf{V}\mathbf{X}_2 &\geq 0 \ \forall \omega \in \mathbb{R} \end{aligned}$$

Multiply the first inequality by $\mu \in [0,1]$, the second one by $(1-\mu)$ and add:

$$\mathbf{Q}+\mathbf{R}[\mu\mathbf{X}_1+(1-\mu)\mathbf{X}_2]+[\mu\mathbf{X}_1+(1-\mu)\mathbf{X}_2]^*\mathbf{R}^*+\mu\mathbf{X}_1^*\mathbf{V}\mathbf{X}_1+(1-\mu)\mathbf{X}_2^*\mathbf{V}\mathbf{X}_2 \geq 0 \ \forall \omega \in \mathbb{R} \tag{B.19}$$

Notice that

$$-\mu(1-\mu)(\mathbf{X}_1+\mathbf{X}_2)^*\mathbf{V}(\mathbf{X}_1+\mathbf{X}_2) \geq 0, \tag{B.20}$$

because $\mathbf{V} \leq 0$ and $\mu \in [0,1]$. Introduce the convex combination

$$\mathbf{X}_\mu := \mu\mathbf{X}_1 + (1-\mu)\mathbf{X}_2.$$

$\mathbf{X}_\mu \in \mathbf{R}\mathcal{H}_\infty$ since both $\mathbf{X}_1, \mathbf{X}_2 \in \mathbf{R}\mathcal{H}_\infty$. Add inequalities (B.19) and (B.20) to obtain

$$\mathbf{Q} + \mathbf{R}\mathbf{X}_\mu + \mathbf{X}_\mu^*\mathbf{R}^* + \mathbf{X}_\mu^*\mathbf{V}\mathbf{X}_\mu \geq 0 \ \forall \omega \in \mathbb{R}. \tag{B.21}$$

Thus $\mathbf{X}_\mu \in \mathbf{S}_l(\mathbf{\Pi})$ $\forall \mu \in [0,1]$ and this set is convex. □□□

Next we reproduce and demonstrate the Proposition 7 in Section 3.2:

Proposition 7 *Let $\mathbf{Z}_1(s) \in \mathbf{R}\mathcal{L}_\infty^{m\times m}, \mathbf{Y}_2(s) \in \mathbf{R}\mathcal{H}_\infty^{m\times m}$ such that the operator $\mathbf{Z}_1 \star \mathbf{Y}_2$ is internally stable. Assume the existence of a Hermitian multiplier $\mathbf{\Pi}(\omega) \in \mathcal{L}_\infty^{2m\times 2m}$ and a scalar $\epsilon > 0$ such that the following conditions are met $\forall \omega \in \mathbb{R}$:*

$$i. \qquad \sigma_l(\mathbf{Y}_2(j\omega), \mathbf{\Pi}(\omega)) \geq 0, \tag{B.22}$$

[1] As usual, we omit the dependence on ω.

$$ii. \qquad \sigma_u(-\mathbf{Z}_1(j\omega), \mathbf{\Pi}(\omega)) \leq -\epsilon I, \tag{B.23}$$

$$iii. \qquad \begin{bmatrix} 0 \\ I_m \end{bmatrix}^* \mathbf{\Pi}(\omega) \begin{bmatrix} 0 \\ I_m \end{bmatrix} \leq 0. \tag{B.24}$$

Then, the feedback interconnection $\mathbf{Z}_1 \star \mathcal{Y}_2$ *is internally stable for all operator* $\mathcal{Y}_2 \in \mathbf{S}_l(\mathbf{\Pi})$ *such that the pair* $\mathbf{Z}_1, \mathcal{Y}_2$ *satisfy Assumption* 9.

Proof: Consider an arbitrary operator $\mathcal{Y}_2$ in the conditions stated in the Proposition. Thus $\mathcal{Y}_2 \in \mathbf{S}_l(\mathbf{\Pi})$ and, by hypothesis i), also $\mathbf{Y}_2 \in \mathbf{S}_l(\mathbf{\Pi})$. Define

$$\Delta := \mathcal{Y}_2 - \mathbf{Y}_2.$$

$\Delta \in \mathbf{R}\mathcal{H}_\infty$ because both terms are in $\mathbf{R}\mathcal{H}_\infty$. Recall partition (3.15) for $\mathbf{\Pi}$ and write

$$\begin{aligned} \sigma_l(\mathcal{Y}_2, \mathbf{\Pi}) &= \sigma_l(\Delta + \mathbf{Y}_2, \mathbf{\Pi}) = \\ &= \begin{bmatrix} I_m \\ \Delta + \mathbf{Y}_2 \end{bmatrix}^* \mathbf{\Pi} \begin{bmatrix} I_m \\ \Delta + \mathbf{Y}_2 \end{bmatrix} = \\ &= \mathbf{Q} + \mathbf{R}(\mathbf{Y}_2 + \Delta) + (\mathbf{Y}_2^* + \Delta^*)\mathbf{R}^* + (\mathbf{Y}_2^* + \Delta^*)\mathbf{V}(\mathbf{Y}_2 + \Delta) = \\ &= \sigma_l(\mathbf{Y}_2, \mathbf{\Pi}) + \mathbf{R}\Delta + \Delta^*\mathbf{R}^* + \Delta^*\mathbf{V}\mathbf{Y}_2 + \mathbf{Y}_2^*\mathbf{V}\Delta + \Delta^*\mathbf{V}\Delta. \end{aligned}$$

Thus

$$\sigma_l(\mathcal{Y}_2, \mathbf{\Pi}) = \begin{bmatrix} I_m \\ \Delta \end{bmatrix}^* \begin{bmatrix} \sigma_l(\mathbf{Y}_2, \mathbf{\Pi}) & \mathbf{R} + \mathbf{Y}_2^*\mathbf{V} \\ \mathbf{R}^* + \mathbf{V}\mathbf{Y}_2 & \mathbf{V} \end{bmatrix} \begin{bmatrix} I_m \\ \Delta \end{bmatrix}. \tag{B.25}$$

Define

$$\mathbf{\Pi}_\Delta := \begin{bmatrix} \sigma_l(\mathbf{Y}_2, \mathbf{\Pi}) & \mathbf{R} + \mathbf{Y}_2^*\mathbf{V} \\ \mathbf{R}^* + \mathbf{V}\mathbf{Y}_2 & \mathbf{V} \end{bmatrix}, \tag{B.26}$$

and notice $\mathbf{\Pi}_\Delta \in \mathcal{L}_\infty$. Since $\mathcal{Y}_2 \in \mathbf{S}_l(\mathbf{\Pi})$, equation (B.25) implies

$$\begin{bmatrix} I_m \\ \Delta \end{bmatrix}^* \mathbf{\Pi}_\Delta(\omega) \begin{bmatrix} I_m \\ \Delta \end{bmatrix} \geq 0; \forall \omega \in \mathbb{R}. \tag{B.27}$$

Since $\Delta \in \mathbf{R}\mathcal{H}_\infty$, the equivalence (B.17) implies that the block Δ satisfies the IQC defined by multiplier $\mathbf{\Pi}_\Delta$. By definition, $\mathbf{\Pi}_\Delta$ satisfies

$$\begin{aligned} \begin{bmatrix} I_m \\ 0 \end{bmatrix}^* \mathbf{\Pi}_\Delta(\omega) \begin{bmatrix} I_m \\ 0 \end{bmatrix} &= \sigma_l(\mathbf{Y}_2(\omega), \mathbf{\Pi}(\omega)) \geq 0 \ \forall \omega \in \mathbb{R}, \\ \begin{bmatrix} 0 \\ I_m \end{bmatrix}^* \mathbf{\Pi}_\Delta(\omega) \begin{bmatrix} 0 \\ I_m \end{bmatrix} &= \mathbf{V}(\omega) \leq 0 \ \forall \omega \in \mathbb{R}, \end{aligned} \tag{B.28}$$

because of, respectively, hypotheses i) and iii). Inequalities (B.28) imply, respectively that $0_{m\times m}$ satisfies the IQC defined by $\mathbf{\Pi}_\Delta(\omega)$ and that the set $\mathbf{S}_l(\mathbf{\Pi}_\Delta)$ is convex. So, all operator $\mu\Delta, \mu \in [0,1]$ satisfies the IQC defined by $\mathbf{\Pi}_\Delta(\omega)$.

Notice that the operator $\mathbf{Z}_1 \star \mathcal{Y}_2$ can be seen as the interconnection of a nominal stable system $\mathbf{G} := -\mathbf{Z}_1[I + \mathbf{Y}_2\mathbf{Z}_1]^{-1} \in \mathbf{R}\mathcal{H}_\infty$ with the stable block Δ, see Figure B.2. Let us compute

$$[I + \mathbf{Y}_2\mathbf{Z}_1]^* \sigma_u(\mathbf{G}, \mathbf{\Pi}_\Delta)[I + \mathbf{Y}_2\mathbf{Z}_1] =$$

$$= \begin{bmatrix} -\mathbf{Z}_1 \\ (I + \mathbf{Y}_2\mathbf{Z}_1) \end{bmatrix}^* \mathbf{\Pi}_\Delta \begin{bmatrix} \mathbf{Z}_1 \\ (I + \mathbf{Y}_2\mathbf{Z}_1) \end{bmatrix}.$$

A routine algebraic manipulation involving definition (B.26) and latter identity allows us to conclude

$$[I + \mathbf{Y}_2\mathbf{Z}_1]^* \sigma_u(\mathbf{G}, \mathbf{\Pi}_\Delta)[I + \mathbf{Y}_2\mathbf{Z}_1] = \sigma_u(-\mathbf{Z}_1, \mathbf{\Pi}).$$

Hypothesis ii) and the existence of an upper bound of $(I + \mathbf{Y}_2\mathbf{Z}_1)^{-1}$ on the imaginary axis imply the existence of a real $\epsilon_1 > 0$ such that

$$\sigma_u(\mathbf{G}, \mathbf{\Pi}_\Delta) \leq -\epsilon_1 I,$$

i.e.

$$\begin{bmatrix} \mathbf{G}(j\omega) \\ I \end{bmatrix}^* \mathbf{\Pi}_\Delta(\omega) \begin{bmatrix} \mathbf{G}(j\omega) \\ I \end{bmatrix} \leq -\epsilon_1 I; \forall \omega \in \mathbb{R}. \tag{B.29}$$

The proof ends verifying that we are in condition to apply the IQC Theorem to conclude the stability of the interconnection of Fig. B.2. In first instance, it is assumed that the interconnection is well possed for all $\mathcal{Y}_2$. So the hypothesis 1 of the IQC Theorem is met. The block $\mu\Delta, \mu \in [0,1]$ was shown to satisfy the IQC defined by Π_Δ. So, hypothesis 2 of the IQC Theorem es also met. Inequality (B.29) is equivalent to the hypothesis 3 of the IQC Theorem. The stability of G and Δ allow us apply the mentioned theorem and conclude the input-output stability of the operator $\mathbf{Z}_1 \star \mathcal{Y}_2$. The closed loop internal stability finally follows from Assumption 9. □□□

Appendix C

On Quadratic Inequalities and LFTs

This appendix introduces some algebraic computations involving Linear Fractional Transformations (LFT), necessary to demonstrate Lemma 8 in Chapter 4. The interested reader can consult reference (Zhou et al., 1996) for a detailed treatment of LFTs.

Consider a complex matrix $N \in \mathbb{C}^{2m\times 2m}$ with a partition

$$N = \begin{bmatrix} N_{11} & N_{12} \\ N_{21} & N_{22} \end{bmatrix},$$

and a matrix $\Delta \in \mathbb{C}^{m\times m}$. Assume the matrix $(I_m - N_{11}\Delta)$ invertible. The (upper) Linear Fractional Transformations $\mathcal{F}_u : \mathbb{C}^{2m\times 2m} \times \mathcal{C}^{m\times m} \to \mathbb{C}^{m\times m}$ is defined by

$$\mathcal{F}_u(N, \Delta) := N_{22} + N_{21}\Delta(I_m - N_{11}\Delta)^{-1}N_{12}.$$

Assume N_{12} invertible. Factorize

$$I_m = N_{12}^{-1}(I_m - N_{11}\Delta)(I_m - N_{11}\Delta)^{-1}N_{12}, \tag{C.1}$$

to write

$$\mathcal{F}_u(N, \Delta) = N_{22}N_{12}^{-1}(I_m - N_{11}\Delta)(I_m - N_{11}\Delta)^{-1}N_{12} + N_{21}\Delta(I_m - N_{11}\Delta)^{-1}N_{12} =$$

$$= [N_{22}N_{12}^{-1}(I_m - N_{11}\Delta) + N_{21}\Delta](I_m - N_{11}\Delta)^{-1}N_{12} =$$

$$= \begin{bmatrix} N_{22}N_{12}^{-1} & N_{21} - N_{22}N_{12}^{-1}N_{11} \end{bmatrix} \begin{bmatrix} I_m \\ \Delta \end{bmatrix} (I_m - N_{11}\Delta)^{-1}N_{12}.$$

Now factorize equation (C.1) to obtain

$$I_m = \begin{bmatrix} N_{12}^{-1} & -N_{12}^{-1}N_{11} \end{bmatrix} \begin{bmatrix} I_m \\ \Delta \end{bmatrix} (I_m - N_{11}\Delta)^{-1}N_{12},$$

and compute

$$\begin{bmatrix} I_m \\ \mathcal{F}_u(N,\Delta) \end{bmatrix} = \begin{bmatrix} N_{12}^{-1} & -N_{12}^{-1}N_{11} \\ N_{22}N_{12}^{-1} & N_{21} - N_{22}N_{12}^{-1}N_{11} \end{bmatrix} \begin{bmatrix} I_m \\ \Delta \end{bmatrix} (I_m - N_{11}\Delta)^{-1}N_{12}.$$

Denote

$$\tilde{N} := \begin{bmatrix} N_{12}^{-1} & -N_{12}^{-1}N_{11} \\ N_{22}N_{12}^{-1} & N_{21} - N_{22}N_{12}^{-1}N_{11} \end{bmatrix}, \ \tilde{M}(\Delta) := (I_m - N_{11}\Delta)^{-1}N_{12},$$

to write

$$\begin{bmatrix} I_m \\ \mathcal{F}_u(N,\Delta) \end{bmatrix} = \tilde{N} \begin{bmatrix} I_m \\ \Delta \end{bmatrix} \tilde{M}(\Delta).$$

Recall the definition (3.14) and compute, for a given $\Pi \in \mathbb{C}^{2m\times 2m}$:

$$\sigma_l(\mathcal{F}_u(N,\Delta),\Pi) = \begin{bmatrix} I_m \\ \mathcal{F}_u(N,\Delta) \end{bmatrix}^* \Pi \begin{bmatrix} I_m \\ \mathcal{F}_u(N,\Delta) \end{bmatrix} =$$

$$= \tilde{M}(\Delta)^* \begin{bmatrix} I_m \\ \Delta \end{bmatrix}^* \tilde{N}^*\Pi\tilde{N} \begin{bmatrix} I_m \\ \Delta \end{bmatrix} \tilde{M}(\Delta).$$

Thus

$$\sigma_l(\mathcal{F}_u(N,\Delta),\Pi) = \tilde{M}(\Delta)^*\sigma_l(\Delta,\tilde{N}^*\Pi\tilde{N}))\tilde{M}(\Delta). \tag{C.2}$$

The previous considerations are the basis of the following lemma:

Lemma 10. *Assume $\Pi \in \mathbb{C}^{2m\times 2m}$ and $N \in \mathcal{C}^{2m\times 2m}$ such that N_{12} and $(I_m - N_{11}\Delta)$ are invertible. Then*

$$\mathcal{F}_u(N,\Delta) \in \mathcal{S}_l(\Pi)$$

if and only if

$$\Delta \in \mathcal{S}_l(\tilde{N}^*\Pi\tilde{N}).$$

Proof The hypotheses imply that the matrix $\tilde{M}(\Delta) := (I_m - N_{11}\Delta)^{-1}N_{12}$ is invertible. Thus, the equation (C.2) implies that

$$\sigma_l(\mathcal{F}_u(N,\Delta),\Pi) \geq 0$$

is equivalent to

$$\sigma_l(\Delta,\tilde{N}^*\Pi\tilde{N})) \geq 0.$$

The proof concludes by recalling definition (4.30). □□□

Appendix D

Small signal models of static loads

Consider the classical polynomial model for the static load, (Kundur, 1994):

$$\begin{array}{rcl} P^d & = & P^\star[p_1(\frac{V}{V^\star})^2 + p_2\frac{V}{V^\star} + p_3][1 + k_{pf}\Delta f] \\ Q^d & = & Q^\star[q_1(\frac{V}{V^\star})^2 + q_2\frac{V}{V^\star} + q_3][1 + k_{qf}\Delta f] \end{array},$$

with Δf the frequency deviations, in p.u., of the bus voltage and $P^\star, Q^\star, V^\star$ the standard variables at the equilibrium. The respective portions of constant impedance, current and power satisfy

$$\sum_{i=1}^{3} p_i = 1, \sum_{i=1}^{3} q_i = 1, p_i \geq 0, q_i \geq 0 \; \forall i = 1..3 \tag{D.1}$$

k_{pf} and k_{qf} represent the power deviations proportional to frequency, see (Kundur, 1994) for a deep discussion. If we recall equations (1.5), we can write

$$\begin{array}{rcl} \mathrm{V}^\top \mathrm{I} & = & P^\star[p_1(\frac{V}{V^\star})^2 + p_2\frac{V}{V^\star} + p_3][1 + k_{pf}\Delta f] \\ \mathrm{V}^\top J\mathrm{I} & = & Q^\star[q_1(\frac{V}{V^\star})^2 + q_2\frac{V}{V^\star} + q_3][1 + k_{qf}\Delta f] \end{array},$$

to obtain the small signal deviations from equilibrium

$$\begin{array}{rcl} \mathrm{V}^{\star\top}\mathrm{i} + \mathrm{I}^{\star\top}\mathrm{v} & = & P^\star[2p_1\frac{v}{V^\star} + p_2\frac{v}{V^\star}] + P^\star k_{pf}\frac{\lambda}{2\Pi f_0} \\ \mathrm{V}^{\star\top}J\mathrm{i} - \mathrm{I}^{\star\top}J\mathrm{v} & = & Q^\star[2q_1\frac{v}{V^\star} + q_2\frac{v}{V^\star}] + Q^\star k_{qf}\frac{\lambda}{2\Pi f_0} \end{array},$$

that is equivalent to

$$\begin{array}{rcl} \mathrm{V}^{\star\top}\mathrm{i} & = & -\mathrm{I}^{\star\top}\mathrm{v} + P^\star[2p_1\frac{v}{V^\star} + p_2\frac{v}{V^\star}] + P^\star k_{pf}\frac{\lambda}{2\Pi f_0} \\ -\mathrm{V}^{\star\top}J\mathrm{i} & = & -\mathrm{I}^{\star\top}J\mathrm{v} - Q^\star[2q_1\frac{v}{V^\star} + q_2\frac{v}{V^\star}] - Q^\star k_{qf}\frac{\lambda}{2\Pi f_0} \end{array}.$$

Recall equations (4.8), (4.15) and the definition $\lambda = \dot{\vartheta}$ to get, in the transformed domain:

$$\hat{v} = k_v\hat{\mathrm{v}} = \frac{\mathrm{V}^{\star\top}}{V^\star}\hat{\mathrm{v}};\; \hat{\lambda} = j\omega\hat{\vartheta} = \frac{j\omega}{V^\star}k_\theta\hat{\mathrm{v}} = -\frac{j\omega}{V^{\star 2}}\mathrm{V}^{\star\top}J\hat{\mathrm{v}}.$$

With the help of these relations, we get

$$\left[\begin{array}{c} \mathrm{V}^{\star\top} \\ -\mathrm{V}^{\star\top}J \end{array}\right]\hat{\mathrm{i}} = -\left[\begin{array}{c} \mathrm{I}^{\star\top} \\ \mathrm{I}^{\star\top}J \end{array}\right]\hat{\mathrm{v}} + \frac{1}{V^{\star 2}}\left[\begin{array}{c} P^{\star}(2p_1+p_2) \\ -Q^{\star}(2q_1+q_2) \end{array}\right]\mathrm{V}^{\star\top}\hat{\mathrm{v}} -$$

$$-\frac{j\omega}{2\Pi f_0 V^{\star 2}}\left[\begin{array}{c} P^{\star}k_{pf} \\ -Q^{\star}k_{qf} \end{array}\right]\mathrm{V}^{\star\top}J\hat{\mathrm{v}}, \qquad \text{(D.2)}$$

Recall the definition of U_θ, equation (4.2), and property (4.3), to get

$$U_\theta = \frac{1}{V^\star}\left[\begin{array}{c} \mathrm{V}^{\star\top} \\ -\mathrm{V}^{\star\top}J \end{array}\right];\ U_\theta^\top = \frac{1}{V^\star}\left[\mathrm{V}^\star \ \ J\mathrm{V}^{\star\top}\right],\ U_\theta U_\theta^\top = U_\theta^\top U_\theta = I_2. \qquad \text{(D.3)}$$

Now, equation (D.2) can be written

$$V^\star U_\theta\hat{\mathrm{i}} = \{-\left[\begin{array}{c} \mathrm{I}^{\star\top} \\ \mathrm{I}^{\star\top}J \end{array}\right] + \frac{1}{V^{\star 2}}\left[\begin{array}{c} P^{\star}(2p_1+p_2) \\ -Q^{\star}(2q_1+q_2) \end{array}\right]\mathrm{V}^{\star\top} - \frac{j\omega}{2\Pi f_0 V^{\star 2}}\left[\begin{array}{c} P^{\star}k_{pf} \\ -Q^{\star}k_{qf} \end{array}\right]\mathrm{V}^{\star\top}J\}\hat{\mathrm{v}}.$$

Recall properties (D.3) and definitions (1.5) to obtain, successively

$$Y_{ZIP} = \frac{1}{V^\star}U_\theta^\top\{-\left[\begin{array}{c} \mathrm{I}^{\star\top} \\ \mathrm{I}^{\star\top}J \end{array}\right] + \frac{1}{V^{\star 2}}\left[\begin{array}{c} P^{\star}(2p_1+p_2) \\ -Q^{\star}(2q_1+q_2) \end{array}\right]\mathrm{V}^{\star\top} -$$

$$-\frac{j\omega}{2\Pi f_0 V^{\star 2}}\left[\begin{array}{c} P^{\star}k_{pf} \\ -Q^{\star}k_{qf} \end{array}\right]\mathrm{V}^{\star\top}J\}U_\theta^\top U_\theta =$$

$$= \frac{1}{V^{\star 2}}U_\theta^\top\{\left[\begin{array}{cc} -P^\star & Q^\star \\ Q^\star & P^\star \end{array}\right] + \left[\begin{array}{cc} P^{\star}(2p_1+p_2) & 0 \\ -Q^{\star}(2q_1+q_2) & 0 \end{array}\right] + \frac{j\omega}{2\Pi f_0}\left[\begin{array}{cc} 0 & P^{\star}k_{pf} \\ 0 & -Q^{\star}k_{qf} \end{array}\right]\}U_\theta =$$

$$= \frac{1}{V^{\star 2}}U_\theta^\top\{\left[\begin{array}{cc} P^{\star}(2p_1+p_2-1) & Q^\star \\ -Q^{\star}(2q_1+q_2-1) & P^\star \end{array}\right] + \frac{j\omega}{2\Pi f_0}\left[\begin{array}{cc} 0 & P^{\star}k_{pf} \\ 0 & -Q^{\star}k_{qf} \end{array}\right]\}U_\theta.$$

The use of constraints (D.1) allows us to conclude

$$Y_{ZIP} = \frac{1}{V^{\star 2}}U_\theta^\top\{\left[\begin{array}{cc} P^{\star}(p_1-p_3) & Q^\star \\ -Q^{\star}(q_1-q_3) & P^\star \end{array}\right] + \frac{j\omega}{2\Pi f_0}\left[\begin{array}{cc} 0 & P^{\star}k_{pf} \\ 0 & -Q^{\star}k_{qf} \end{array}\right]\}U_\theta. \qquad \text{(D.4)}$$

Uncertainty model Suppose that the nominal ZIP model is given by the triads $p_i^\star, q_i^\star, i = 1..3$ and $k_{pf}^\star, k_{qf}^\star$. The family of ZIP models able to be obtained by parameter variation constrained by (D.1) can be written

$$\mathcal{Y}_{\mathcal{ZIP}}(\Delta) : Y_{ZIP}^\star + \frac{1}{V^{\star 2}}U_\theta^\top\left[\begin{array}{cc} P^\star & 0 \\ 0 & -Q^\star \end{array}\right]\left[\begin{array}{cc} \Delta_{11} & \Delta_{12} \\ \Delta_{21} & \Delta_{22} \end{array}\right]\left[\begin{array}{cc} 1 & 0 \\ 0 & \frac{j\omega}{2\Pi f_0} \end{array}\right]U_\theta, \qquad \text{(D.5)}$$

with

$$\Delta_{11} := p_1 - p_3 - (p_1^\star - p_3^\star); \Delta_{12} := k_{pf} - k_{pf}^\star,$$

$$\Delta_{21} := q_1 - q_3 - (q_1^\star - q_3^\star); \Delta_{22} := k_{qf} - k_{qf}^\star.$$

Bounds on k_{pf}, k_{qf} and the constraints (D.1) yield the set

$$\mathcal{D}_\Delta : \{\Delta \subset \mathbb{R}^{2\times 2} \textit{ such that } \begin{cases} -1 \leq & \Delta_{11} + p_1^\star - p_3^\star & \leq 1, \\ -1 \leq & \Delta_{21} + q_1^\star - q_3^\star & \leq 1, \\ \underline{k_{pf}} \leq & \Delta_{12} + k_{pf}^\star & \leq \overline{k_{pf}}, \\ \underline{k_{qf}} \leq & \Delta_{22} + k_{qf}^\star & \leq \overline{k_{qf}}, \end{cases} \}, \tag{D.6}$$

which is compact and convex.

Bibliography

Abdel-Magid, Y., Abido, M. and Mantaway, A. (2000). Robust tuning of power system stabilizers in multimachine power systems, *Power Systems, IEEE Transactions on* **15**(2): 735 –740.

Anderson, P. and Fouad, A. (1993). *Power System Control and Stability*, IEEE Press.

Athay, T., Podmore, R. and Virmani, S. (1979). A practical method for the direct analysis of transient stability., *IEEE Trans. on Power App. Syst.* pp. 573–582.

Azbe, V., Gabrijel, U., Povh, D. and Mihalic, R. (2005). The energy function of a general multimachine system with a unified power flow controller., *IEEE Transactions on Power Systems* **20**(3): 1478–1485.

Bergen, A. and Hill, D. (1981). A structure preserving model for power system stability analysis, *IEEE Trans Power App. Syst.* **PAS 100**(1): 25–35.

Boukarim, G., Wang, S., Chow, J., Taranto, G. and Martins, N. (2000). A comparison of classical, robust, and decentralized control designs for multiple power system stabilizers, *Power Systems, IEEE Transactions on* **15**(4): 1287 –1292.

Castellanos, R., Juárez, C., Hernández, J. and Messina, A. (2006). Robustness analysis of large power systems with parametric uncertainties, *Power Engineering Society General Meeting, 2006. IEEE* .

Chen, C.-T. (1984). *Linear System Theory and Design*, Holt, Rinehart and Winston, Inc.

Chiang, H.-D. (1989). Study of the existence of energy functions for power systems with losses, *Circuits and Systems, IEEE Transactions on* **36**(11): 1423 –1429.

Chiang, H.-D., Wu, F. and Varaiya, P. (1987). Foundations of direct methods for power system transient stability analysis, *Circuits and Systems, IEEE Transactions on* **34**(2): 160 – 173.

Chiang, H.-D., Wu, F. and Varaiya, P. (1994). A BCU method for direct analysis of power system transient stability, *Power Systems, IEEE Transactions on* **9**(3): 1194 –1208.

Chilali, M. and Gahinet, P. (1996). H_∞ design with pole placement constraints: An LMI approach., *IEEE Transactions on Automatic Control* **41**: 358–367.

Cigré, S. C. . (1996). Analysis and control of power system oscillations, *Technical report*, Cigré.

Commitee, W. S. (2004). Wecc power system stabilizer tuning guidelines, *Technical report*, WECC.

Conway, J. B. (1985). *A Course in Functional Analysis*, Springer-Verlag.

DeMello, F. and Concordia, C. (1969). Concepts of synchronous machine stability as affected by excitation control, *IEEE Transactions on Power Apparatus and systems* **PAS-88**: 316–329.

Djukanovic, M., Khammash, M. and Vittal, V. (1999). Sequential synthesis of structured singular value based decentralized controllers in power systems, *Power Systems, IEEE Transactions on* **14**(2): 635 –641.

Dommel, H. (1969). Digital computer solution of electromagnetic transients in single-and multiphase networks, *Power Apparatus and Systems, IEEE Transactions on* **PAS-88**(4): 388–399.

Doyle, J. (1982). Analysis of feedback systems with structured uncertainty, *Proc. Inst. Elect. Eng.* **D-129**: 242–251.

Doyle, J. (1985). Structure uncertainty in control system design, *Proceedings of 24th Conference on Decision and Control* pp. 260–265.

Doyle, J., Francis, B. and Tannembaum, A. (1992). *Feedback Control Theory*, Macmillan Publishing Company.

Fan, M., Tits, A. and Doyle, J. (1991). Robustness in presence of mixed parametric uncertainty and unmodeled dynamics, *IEEE Transactions on Automatic Control* **36**: 25–38.

Gahinet, P., Nemirovski, A., Laub, A. and Chilali, M. (1995). *LMI Control Toolbox for use with MATLAB*.

Galaz, M., Ortega, R., Bazanella, A. and Stankovic, A. (2001). A control strategy for controllable series capacitor in electric power systems, *Automatica* **37**: 1575–1583.

Giusto, A. (2007a). On some dissipativity properties of a class of power system models, *3rd. IFAC Symposium on System, Structure and Control, Foz do Iguazú, Brasil* .

Giusto, A. (2007b). On some frequency domain properties of small signal models of a class of power systems, *IEEE Conference on Decision and Control, 46th. Florida, USA*.

Giusto, A. (2010). Application of frequential properties of power systems in robustness analysis, *2010 American Control Conference, Baltimore, USA*.

Giusto, A., Ortega, R. and Stankovic, A. (2006a). On Transient Stabilization of Power System: a Power–Shaping Solution for structure–preserving models, *IEEE Conference on Decision and Control*, San Diego, USA.

Giusto, A., Ortega, R. and Stankovic, A. (2006b). A Power-Shaping solution for the Transient Stabilization of Power Systems, *Congresso Brasileiro de Automatica*, Salvador, Brazil.

Giusto, A., Stankovic, A. and Ortega, R. (2008). Dissipativity properties of detailed models of synchronous generators, *IEEE Conference on Decision and Control*, Cancún, México.

Hill, D. J. and Moylan, P. J. (1980). Dissipative dynamical systems: Basic input–output and state properties., *Journal of the Franklin Institute* **309**(5): 327–357.

Hill, D. and Mareels, I. (1990). Stability theory for differential/algebraic systems with application to power systems., *IEEE Transactions on Circuits and Systems* **37**(11): 1416–1423.

Hiskens, I. and Hill, D. (1992). Incorporation of SVCs into Energy Function Methods, *IEEE Transactions on Power Systems* **7**(1): 133–140.

Horowitz, I. (1993). *Quantitative Feedback Design Theory*, QFT Publications.

Iwasaki, T. and Hara, S. (2005). Generalized KYP Lemma: Unified frequency domain inequalities with design applications., *IEEE Transactions on Automatic Control* **50**: 41–59.

Khalil, H. (1996). *Nonlinear Systems*, Prentice-Hall.

Kimbark, E. (1948). *Power System Stability*.

Klein, M., Rogers, G., Moorty, S. and P.Kundur (1992). Analytical investigation of factors influencing power system stabilizers performance, *IEEE Trans. on Energy Conversion* **7**: 382–390.

Kundur, P. (1994). *Power Systems Stability and Control*, McGraw-Hill, New York.

Kundur, P., Klein, M., Rogers, G. and Zywno, M. (1989). Application of power system stabilizers for enhancement of overall system stability, *IEEE Transactions on Power Systems* **4**(2).

Lee, D., Beaulieu, R. and Service, J. (1981). A Power System Stabilizer using speed and electrical power inputs. Design and field experience, *IEEE Transactions on Power Apparatus and Systems* **PAS-100**: 4151–4157.

Mattavelli, P., Verghese, G. and Stankovic, A. (1997). Phasor dynamics of thyristor-controlled series capacitor systems, *Power Systems, IEEE Transactions on* **12**(3): 1259–1267.

Megretski, A. and Rantzer, A. (1997). System analysis via integral quadratic constraints, *IEEE Transactions on Automatic Control* **42**(6): 819–830.

Milano, F. (2005). An open source power system analysis toolbox, *IEEE Transactions on Power Systems* **20**: 1199–1206.

Ortega, R., Galaz, M., Astolfi, A., Sun, Y. and Shen, T. (2005). Transient stabilization of multimachine power systems with nontrivial transfer conductances, *IEEE Transactions on Automatic Control* **50**(1).

Ortega, R., Jeltsema, D. and Scherpen, J. (2003). Power shaping: A new paradigm for stabilization of nonlinear RLC circuits., *IEEE Transaction on Automatic Control* **48**(10).

Ortega, R., Stankovic, A. and Stefanov (1998). A passivation approach to power systems stabilization., *IFAC Symp. Nonlinear Control Systems Design, Enschede, NL* .

Ortega, R., Van Der Schaft, A., Mareels, I. and Maschke, B. (2001). Putting energy back in control, *Control Systems Magazine, IEEE* **21**(2): 18 –33.

Ortega, R., Van der Schaft, A., Maschke, B. and Escobar, G. (2002). Interconnection and damping assignment passivity–based control of port–controlled hamiltonian systems., *Automatica* **38**(4).

Overbye, T. and DeMarco, C. (1991). Improved techniques for power system voltage stability assessment using energy methods, *Power Systems, IEEE Transactions on* **6**(4): 1446 –1452.

Paganini, F. and Lesieutre, B. (1999). Generic properties, one-parameter deformations, and the BCU method, *IEEE Transactions on Circuits and Systems I: Fundamental Theory and Applications* **46**(6): 760 –763.

Pai, M. (1989). *Energy Function Analysis for Power System Stability.*, Kluwer Academic Publishers, Boston, MA.

Pal, B. and Chaudhuri, B. (2005). *Robust Control in Power Systems*, Springer Science.

Powertech Labs Inc. (n.d.). DSATools. Dynamic Security Assessment Software. www.powertechlabs.com.

Rantzer, A. (1996). On the Kalman-Yakubovic-Popov lemma, *Systems and Control Letters* **28**(1): 7–10.

Sanders, S., Noworolski, J., Liu, X. and Verghese, G. (1991). Generalized averaging method for power conversion circuits, *Power Electronics, IEEE Transactions on* **6**(2): 251–259.

Sauer, P. and Pai, M. (1998). *Power System Dynamic and Stability.*, Prentice Hall, N.J.

Shen, T., Ortega, R., Lu, Q., Mei, S. and Tamura, K. (2003). Adaptive disturbance attenuation of hamiltonian systems with parametric perturbations and application to power systems, *Asian Journal of Control* **5**(1).

Stankovic, A. and Aydin, T. (2000). Analysis of asymmetrical faults in power systems using dynamic phasors, *Power Systems, IEEE Transactions on* **15**(3): 1062–1068.

Stankovic, A., Stefanov, P., Tadmor, G. and Sobajic, D. (1999). Dissipativity as a unifying control design framework for suppression of low frequency oscillations in power systems, *IEEE Transactions on Power Systems* **14**(1): 192–199.

Sun, Y., Song, Y. and Li, X. (2000). Novel energy-based Lyapunov function for controlled power systems., *IEEE Power Engineering Review* pp. 55–57.

Tsolas, N., Arapostathis, A. and Varaiya, P. (1985). A structure preserving energy function for power system transient stability analysis., *IEEE Transactions on Circuits and Systems* **32**: 1041–1049.

Van Cutsem, T. and Ribbens-Pavella, M. (1985). Structure preserving direct methods for transient stability analysis of power systems., *Proc. of the 24th IEEE Conf. on Decision and Control* pp. 70–76.

Van der Schaft, A. (2000). *L_2 Gain and Passivity Techniques in Nonlinear Control*, 2nd edn, Springer Verlag.

Varaiya, P., Wu, F. and R.-L., C. (1985). Direct methods for transient stability analysis of power systems: Recent results, *Proceedings of the IEEE* **73**(12): 1703–1715.

Vidyasagar, M. (1993). *Nonlinear Systems Analysis*, 2nd edn, Prentice-Hall.

Wang, Y., Daizhan, C., Chunwen, L. and You, G. (2003). Dissipative hamiltonian realization and energy-based l_2 disturbance attenuation control of multimachine power systems., *IEEE Transactions on Automatic Control* **48**(8): 1428–1433.

Willems, J. (1971). Least squares stationary optimal control and the algebraic Riccati equation, *IEEE Transactions on Automatic Control,* **16**(6): 621 – 634.

Willems, J. (1972). Dissipative dynamical systems. part i: General theory; part II: Linear systems with quadratic supply rates, *Arch. Rational Mech. Anal.* **45**: 321–393.

Willems, J. L. (1974). A partial stability approach to the problem of transient power system stability, *Int. J. of Control* **19**(1): 1–14.

Wyatt, J., Chua, L., Gannett, J., Goknar, I. and Green, D. (1981). Energy concepts in the state-space theory of nonlinear n-ports: Part i-passivity, *IEEE Trans. on Circuit and Systems* **28**(1): 48–61.

Zhou, K., Doyle, J. and Glover, K. (1996). *Robust and Optimal Control*, Prentice-Hall.